ARS JOURNAL
RUSSIAN SUPPLEMENT

J. George Adashko, Editor

Published Under National Science Foundation Grant-in-Aid

On the Design of Nozzles

I. M. YUR'EV

WE OBTAINED an exact particular solution of the nonlinear equation, which is the principal portion of the exact equation of three-dimensional gas flow over a large range of Mach numbers ($0 < M < 1.7$). The result is applicable to the design of nozzles.

1 Let the gas move essentially along the x axis. Let us imagine, for example, sufficiently long nozzles, which become an elementary small jet in the limit, and assume that we want to find more rigorous solutions over a larger range of Mach number variation than obtainable under the assumption of a small jet. It is clear that for such a flow it is possible to discard all the terms with mixed derivatives φ_{xy}, φ_{xz} and φ_{yz} from the exact equation of motion of gas

$$\left(1-\frac{u^2}{c^2}\right)\varphi_{xx}+\left(1-\frac{v^2}{c^2}\right)\varphi_{yy}+\left(1-\frac{w^2}{c^2}\right)\varphi_{zz}-\frac{2uv}{c^2}\varphi_{xy}-\frac{2uw}{c^2}\varphi_{xz}-\frac{2vw}{c^2}\varphi_{yz}=0 \quad [1.1]$$

by virtue of the smallness of $v = \varphi_y$ and $w = \varphi_z$, and it is also possible to neglect the quantities v^2 and w^2 in the coefficients of φ_{xx}, φ_{yy} and φ_{zz}. We thus arrive at the equation

$$F(u)\varphi_{xx}+\varphi_{yy}+\varphi_{zz}=0$$

or

$$F[c_*(1+u')]\varphi_{xx}'+\varphi_{yy}'+\varphi_{zz}'=0$$

$$\left(\varphi'=\frac{\varphi}{c_*}-x \qquad u=c_*(1+u')\right) \quad [1.2]$$

where

$$u'=\varphi_x' \qquad F(u)=\frac{c_*^2-u^2}{c_*^2-u^2/h^2} \qquad \left(h^2=\frac{\kappa+1}{\kappa-1}\right) \quad [1.3]$$

and c_* is the critical velocity of sound. The steeper the walls of the nozzle, the less exact is Equation [1.2]. However, even here Equation [1.2] is the principal part of the exact Equation [1.1] in the vicinity of the velocity of sound and in the region of small subsonic velocities. Apparently, the best results can be obtained with Equation [1.2] in the design of an axially symmetrical nozzle, for in this case definite velocities are reached at the minimum expansion. The solution can be obtained, however, only for the equation

$$-[(\kappa+1)u'+\kappa u'^2]\varphi_{xx}'+\varphi_{yy}'+\varphi_{zz}'=0 \quad [1.4]$$

In the figure, curve 1 represents the exact function F, line 2 represents $-(\kappa+1)u'$, which corresponds to the Tricomi equation, and curve 3 represents the function $-[(\kappa+1)u'+\kappa u'^2]$. In the vicinity of $u = c_*$ (i.e., $u' = 0$), Equation [1.4], like Equation [1.2], is equivalent to the Tricomi equation.

2 As in (1),[1] we seek for Equation [1.4] a particular solution of the form

$$\varphi'=f_1(y,z)x^2+f_2(y,z)x+f_3(y,z) \quad [2.1]$$

Substituting [2.1] into [1.4] and setting equal to zero the coefficients of the powers of x, we obtain the system of equations

$$\frac{\partial^2 f_1}{\partial y^2}+\frac{\partial^2 f_2}{\partial z^2}-8\kappa f_1^3=0$$

$$\frac{\partial^2 f_2}{\partial y^2}+\frac{\partial^2 f_2}{\partial z^2}-8\kappa f_1^2 f_2-4(\kappa+1)f_1^2=0 \quad [2.2]$$

$$\frac{\partial^2 f_3}{\partial y^2}+\frac{\partial^2 f_3}{\partial z^2}-2f_1[(\kappa+1)f_2+\kappa f_2^2]=0$$

For axially symmetrical flow, the system [2.2] becomes a system of ordinary differential equations

$$\frac{d^2 f_1(r)}{dr^2}+\frac{1}{r}\frac{df_1(r)}{dr}-8\kappa f_1^3(r)=0 \quad [2.3]$$

$$\frac{d^2 f_2(r)}{dr^2}+\frac{1}{r}\frac{df_2(r)}{dr}-8\kappa f_1^2(r)f_2(r)-4(\kappa+1)f_1^2(r)=0 \quad [2.4]$$

$$\frac{d^2 f_3(r)}{dr^2}+\frac{1}{r}\frac{df_3(r)}{dr}-2f_1(r)[(\kappa+1)f_2(r)+\kappa f_2^2(r)]=0 \quad [2.5]$$

where $r=\sqrt{y^2+z^2}$. Equation [2.3] is satisfied by $1/2\sqrt{2\kappa}\,r$.

Let us consider, however, a solution that is continuous on the symmetry axis. In general form, such a solution of Equation [2.3] is

$$f_1=Ap(Ar) \quad [2.6]$$

where A is an arbitrary constant and $p(r)$ is a particular solution. Let, for the sake of being definite, $p(0) = 1$. Obviously $p'(0) = 0$. The function $f_1(r)$ is simultaneously the particular solution of the homogeneous equation corresponding to [2.4]. From this we have

$$f_2(r)=\left\{B+4(\kappa+1)\int_0^r r^{-1}f_1^{-2}(r)\left(\int_0^r rf_1^3(r)dr\right)dr\right\}f_1(r) \quad [2.7]$$

where B is an arbitrary constant. For [2.5] we have

$$f_3(r)=2\int_0^r\frac{dr}{r}\left\{\int_0^r[(\kappa+1)f_2(r)+\kappa f_2^2(r)]f_1(r)\,rdr\right\} \quad [2.8]$$

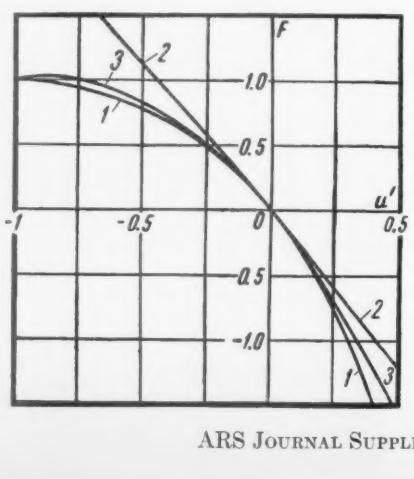

Translated from *Izvestiia Akademii Nauk SSSR, Otdelenie Tekhnicheskikh Nauk, Mekhanika i Mashinostroenie* (*Bull. USSR Acad. Sci., Div. Tech. Sci., Mechanics and Machine Building*), no. 4, 1959, pp. 140–141.

[1] Numbers in parentheses indicate References at end of paper.

The values for $p(r)$ and $p'(r)$ are best obtained by numerical interpolation of the equation with respect to the function

$$k(r) = f_1^{-2}(r) \qquad [2.9]$$

The function $p(r)$ is approximated quite closely by the function sec $(2.2335\ r)$. We obtain the wall of the nozzle by calculating the streamline

$$\frac{dr}{dx} = \frac{\varphi_r'}{1 + \varphi_x'} \qquad [2.10]$$

The sonic line passes through the origin for $B = 0$.

Calculations for $B = 0$ and $A = 1$ show that short transonic and subsonic sections have nozzles with ordinates $y \geq 0.2$ at $x = 0$.

On the symmetry axis we have in this case $\lambda = 1 + 2x$.

Reference

1 Yur'ev, I. M., "On Nozzle Design," *Prikladnaya Matematika i Mekhanika (Applied Math. and Mechanics)*, vol. 19, no. 1, 1955.

—Original received August 5, 1958

Reviewer's Comment

It is the opinion of the reviewer that the inclusion of the second-order term in Equation [1.4] is not necessary in considering nozzle flows in the throat region. However, in treating flow problems containing stagnation points, it would be necessary to use an equation such as Equation [1.4] for proper representation of the function F. Tomotika and Tamada (1) also have treated the problem, including a second-order term, for similar reasons, but the method given by Yur'ev here lends itself to easy numerical calculations.

G. V. R. Rao
Rocketdyne Division
North American Aviation, Inc

[1] Tomotika, S. and Tamada, K., "Studies on Two-Dimensional Transonic Flows of Compressible Fluid—Part III," *Quart. Appl. Math.*, vol. IX, no. 2, July 1951, pp. 129–147.

Calculation of the Heating of Shells at High Speeds

I. N. SOKOLOVA

The shell of an aircraft may become highly heated when flying at high speed. Thin metallic shells, thanks to the high heat conduction of the metal, rapidly heated throughout their thickness to an equal temperature. In nonmetallic shells, even thin ones, the heating is much slower than in metallic ones, and the temperature of the internal surface may be considerably different from that of the outer surface. The solution of the problem of heating such shells under nonstationary conditions involves considerable difficulty, since the connection between the heat flux inside the wall and the surface temperature must be determined from the heat conduction equation, an exact solution of which is difficult to obtain for arbitrary boundary conditions. An attempt is given to obtain an approximate solution of such a problem.

1 Statement of the Problem

WE CONSIDER the heating of a shell placed in a stream of gas of variable velocity, pressure and density. The inner surface of the shell is assumed to be thermally insulated. It is assumed that the heat flow along the surface can be neglected compared with the transverse flow, a condition that is satisfied when

$$\delta^*(d \ln k_n/dx) \ll 1$$

where

δ^* = the thickness of the shell
k_n = heat transfer coefficient
x = coordinate along the shell

In this case the problem becomes one-dimensional. We choose the origin on the external surface of the shell and direct the only spatial axis y from the outer into the inner surface. The temperature distribution over the thickness of the shell is determined by the heat conduction equation

$$\frac{\partial T}{\partial t} = k^* \frac{\partial^2 T}{\partial y^2} \qquad [1.1]$$

where

T = temperature
t = time
k^* = coefficient of heat conduction of the material

On the outer surface we have the condition of heat balance

$$k_n \rho_\infty U_\infty c_p (T^\circ - T_1) + \lambda^* (\partial T/\partial y)_{y=0} - \epsilon\sigma(T_1^4 - T_\infty^4) = 0 \qquad [1.2]$$

Translated from *Izvestiia Akademii Nauk SSSR, Otdelenie Tekhnicheskikh Nauk, Energetika i Avtomatica (Bull. USSR Acad. Sci., Div. Tech. Sci., Power and Automation)*, no. 3, 1959, pp. 90–94.

where

$\rho_\infty, U_\infty, T_\infty$ = density, velocity and temperature in the incoming stream
c_p = specific heat at constant pressure
T° = adiabatic wall temperature
T_1 = temperature of the outer surface
λ^* = coefficient of heat conduction of the material of the plate
σ = Stefan-Boltzmann coefficient
ϵ = emissivity coefficient

On the inner surface the condition of heat insulation is satisfied

$$(\partial T/\partial y)_{y=\delta^*} = 0 \qquad [1.3]$$

The initial condition is

$$T = T_0 \quad \text{at} \quad t = 0 \qquad [1.4]$$

The flow parameters M_∞, p_∞, ρ_∞ and T_∞ are arbitrary functions of time. The heat transfer coefficient k_n depends on the numbers M_∞ and R_∞, and on the structure of the boundary layer.

2 The Method of Parabolas

Since an exact solution of the equation of heat conduction, satisfying the foregoing boundary conditions, is very difficult to find, we shall try an approximate solution. The approximation will consist of replacing the actual temperature profile along the thickness of the wall by a parabolic profile

$$T = T_2 + [(T_1 - T_2)/\delta^{*2}](\delta^* - y)^2 \qquad [2.1]$$

(T_2 is the temperature of the internal surface), and of solving the equation of heat conduction in the mean. We integrate the equation of heat conduction over the thickness of the wall, substituting Equation [2.1] for the temperature, and obtain

$$\frac{dT_2}{dt} + \frac{1}{2}\frac{dT_1}{dt} = \frac{3k^*}{\delta^{*2}}(T_1 - T_2) \qquad [2.2]$$

In the heat balance equation, for the sake of simplicity, we linearize the radiated heat flux

$$T_1^4 - T_\infty^4 = 4T_\infty^3(T_1 - T_\infty) \qquad [2.3]$$

which makes for a somewhat excessive value for the sought temperature. After this simplification the equation of heat balance becomes

$$k_n\rho_\infty U_\infty c_p(T^\circ - T_1) - (2\lambda^*/\delta^*)(T_1 - T_2) = 4\epsilon\sigma T_\infty^3(T_1 - T_\infty) \qquad [2.4]$$

We introduce

$$\begin{aligned} A &= 3k^*/\delta^{*2} \\ V &= k_n\rho_\infty U_\infty c_p + 2\lambda^*/\delta^* + 4\epsilon\sigma T_\infty^3 \\ M &= -2\lambda^*/\delta^* \\ Q &= 4\epsilon\sigma T_\infty^4 + k_n\rho_\infty U_\infty c_p T^\circ \end{aligned} \qquad [2.5]$$

With this notation, Equations [2.2 and 2.3] become

$$MT_2 + NT_1 = Q \qquad \frac{d}{dt}\left(T_2 + \frac{1}{2}T_1\right) = A(T_1 - T_2) \qquad [2.6]$$

Introducing

$$z = T_2 + (1/2)T_1 \qquad [2.7]$$

the system [2.6] can be reduced to a single equation

$$\frac{dz}{dt} = A\left\{\frac{M+N}{(1/2)M - N}z - \frac{(3/2)Q}{(1/2)M - N}\right\}$$

the solution of which is found in quadratures

$$z = F(t)\left[\text{constant} - \frac{3}{2}A\int_{t_1}^{t}\frac{Q\,dt}{F(t)[(1/2)M - N]}\right]$$

$$\left(F = (t)\exp A\int_{t_1}^{t}\frac{M-N}{(1/2)M - N}\,dt\right) \qquad [2.8]$$

After determining z the quantities T_1 and T_2 are calculated from

$$T_1 = \frac{Mz - Q}{(1/2)M - N} \qquad T_2 = \frac{(1/2)Q - Nz}{(1/2)M - N} \qquad [2.9]$$

The constant in the expression for z is determined at a certain value $t = t_1$, different from 0. Near the start of motion, i.e., before the instant t_1 is reached, it is necessary to solve the problem by a somewhat different method. The point is that the profiles of the temperature at the initial period of motion are poorly approximated by a parabola extending over the entire thickness of the shell, since actually the wall is heated in a short time to a smaller depth than that given by a parabolic profile. Therefore in the first instant of motion the temperature must be determined by a more accurate method.

3 Method of Incomplete Parabolas

We shall approximate the temperature profile by means of a parabola not over the entire thickness of the wall δ^*, but only over a thickness $\delta(t)$, on the inner boundary of which $y = \delta(t)$ the condition $\partial T/\partial y = 0$ is satisfied.

Thus, we assume that the heat wave is propagated not instantaneously, but at a corresponding thickness $\delta(t)$ at each instant. Consequently, the temperature profile will have the form

$$T = T_0 + (T_1 - T_0)\{[\delta(t) - y]^2/\delta^2(t)\} \qquad [3.1]$$

As before, the equation of heat conduction will be solved in the mean. Integrating the equation of heat conduction from 0 to $\delta(t)$ and inserting the expression for T and for $(\partial T/\partial y)_{y=0}$, we get

$$\frac{d}{dt}[\delta(t)(T_1 - T_0)] = \frac{6k^*}{\delta(t)}(T_1 - T_0) \qquad [3.2]$$

subject to initial conditions [1.4].

In this equation the unknowns are $\delta(t)$ and T_1. They are determined by simultaneous solution of this equation and the equation of heat balance. We introduce the notation

$$\delta(t)(T_1 - T_0) = S \qquad [3.3]$$

Then the system of Equations [2.2 and 2.4] assumes the form

$$\frac{dS}{dt} = \frac{6k^*}{\delta(t)^2}S \qquad q\delta(t)^2 - [k_n\rho_\infty U_\infty c_p + 4\epsilon\sigma T_\infty^3]S\delta(t) - 2\lambda^* S = 0 \qquad [3.4]$$

where

$$q = k_n\rho_\infty U_\infty c_p(T - T_0) + 4\epsilon\sigma T_\infty^3(T_\infty - T_0) \qquad [3.5]$$

From a solution of this system we determine S and $\delta(t)$, and T_1 is determined from Equation [3.3]. The solution is carried out by this method up to the instant t_1, at which $\delta(t)$ becomes equal to the thickness of the wall δ^*.

The constant in the form [2.8] is determined at $t = t_1$ from the value $T_1(t_1)$

$$\text{constant} = T_0 + (1/2)T_1(t_1) \qquad [3.6]$$

4 Estimate of the Accuracy of the Approximate Solution

To estimate the accuracy of the foregoing approximate

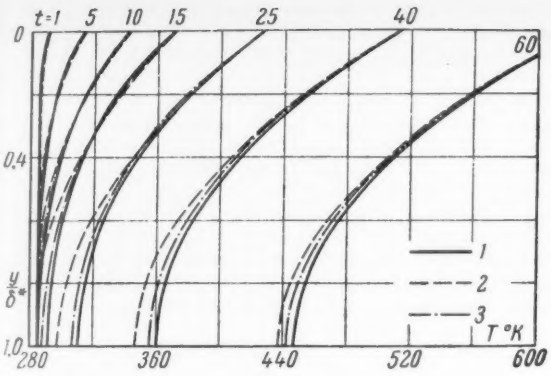

Fig. 1

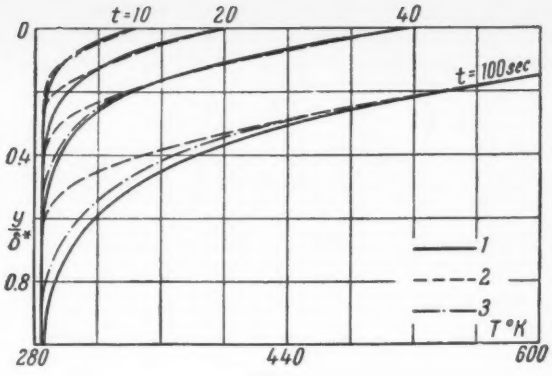

Fig. 2

solution for the heat conduction equation, let us compare the exact and approximate solutions obtained for particular specified boundary conditions.

a) The temperature of the external surface is specified in the form

$$T_1 = at + b \qquad [4.1]$$

The exact solution of the heat conduction equation, subject to such a choice of T_1, has the form

$$T = T_1 - \frac{16a\delta^{*2}}{k^*\pi^3} T_0 \sum_0^m \frac{1}{(2m+1)^3} \times \left[1 - \exp\left(\frac{-k^*(2m+1)^2\pi^2}{4\delta^{*2}} t\right)\right] \sin\frac{(2m+1)\pi y}{2\delta^*} \qquad [4.2]$$

The approximate solution for the same problem has the form

$$T = T_0\left[1 + \frac{a}{k^*}\left(\sqrt{4k^*t} - y\right)^2\right] \quad \text{for} \quad t < \frac{\delta}{4k^*} \qquad [4.3]$$

$$T = T_0\left\{1 + at - \frac{a\delta^{*2}}{2k^*} - \left(at_1 - \frac{a\delta^{*2}}{2k^*}\right) \exp\left[-\frac{3k^*}{\delta^{*2}}(t - t_1)\right] + \left[\frac{a\delta^*}{2k^*} + \left(at_1 - \frac{a\delta^{*2}}{2k^*}\right) \times \exp\left(-\frac{3k^*}{\delta^{*2}}(t - t_1)\right)\right] \frac{(\delta^* - y)^2}{\delta^{*2}}\right\} \quad \text{for} \quad t > \frac{\delta^{*2}}{4k^*} \qquad [4.4]$$

Figs. 1 and 2 show a comparison of the temperature profiles, calculated from the exact (curve 1) and approximate (curve 2, approximation by one parabola) equations for plates 30-mm thick, at values of k^* equal to 0.12 cm² per sec and 0.008 cm² per sec, and for the different values of t as indicated on these curves. The maximum discrepancy between the exact and approximate solutions amounts to approximately 7 per cent.

b) The temperature gradient is specified

$$\left.\frac{\partial T^*}{\partial y}\right|_{y=0} = f(t) \qquad [4.5]$$

In this case the exact solution of the heat conduction equation has the form

$$T(y,t) = T_0 - \frac{k^*}{\delta^*}\int_0^t f(t)dt - \frac{2k^*}{\delta^*}\sum_1^\infty \left\{\exp\left(-\frac{k^*n^2\pi^2}{\delta^{*2}} t\right)\int_0^t f(\xi)\exp\left(\frac{k^*n^2\pi^2}{\delta^{*2}}\right)d\xi\right\} \cos\frac{n\pi y}{\delta^*} \qquad [4.6]$$

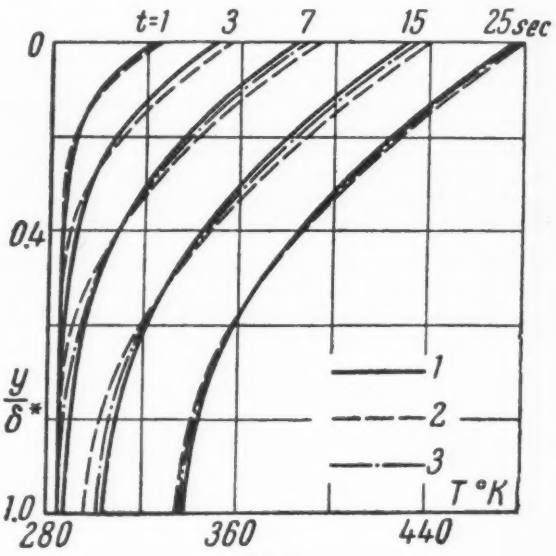

Fig. 3

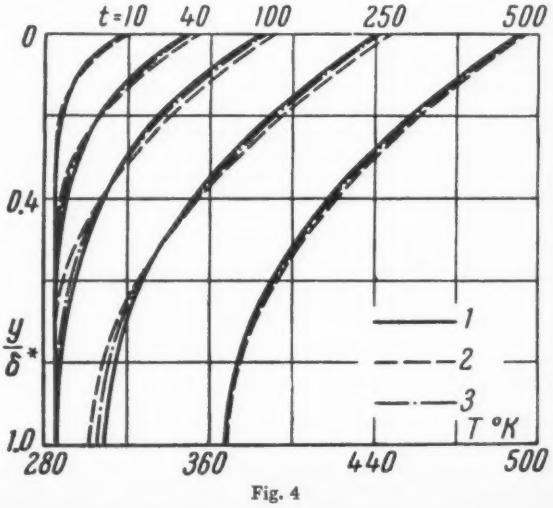

Fig. 4

For the sake of simplification, we put $f(t) = \text{constant} = B$. Then the exact temperature $T = T(y, t)$, after improving the convergence, becomes

$$T = T_0 + yB\left(1 - \frac{y}{2\delta^*}\right) - \frac{k^*Bt}{\delta^*} - \frac{B\delta^*}{3} + \frac{2\delta^*B}{\pi^2}\sum_1^\infty \frac{1}{n^2}\exp\left(-\frac{k^*n^2\pi^2}{\delta^*}t\right)\cos\frac{n\pi y}{\delta^*} \quad [4.7]$$

The corresponding approximate solution will be

$$T(y, t) = T_0 - \frac{B}{2\sqrt{6k^*t}}\left[\sqrt{6k^*t} - y\right]^2 \quad \text{for } t \leq \frac{\delta^{*2}}{6k^*} \quad [4.8]$$

$$T(y, t) = T_0 - \frac{k^*B}{\delta^*}(t - t_1) - \frac{B}{2\delta^*}(\delta^* - y)^2 \quad \text{for } t \geq \frac{\delta^{*2}}{6k^*} \quad [4.9]$$

Figs. 3 and 4 show a comparison of the exact and approximate solutions for the foregoing two plates: Curves 1 are for the exact solution, curves 2 are for approximation by one parabola. The error in this case does not exceed 4 per cent.

From a comparison of the exact and approximate solutions for particular types of boundary conditions, it can be assumed that the accuracy of the approximate method is of the same order of magnitude even for arbitrary boundary conditions.

Greater accuracy can be attained by approximating the temperature profile by two parabolas, each satisfying, in the mean, the equation of heat conductions at half the thickness $\delta(t)$. We choose the parabolas in the form

$$T^{(1)} = a_1 + b_1y + c_1y^2 \quad \text{for} \quad 0 \leq y \leq (1/2)\delta(t) \quad [4.10]$$

$$T^{(2)} = a_2 + b_2\left(y - \frac{1}{2}\delta(t)\right) + c_2\left(y - \frac{1}{2}\delta(t)\right)^2 \quad \text{for} \quad \frac{1}{2}\delta(t) \leq y \leq \delta(t) \quad [4.11]$$

The coefficients of the parabolas are determined from the boundary conditions and from the condition of the joining of the parabolas—the equality of the temperatures and their derivatives at $y = (1/2)\delta(t)$.

Let us use the previous examples to follow the variation in the accuracy in the case when the temperature profile is approximated by two parabolas.

Case a) $T_1 = at$

By solving the equations of heat conductions in the mean, we obtain at $t \geq \delta^{*2}/8k^*$

$$\Theta = (1/8)at \qquad \delta(t) = \sqrt{8k^*t} \quad [4.12]$$

where Θ is value of the temperature on the line where the parabolas join.

The temperature profiles are determined from the expressions

$$T^{(1)} = at\left[1 - \frac{3}{\sqrt{8k^*t}}y + \frac{5}{2}\frac{y^2}{8k^*t}\right]$$

$$T^{(2)} = \frac{1}{2}at\left[1 - \frac{y}{\sqrt{8k^*t}}\right]^2 \quad \ldots\ldots [4.13]$$

The unknown Θ and T_2 at $t \geq \delta^{*2}/8k^*$ are found by solving the heat conduction equation in the mean; we shall not give these expressions here because of their complexity. The expressions for the temperature profiles will be

$$T^{(1)} = T_1 + (8\Theta - 4T_2 - 4T_1)\frac{y}{\delta^*} + (4T_1 + 8T_2 - 12\Theta)\frac{y^2}{\delta^{*2}} \quad [4.14]$$

$$T^{(2)} = \Theta + (4T_2 - 4\Theta)\frac{y - (1/2)\delta^*}{\delta^*} + (4\Theta - 4T_2)\frac{[y - (1/2)\delta^*]^2}{\delta^{*2}}$$

Case b)

$$\left.\frac{\partial t}{\partial y}\right|_{y=0} = B \quad [4.15]$$

The approximate solution at $t \leq \delta^{*2}/9.6k^*$ yields in this case

$$\delta(t) = \sqrt{9.6kt} \qquad \Theta = -B\delta(t)/16.5 \quad [4.16]$$

The temperature profiles have the form

$$T^{(1)} = -B\delta(t)\left[0.3712 - \frac{y}{\delta(t)} + 0.7576\frac{y^2}{\delta^2(t)}\right]$$

$$T^{(2)} = -0.2424B\delta(t)[1 - y/\delta(t)]^2 \quad \ldots\ldots [4.17]$$

When $t \geq \delta^{*2}/9.6$

$$T^{(1)} = \left(2\Theta - T_2 - \frac{B\delta(t)}{4}\right) + By + \left[(4T_2 - 4\Theta)\frac{1}{\delta(t)^2} - \frac{B}{\delta(t)}\right]y^2$$

$$T^{(2)} = \Theta + (4T_2 - \Theta)\frac{y - (1/2)\delta(t)}{\delta(t)} + (4\Theta - 4T_2)\frac{(y - (1/2)\delta(t))^2}{\delta(t)^2} \quad \ldots\ldots [4.18]$$

Θ and T_2 are determined when $t \geq \delta^{*2}/9.6$ from the solution of the equations of heat conduction in the mean.

The temperatures, calculated from these formulas, are also shown in Figs. 1, 2, 3 and 4 (curves 3). The accuracy is considerably increased when approximation with two parabolas is used.

Original submitted Aug. 13, 1958

Reviewer's Comment

This paper represents an interesting application of an approximate technique of solving partial differential equations known as the integral method. In this type of approach the equation is satisfied in the mean, the mean being taken over a certain thickness variously called the boundary layer thickness or the thermal thickness, depending on the physical problem considered.

Von Karman (1) and Pohlhausen (2) originally developed the method. It was extended by Gruschwitz (3), and Wieghardt (4) applied it to the solution of the energy equation.

Most recently, it has been utilized in a series of papers by Goodman (5) in treating Stefan's problem (heat transfer at a moving boundary).

In the present paper, Sokolova has treated heat transfer with either a stationary or moving inner boundary. He finds that the use of two polynomials leads to greater accuracy than the use of a single polynomial (parabola). It would have also been interesting for the author to compare his two-parabola approach with the use of an exponential curve which also satisfies the boundary conditions.

Another extension of the present work, which would be of great interest, would be the specification of the environmental conditions ρ_∞ and T_∞, and the flight speed U_∞ as a function of time, rather than the boundary conditions [4.1] or [4.5] selected by the author.

—Sinclaire M. Scala
General Electric Co.

[1] von Karman, T., "Über laminare und turbulente Reibung," *Z. Angewandte Math. und Mech.*, vol. 1, 1921, translated as NACA TM 1092.

[2] Pohlhausen, J., "Zur naherungsweisen Integration der Differential gleichungen der laminaren Grenzschicht," *Z. Angewandte Math. und Mech.*, vol. 1, 1921, p. 252.

[3] Gruschwitz, E., "Die turbulente Reibungsschicht in ebener Strömung die Druckabfall und Druckansteig," *Ing. Arch.*, vol. 2, 1931, p. 321.

[4] Wieghardt, K., "Uber einen Energiesatz zur Berechnung laminaren Grenzschichten," *Ing. Arch.*, vol. 16, 1948, p. 231.

[5] Goodman, T. R., "The Heat Balance Integral and its Application to Problems Involving a Change of Phase," Trans. ASME, 1958, p. 335.

Analysis of Operation of Simplest Ramjet Combustion Chamber Under Flying Conditions

A. V. Talantov

Kazan' Aviation Institute

THE PARAMETERS at the inlet of a ramjet combustion chamber are subject to considerable variation in flight. The variations will be particularly strong for launching-type engines. The pressure and the temperature at the chamber inlet depend on the altitude and velocity of flight. In addition, under different control methods, the rate of flow into the chamber and the composition of the mixture do not remain constant. All this naturally influences the operation of the chamber and the heat release ratio.

In this paper we analyze the influence of flight conditions on the required dimensions of the combustion chamber. Such an analysis is made possible by the existence of equations that relate the principal combustion characteristics with the pressure, temperature, mixture composition and flow turbulence. These relations have been investigated essentially for combustion in a turbulent homogeneous mixture, in which the evaporation of the fuel and the mixing of the fuel vapor with the air are fully completed by the instant combustion begins. Such conditions occur at high temperatures at the chamber inlet, i.e., at high flight velocities ($M \geq 3$). However, even at lower temperatures (lower flight velocities), when the fuel does not have time to evaporate completely, it is also possible to use as a first approximation the equations for a homogeneous mixture, since they are quite close to the relations that hold for an inhomogeneous mixture.

Let us first establish the variation of the speed of flame propagation in a turbulent stream u_t and of the combustion time t, as functions of the pressure and temperature. Although the dependence of the speed of flame propagation and of the combustion time on the pulsational speed w' and on the normal speed u_n have by now been sufficiently well investigated, the influence of pressure and temperature has not been so well studied. We shall attempt to establish the influence of these factors, using the customary relations for the speed u_t and the time t.

In accordance with the theory of "surface" combustion and with experiment (1,2),[1] the speed of flame propagation in a turbulently flowing homogeneous mixture can be written

$$u_t = A \cdot w'^a u_n^{1-a} \qquad [1]$$

where

$A \approx 5.4$
$a = 0.6$ to 0.8

There are no indications in the literature concerning the dependence of the pulsational speed on the stream temperature (4). The normal speed is proportional to the 1.8 power of the temperature (3). In the range of moderate ratios of pulsational to normal speed, which is the range of practical interest (but at $w'/u_n > 1$), we can assume $a \approx 0.8$. Then

$$u_t \sim T^{0.4} \qquad [2]$$

This result is in satisfactory agreement with experiment (1,4).

The pressure dependence of u_t computed from Equation [1] is less than that found from experiment (4,5).

In accordance with (3 and 4), we can assume

$$u_n \sim p^{-0.25} \qquad w' \sim p^{0.25}$$

Then the pressure dependence on the speed of flame propagation in turbulent flow becomes

$$u_t \sim w'^{0.8} \qquad u_n^{0.2} \sim p^{0.25 \cdot 0.8} \qquad p^{-0.25 \cdot 0.2} \sim p^{0.15}$$

Translated from *Izvestiia Vysshych Uchebnykh Zavadenii MVO, Aviationnaya Tekhnika* (*Bull. Higher Institute of Learning, Aviation Engng.*), no. 2, 1959, pp. 122–133.

[1] Numbers in parentheses indicate References at end of paper.

On the other hand, experiment yields (4,5)

$$u_t \sim p^{0.5}$$

One cause for this disagreement is the damping of the turbulence behind the grids (4). As the pressure is reduced and the speed u_t is decreased, the flame becomes longer. Consequently the average value of the pulsational speed, which determines u_t, decreases, and this causes an increase in the exponent for p. In practice we frequently produce forced turbulization of the stream, and we shall therefore assume in our calculations the experimental value

$$u_t \sim p^{0.5} \qquad [3]$$

We estimate the combustion time from the following relation, which is theoretically derived (2)

$$t = B \frac{l_0}{w'} \ln\left(1 + \frac{w'}{u_n}\right) \qquad [4]$$

Here l_0 is the scale of turbulence.

This relation is in satisfactory agreement with the experimental data on the effects of l_0, w' and u_n at $B = 3$.

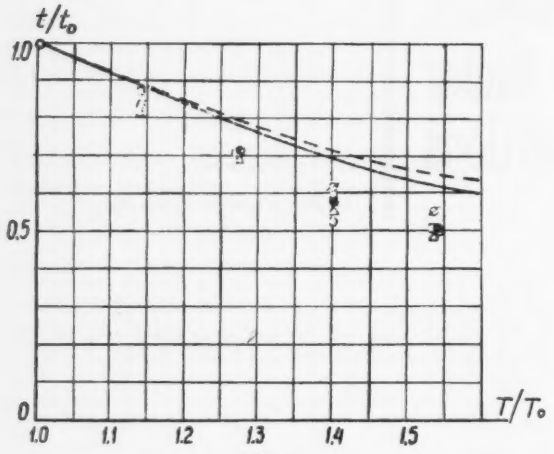

Fig. 1

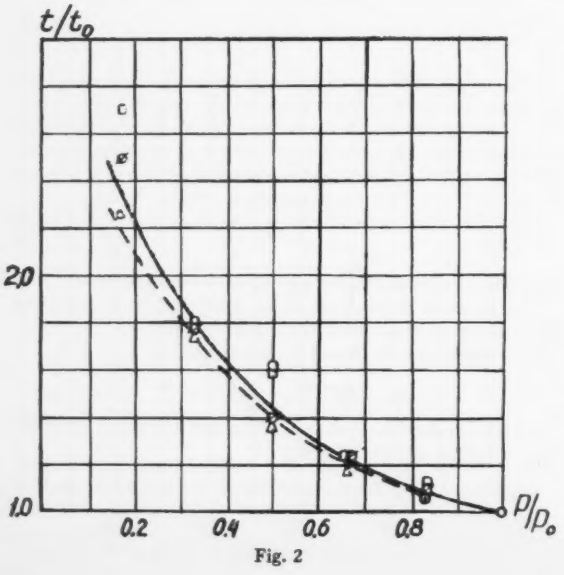

Fig. 2

If it is assumed that the pulsational speed and the scale of turbulence are independent of the temperature (4), then the dependence of the combustion time on the temperature, with allowance for the influence of the temperature on the normal speed, can be written

$$t = t_0 \cdot \frac{\ln\left[1 + \frac{w'}{u_{n_0}}\left(\frac{T_0}{T}\right)^{1.8}\right]}{\ln\left(1 + \frac{w'}{u_{n_0}}\right)} \qquad [5]$$

We shall compare this theoretical equation with the only experimental data known on this subject, namely those of Doroshenko and Nikitskii (4).

The points on Fig. 1 show the dimensionless values of the combustion time vs. the temperature. The curves represent the values calculated from Equation [5]. The solid line is for a pressure of 200 mm mercury, the dotted one for 600 mm mercury.

Thus, theory and experiment show that the combustion time decreases with increasing temperature. It is possible to use Equation [5] in approximate calculations.

In examining the pressure dependence of the combustion time it is necessary to take into account not only the influence of the pressure on the normal and pulsational speeds, but also on the turbulence scale (4)

$$l \sim p^{-0.5}$$

Taking all this into account, we can write for the combustion time

$$t = t_0 \cdot \left(\frac{p}{p_0}\right)^{-0.75} \frac{\ln\left[1 + \left(\frac{w'}{u_n}\right)_0 \left(\frac{p}{p_0}\right)^{0.5}\right]}{\ln\left[1 + \left(\frac{w'}{u_n}\right)_0\right]} \qquad [6]$$

The ratio of the combustion time to the initial time, calculated from Equation [6], as well as the results of the experiment of Doroshenko and Nikitskii (4), are plotted against the pressure ratio in Fig. 2. As in the case of the temperature dependence of the time, the curves differ little at various ratios of w'/u_n The solid line on the curve corresponds to a temperature of 373 deg abs, the dotted line is for 573 deg abs.

It is seen that both theory and experiment, which are in satisfactory agreement, evidence a rather intense increase in combustion time with decreasing pressure. We shall use Equation [6] in further calculations.

When the pressure and temperature change simultaneously with the mixture composition and the flow rate, the equation for the combustion time becomes

$$t = t_0 \cdot \left(\frac{p}{p_0}\right)^{-0.75} \cdot \left(\frac{w_0}{w}\right) \cdot \frac{\ln\left[1 + \left(\frac{w'}{u_n}\right)_0 \left(\frac{p}{p_0}\right)^{0.5} \left(\frac{T_0}{T}\right)^{1.8} \left(\frac{w}{w_0}\right) \cdot \left(\frac{u_{n\alpha_0}}{u_{n\alpha}}\right)\right]}{\ln\left[1 + \left(\frac{w'}{u_n}\right)_0\right]} \qquad [7]$$

Here, as before, the subscript zero pertains to initial values, for which the initial time t_0 was determined, and u_{n_α} and $u_{n_{\alpha_0}}$ are the normal speeds at the current and initial values of α. This equation is correct only when the effect of each factor is independent of the remaining parameters.

The foregoing equations make it possible to calculate the length that the combustion chamber must have in order for the process to be completed in it.

To calculate the first component X_1 of the chamber length, from the edge of the stabilizers to the place where the flames join, we can use a system of equations similar to that given in (6). To simplify the calculations we shall assume, in addition to the other assumptions made in that paper, that

the flame is infinitesimally thin. The system of equations is then written in the following form:

Equation of conservation of energy for a fresh mixture

$$\tau_m = 1 - \frac{k-1}{2} M_0^2(u_m^2 - 1) \qquad [8]$$

where

τ_m, u_m = dimensionless temperature and speed of fresh mixture, referred to the corresponding parameters at the chamber inlets

M_0 = Mach number at the chamber inlet

Adiabatic equation for the fresh mixture

$$\tau_m = \pi^{(k-1)/k} \qquad [9]$$

where π is the pressure in the section under consideration divided by the pressure at the chamber inlet.

Equation of conservation of energy for the flow of combustion products

$$\tau_p = \lambda_p - \frac{k-1}{2} M_0^2(u_p^2 - 1) \qquad [10]$$

where

τ_p, u_p = dimensionless temperature and speed of combustion products

λ_p = $1 + q/c_pT_0$

q = heat supplied per kg of air

Equation of conservation of mass

$$\frac{\pi}{\tau_m} u_m(1 - \eta) + \frac{\pi}{\tau_p} u_p\eta = 1 \qquad [11]$$

where η is the dimensionless ordinate of the flame front, referred to half the gap between stabilizers.

Momentum equation

$$\frac{\pi}{\tau_m} u_m^2(1 - \eta) + \frac{\pi}{\tau_p} u_p^2\eta = 1 + \frac{1}{kM_0^2}(1 - \pi) \qquad [12]$$

Equation for the fraction of heat liberated

$$r = (\pi/\tau_p)u_p\eta \qquad [13]$$

Equation of conservation of mass of fresh mixture for two neighboring sections, $i - 1$ and i, in converted form

$$\Delta\bar{X} = \sqrt{\left\{r\frac{(\pi/\tau_m)_{i-1}(1 - \eta_{i-1})u_{mi-1} - (\pi/\tau_m)_i(1 - \eta_i)u_{mi}}{[(\pi/\tau_m)_{i-1} + (\pi/\tau_m)_i]\bar{u}_t}\right\}^2 - (\eta_i - \eta_{i-1})^2} \qquad [14]$$

Here

$\bar{u}_t = w_t/w_0$ = dimensionless speed of flame propagation, referred to the speed at the chamber inlet

$\Delta\bar{X}$ = dimensionless distance along the axis between neighboring sections $i - 1$ and i, referred to half the gap between stabilizers

It is also possible to use the approximate relation

$$\tau_p/\tau_m = \lambda_p \qquad [15]$$

These equations are sufficient to determine the unknown values of π, u_m, u_p, τ_m, τ_p, η, r and $\Delta\bar{X}$, one of which serves as the independent variable.

The calculation is best carried out in the following sequence. We first find the dependence of the dimensionless ordinate η and of the other parameters on the combustion coefficient r. Then we use Equation [14] to calculate the value of $\Delta\bar{X}$, which when summed yields $\bar{X}_f$.

The second component X_s of the chamber length, from the point of joining of the flame fronts to the completion of combustion, can be found by integrating the equation of motion of the mixture in the zone

$$dX = w_s \cdot dt$$

Here w_s is the rate of displacement of the mixture in the zone.

This rate is usually variable and a function of the heat liberation and—the burnup (r) in the zone. An exact calculation of X is possible by means of a procedure detailed in (6). Taking into account the fact that in this case the main variation of the parameters is in the axial direction, and neglecting the change in the parameters in the transverse direction, we can determine X approximately by considering the problem as one-dimensional. The rate of flow in this zone can be written in this case as

$$w_s = w_0[1 + r(\theta - 1)]$$

where $\theta = T_c/T_0$ is the ratio of the combustion temperature to the temperature at the entrance to the zone. This equation for the rate takes into account only the density changes due to combustion; the compressibility is disregarded and the formulation of the problem is hydrodynamic.

The distance X becomes

$$X = \int_0^t w_0[1 + r(\theta - 1)]dt$$

Here r is a function of time. The form of this function is given in (2) as

$$r = 3\left(1 + \frac{u_n}{w'}\right)^3\left[\frac{1}{3}(1 - e^{-3t/t_z}) - \frac{1}{1 + w'/u_n}(1 - e^{-2t/t_z}) + \frac{1}{(1 + w'/u_n)^2}(1 - e^{-t/t_z})\right] \qquad [16]$$

where $t_z = l_0/w'$ is the characteristic time. Inserting r and integrating we get

$$X = w_0t + 3w_0(\theta - 1)\left(1 + \frac{u_n}{w'}\right)^3 t_z \times \left[\frac{1}{3}\left(\frac{t}{t_z} + \frac{1}{3}e^{-3t/t_z} - \frac{1}{3}\right) - \frac{1}{1 + w'/u_n} \times \left(\frac{t}{t_z} + \frac{1}{2}e^{-2t/t_z} - \frac{1}{2}\right) + \frac{1}{(1 + w'/u_n)^2}\left(\frac{t}{t_z} + e^{-t/t_z} - 1\right)\right] \qquad [17]$$

The total length of the combustion zone can be obtained from this expression by putting $t = t_p$

$$X_3 = Bw_0\frac{l_0}{w'}\ln\left(1 + \frac{w'}{u_n}\right) + 3Bw_0\frac{l_0}{w'}(\theta - 1) \times \left(1 + \frac{u_n}{w'}\right)^3\left\{\frac{1}{3}\left[\ln\left(1 + \frac{w'}{u_n}\right) + \frac{1}{3[1 + (w'/u_n)]^3} - \frac{1}{3}\right] - \frac{1}{1 + (w'/u_n)}\left[\ln\left(1 + \frac{w'}{u_n}\right) + \frac{1}{2[1 + (w'/u_n)]^2} - \frac{1}{2}\right] + \frac{1}{[1 + (w'/u_n)]^2}\left[\ln\left(1 + \frac{w'}{u}\right) + \frac{1}{[1 + (w'/u_n)]} - 1\right]\right\} \qquad [18]$$

Experiment yields that B is equal to 3. Knowledge of the path X covered by the hot mixture (Eq. [17]) and the knowledge of the burnup r (Eq. [16]), as functions of the time make it also possible to calculate the heat liberated along

the length, $r = f(X)$. The burnup is found to be quite sluggish in the final portion, where a change in the coefficient of heat liberation r from 0.95 to 1 requires approximately the same distance as a change of r from 0 to 0.95. In real chambers it is therefore useless to strive for complete heat liberation in the final portion at the expense of considerably lengthening the chamber, for in the final analysis, the losses produced thereby will offset any gain from the increased heat liberation.

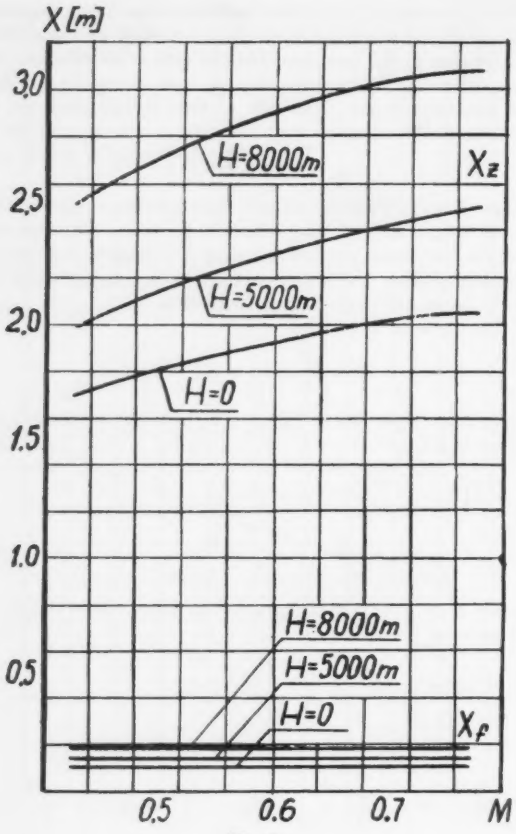

Fig. 3

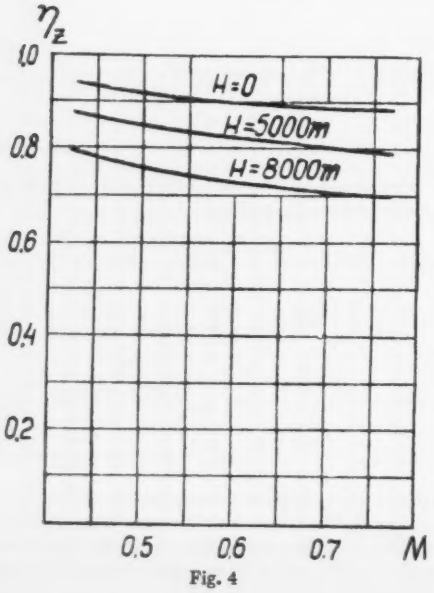

Fig. 4

We used the foregoing procedure and the derived equations to calculate the combustion process in ramjet engine chambers.

One of the objects of calculation was a subsonic ramjet engine with nonadjustable transition sections, operating at altitudes from 0 to 8000 m in the range of $M = 0.4$ to 0.8. The characteristic distance l between stabilizers was taken to be 40 mm, the degree of turbulence $\epsilon = 0.1$, the turbulence scale $l_0 = 0.5$ cm. The fuel was gasoline and the mixture composition stoichiometric. The parameters of the mixture entering into the combustion chamber were calculated by the procedure customarily used in engine theory.

Fig. 3 shows the required lengths X_f and X_z as functions of the rate of flow (Mach number) for 0, 5000 and 8000 m.

An examination of the results obtained makes it possible to draw the following conclusions.

The principal portion of the chamber, for a chosen size of gap between stabilizers, is the combustion zone. The actual distance from the section through the stabilizers to the point of joining of the flame fronts is less than 10 per cent of the total length of the flame. Consequently, in those cases when no great accuracy is required, this quantity can be neglected to simplify the calculations. It is appropriate to emphasize the need for a thorough investigation of the combustion time in turbulent stream, in contrast with the heretofore preferred investigation of the rate of flame propagation.

In accordance with the preceding, the dependence of the total length of the combustion chamber on the altitude and on the flying speed are determined essentially by the combustion time. As the flight speed is increased, the temperatures and the pressure at the inlet to the chamber increase, and this should lead to a reduction in the required length. This does not happen, however, owing to the increase in speed of flow through the engine, including the chamber inlet, with increasing Mach number.

The required chamber dimensions are greatly influenced by the change in flying altitude. As this altitude increases the combustion conditions are substantially worse; the length of the chamber for complete combustion increases.

It is easy to determine the coefficient of completeness of heat liberation in the chamber if its actual length is specified and the variation of burnup along the length of the chamber is known. Fig. 4 shows the dependence of completeness of heat liberation η_z for the engine under consideration, for a chamber 1.3 m long. The resultant relations are in satisfactory agreement with the actual variation of η_z with altitude and with Mach number.

We also used the procedure developed here to calculate the dimensions of a combustion chamber for engines operating at higher speeds, $M = 1$ to 4, and at altitudes from 0 to 20,000 m.

It must be borne in mind that these results were obtained not for one particular engine operating under different conditions, but for a series of engines, each designed for its own operating mode.

The coefficient of speed at the chamber inlet was assumed to be 0.2 for all modes with the exception of $M = 1$, where $\lambda = 0.15$. The coefficient of pressure recovery σ in the system of steps at the inlet to the engine was assumed to have values of 1, 0.9, 0.7 and 0.5 for $M = 1$, 2, 3 and 4, respectively. The composition of the mixture was assumed stoichiometric. The turbulence scales were 0.5 and 1 cm; the degree of turbulence ϵ was 0.1.

The results of calculations are shown in Figs. 5–8. One of the interesting results of the calculation is that in the region of $M = 4$, owing to the high temperatures and large pressures at the chamber inlet, the rate of flame propagation becomes equal to the flow rate and even exceeds it. These results are reliable only to the extent that the foregoing relations, obtained for small pressures and moderate temperatures, can be extended to include large pressures and high temperatures.

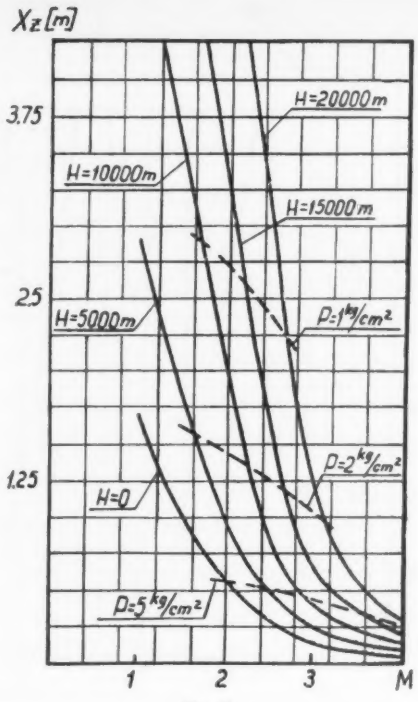

Fig. 5

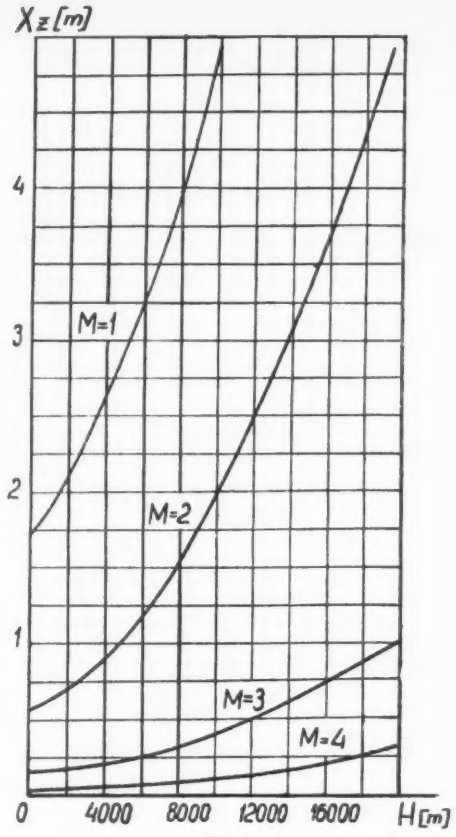

Fig. 6

A direct experimental verification of these relations in this region has not yet been made. It is possible that the velocity u_t and the combustion time t will not obey the foregoing relations because of processes that may occur in the mixture of high temperatures prior to ignition. Equally valid is the assumption that owing to the high temperatures the principal process whereby heat is supplied to the chamber under these conditions ($M \geq 4$) is self-ignition, rather than flame propagation. However, with all this, one can expect the parameters of the combustion chamber to be of the same order of magnitude, and in any case not worse than those obtained in the foregoing calculations.

At $M = 1$ or 2, the size of the initial section X_f is relatively small. Thus, for supersonic engines, as for subsonic ones, it is possible to neglect in approximate calculations the length of the initial section (before joining of the flame fronts).

The value of the combustion time and the corresponding required chamber length for a supersonic engine depend very strongly on the flying altitude and speed. The length of the chamber decreases with increasing Mach number. The effect of the flying speed is explained by the increased temperature and pressure at the inlet to the chamber, which lead to a reduction in the combustion time. A certain increase in the speed of the stream entering the chamber at constant λ, contributing to a lengthening of the zone, does not exert a decisive influence. However, the dependence of the required length of the combustion chamber on the flying speed could actually be somewhat weaker. The point is that, at a constant amount of heat delivered per kilogram of mixture, the relative heat delivery decreases with increasing flying speed and consequently with increasing stagnation temperature. By virtue of this, the maximum possible speed coefficient at the chamber inlet increases, and, if the maximum is reached, this leads to a lengthening of the zone (the other parameters remaining constant) and to a slowing down in the rate of decrease of chamber length with increasing flying speed. In the subsonic region, an increase in flying speed leads to a slight increase in the stagnation temperature and pressure; the increase in the speed of the stream entering the chamber exerts the decisive influence, and the chamber length increases with increasing flying speed.

As the flying altitude is increased, the required chamber dimensions increase because of the drop in temperature and pressure.

From an examination of the curves of Figs. 5 and 6 it follows that to design a ramjet engine that operates satisfactorily in the subsonic region ($M \leq 1$) at altitudes greater than 10 km, serious difficulties are encountered from the point of view of effecting combustion with ordinary fuels. The required length of the combustion chamber under these conditions will be measured in meters, which will lead to large energy losses and to an excessive increase in the structure weight.

It must be borne in mind that the foregoing required chamber lengths are calculated for complete heat liberation, including the final stagnant section of the burnup. The turbulence scale in these calculations, equal to 0.5 or 1 cm, is not the minimum for real chambers. Consequently, the length obtained must be considered only as the upper limit.

It is interesting to determine the change in the necessary longitudinal dimensions of a combustion chamber for engines having an identical pressure at the chamber inlet. The point is that for identical specific rated wing load in horizontal flight, the pressure in a ramjet combustion chamber will have approximately the same value for different altitudes and flying speeds. Therefore, for real engines, intended to fly under different conditions, the pressure in the chamber still changes insignificantly. The dotted curve of Fig. 5 is drawn through

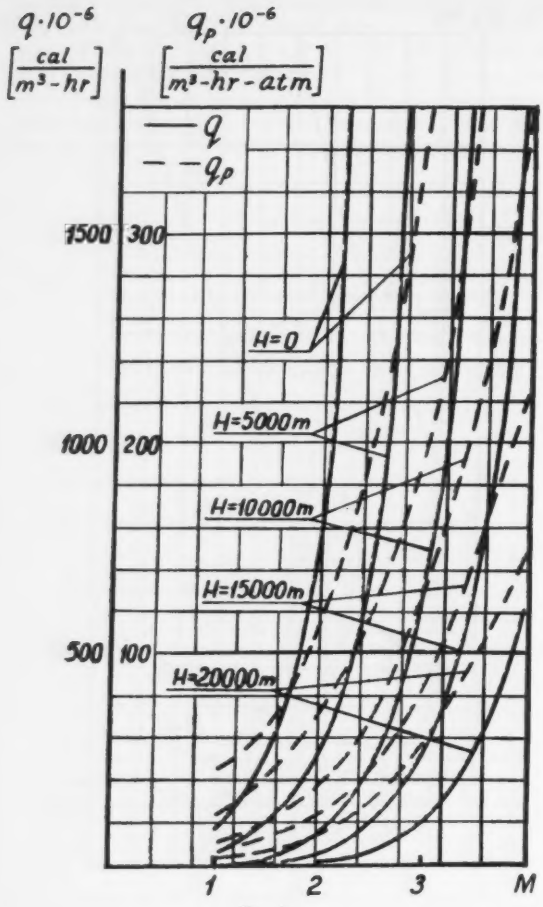

Fig. 7

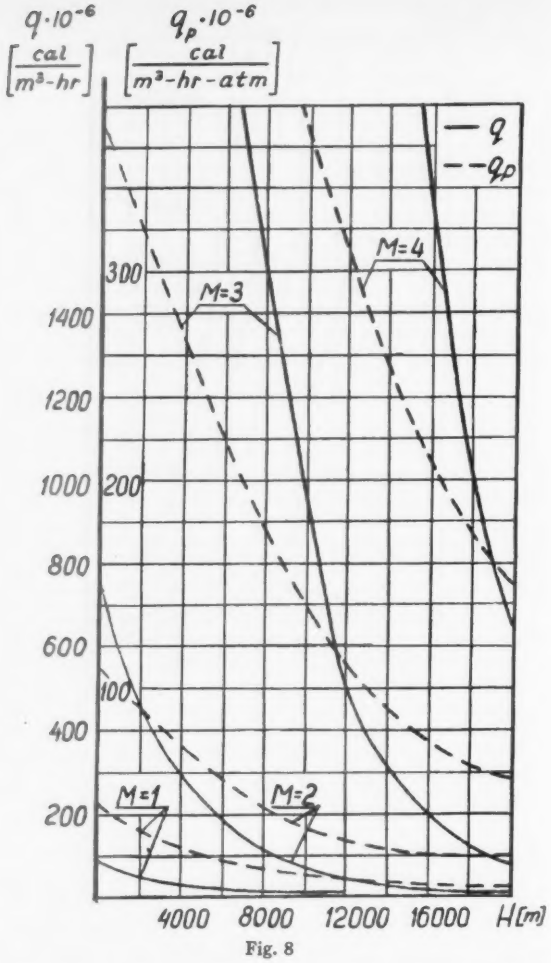

Fig. 8

the points for chamber pressures of 1, 2 and 5 atm. It is seen that the necessary chamber dimensions change little at constant pressure. As the altitude is increased and as the flying speed is increased, the condition that the pressure be maintained constant necessitates some reduction in the dimensions of the chamber. This is explained by the increase in temperature at the combustion chamber inlet, leading to a reduction in the combustion time, in spite of the increase in flow speed w. If one assumes $w \sim \sqrt{T}$ (at constant λ), and if the dependence of time on temperature is taken in accordance with Equation [5], then the length of the combustion zone, proportional to the product of the velocity and the time, will obey the following law

$$X_z \sim wt \sim \sqrt{T} \cdot \ln\left[1 + \frac{w'}{u_n} \cdot \left(\frac{T_0}{T}\right)^{1.3}\right]$$

It is easy to verify that as the temperature increases X_z decreases. The dependence of the total heat release rate q and of the space heating rate per atmosphere q_p on altitude and flying speed are shown in Figs. 7 and 8. What is striking is the exceedingly strong dependence of q and q_p on the flying conditions, their decrease with increasing altitude, and their increase with increasing flight speed. The dependence of the total heat release rate on the flying speed may be even stronger, if the increase of λ at the chamber inlet, noted previously, takes place. An increase in the flow rate at the chamber inlet leads to a proportional increase in the heat delivered to the chamber; lengthening of the zone is not decisive in this case. The total heat release rate q under certain conditions reaches hundreds of millions and billions of cal/m³-hr, which becomes comparable to the heat release rate in liquid fuel engines. The space heating rate per atmosphere reaches hundreds of millions of calories.

What is interesting is not only the values of the mean space heating rate but also the space heating rate per atmosphere change with the flying conditions. This indicates that the method used to design chambers for an average value of q is defective, even if one takes for q its value per atmosphere.

The analysis performed makes possible several recommendations toward improving the parameters of the process in the chamber under fixed flight conditions.

In accordance with the foregoing, we propose that the factor determining the chamber length is the combustion time, which obeys Equation [4]. The value of t is affected by the normal and pulsational speeds and by the turbulence scale. For chambers operating with stoichiometric mixtures of ordinary hydrocarbon fuels, such as gasoline, kerosene and others, there is no possibility of forced operation by increasing the normal speed. At the same time, one cannot exclude the use of new fuels, which yield substantially greater values of normal speed, or the use of additives to the fuel so as to increase the normal speed.

In the case when the speed coefficient λ in the chamber is quite different from the maximum possible one, an increase in this coefficient makes it possible to increase the calorific value somewhat. A certain possibility of forcing is contained also in an increase of the pulsational speed by insertion of specially selected turbulizing grids.

One opportunity, so far not used, for forcing the chamber is to reduce the turbulence scale. This can be done by inserting

suitable grids of thin rods. It is desirable to install the grids as close as possible to the combustion zone, so as to avoid damping of the turbulence with increasing distance from the grids, i.e., an increase in the scale and a decrease in the pulsational speed.

References

1 Vlasov, K. P. and Inozemtsev, N. N., "Influence of Initial Parameters of Flow on the Velocity of Propagation of the Flame of Homogeneous Fuel-Air Mixtures," *Izvestiia Vyshikh Uchebnykh Zavedenii, "Aviatsionnaya tekhnika"* (*News of the Higher Institutions of Learning, "Aviation Engineering"*) 1959, no. 5.

2 Talantov, A. V., "Investigation of Combustion in a Turbulent Flow of a Homogeneous Gas Mixture," Trudy MAP (Trans. of the Ministry of Aviation Industry), 1955, no. 8.

3 Inozemtsev, N. N., "Use of Normal Speed of Flame Propagation of Fuels," *Izvestiia Vyshikh Uchebnykh Zavedenii, "Aviatsionnaya tekhnika"* (*News of the Institutions of Higher Learning, "Aviation Engineering"*) 1955, no. 4.

4 Doroshenko, V. E. and Nikitskii, A. I., "Investigation of the Effect of Pressure and Temperature on the Process of Turbulent Combustion of a Homogeneous Fuel-Air Mixture," Trudy MAP (Trans. of the Ministry of Aviation Industry), 1956, no. 2, p. 182.

5 Gol'denberg, S. A. and Pelevin, V. S., "Effect of Pressure on the Velocity of Propagation of a Flame in Turbulent Flow," *Issledovaniya protsessov goreniya* (Investigation of Combustion Processes) USSR, Academy of Sciences, 1958.

6 Talantov, A. V., "Principles of Design of Simplest Principles of Calculation of Simplest Ramjet Combustion Chamber," *Izvestiia Vyshkh Uchebnykh Zavedenii, "Aviatsionnaya tekhnika"* (*News of Institutions of Higher Learning, "Aviation Engineering"*) 1958, no. 2.

Reviewer's Comment

The results of Talantov's calculations are qualitatively correct, although the degrees of some of the effects noted in the figures are questionable with respect to real engines. For example, in the flight speed range between Mach 3 and Mach 4, the engine will be getting into the spontaneous ignition regime, particularly at the lower altitudes where stagnation pressures and temperatures are higher for a given flight speed. (For altitudes above the isothermal range, i.e., above 26,000; M, temperatures again rise.) In such engines, it is a poor assumption that the combustion chamber will receive a homogeneous mixture, or even a good distribution of liquid fuel at the combustor inlet, because the fuel injectors should be placed close to the flameholders to prevent premature burning. Significant lengths, relative to the X_c's shown, will be required simply for fuel distribution and mixing of burned and partially burned parcels of gas in order to obtain reasonable engine efficiencies. Hence the engine lengths shown for the Mach 3 to 4 range in Fig. 5 and 6 are inordinately small, and the statement that "... the (combustion chamber) length obtained must be considered only as the upper limit" is incorrect for these high speed engines.

With respect to the theoretical bases for the analysis, there are questions with regard to the assumptions employed for both the flame spreading length and the subsequent burnup length. The effects of temperature and pressure on turbulent flame velocity used by Talantov are presumably based on experiments with *open* or burner-type turbulent flames. Although the reviewer did not have access to the references cited by Talantov, the relationships for the effect of pressure on U_t quoted are similar to those presented by Goldenberg and Pelevin (1) and Khramtsov (2), both of whom employed open flames. On the other hand, Scurlock (3) found little effect of approach stream turbulence on spreading rate of *confined* turbulent flames such as we must consider in a ramjet combustor. Scurlock and others have shown that a large part of the turbulence in confined flames is due to shear between burned and unburned gas flows in two regions: Immediately behind the flameholder the unburned mixture moves faster than the recirculating burned gas, and downstream of this piloting recirculation zone the situation is reversed as the burned gas accelerates. Further, Markstein (4) points out that for flames in ducts the "noise" mode of generation of random disturbances (due to pressure oscillations) may have a larger effect than shear flow disturbances. Thus for ramjet flames there is little connection between the local turbulence scale and intensity in either burning region and the turbulence parameters of the combustor inlet flow.

Another point with regard to flame spreading is that experiments have shown that the flame spreading begins toward the rear end of the recirculation zone, the length of which could be of the same order as the calculated flame spreading length when practical sized flameholders are used. This would be important for the higher flight speeds; the temperature ratio λ, which influences the shear generated turbulence mentioned in the foregoing is smaller.

For the second, or burnup region treated by Talantov, this reviewer wonders what Talantov has used for normal burning velocity, U_n, in Equations (16–18). Since all of the material reaching this region has already traversed the turbulent flame front, it is both hotter than T_0 and diluted with reaction products. For such material, U_n is probably 2 to 6 times that for the unburned mixture at room conditions (5). The same reservations regarding suitable values of turbulence characteristics for this region apply as noted in the foregoing for the flame spreading region.

Spalding (6) has proposed that, for the high flow velocities of practical interest in ramjet design, the length required for flame spreading in a duct may be determined largely by entrainment of unburned gas into the hot gas jet which commences behind the recirculation zone. This approach leads to the conclusions that an axial length of 3 to 5 duct widths (or flameholder spacing widths) must be allowed for flame spreading and that little can be done to alter this required length; for example, the analysis suggests that preheating (e.g., from higher flight speed) leads to greater lengths because of the reduction in λ.

Thus the reviewer believes that the results of this paper should be considered only for the purpose of predicting qualitative trends for ramjet length requirements, which have already been established by development experience. Probably of more value are papers such as Spalding's (6) which stimulates thought on new theoretical approaches to the conventional ramjet problem, and papers challenging the experimentalist or designer to conceive new higher output designs for ramjets such as the one by Avery and Hart (7), which dealt with maximum attainable heat release rates in hypothetical combustors with instantaneous mixing of unburned and burning gas.

In spite of the foregoing comments, however, it is encouraging to find papers such as Talantov's which attempt to make practical use of some of the large mass of data from bunsen burner flame studies.

—Gordon L. Dugger
Applied Physics Laboratory
The Johns Hopkins University

1 Goldenberg, S. A. and Pelevin, V. S., "Influence of Pressure on Rate of Flame Propagation in Turbulent Flow," in "Seventh Symposium (International) on Combustion," Butterworths Scientific Publications, London, 1959, p. 590.

2 Khramtsov, V. A., "Investigation of Pressure Effect on the Parameters of Turbulence and on Turbulent Burning," in "Seventh Symposium (International) on Combustion," Butterworths Scientific Publications, London, 1959, p. 609.

3 Scurlock, A. C., "Flame Stabilization and Propagation in High-Velocity Gas Streams," Meteor Rep. 19, Fuels Research Lab., MIT, 1948. *See also* Williams, G. C., Hottell, H. C. and Scurlock, A. C., in "Third Symposium (International) on Combustion," Williams and Wilkins, Baltimore, 1949, p. 21.

4 Markstein, G. H., comment in "Seventh Symposium (International) on Combustion," Butterworths Scientific Publications, London, 1959, p. 634.

5 Dugger, G. L., Weast, R. C. and Heimel, S., "Effect of Preflame Reaction on Flame Velocity of Propane-Air Mixtures," in "Fifth Symposium (International) on Combustion," Reinhold Publishing Corp., New York, 1955, p. 589.

6 Spalding, D. B., "Theory of Rate of Spread of Confined Turbulent Pre-Mixed Flames," in "Seventh Symposium (International) on Combustion," Butterworths Scientific Publications, London, 1959, p. 595.

7 Avery, W. H. and Hart, R. W., "Combustor Performance with Instantaneous Mixing," *Ind. Engng. Chem.*, vol. 45, 1953, p. 1634.

Puncture Problem at Cosmic Velocities

M. A. LAVRENT'EV

IT IS known from the theory of cumulative charges that the mechanism of puncturing of metallic plates by cylinders or by balls differs greatly at 3–10 km/sec from the mechanism at velocities up to 1000 m/sec. Two stages take place at high velocities: a—The ball or cylinder, penetrating into the obstacle, flows over the surface of the punched-out crater; b—inertial expansion of the cavity takes place after the "bullet has been annihilated." The first part can be calculated with sufficient accuracy by using an ideal incompressible liquid as a model, but the calculation of the second part is more difficult, although the results available indicate that the principal difficulties can be overcome. The computational schemes yield good agreement with experiment.

Much less investigated is the puncturing problem at 50–100 km/sec; the experimental difficulties at such velocities require particular caution as regards the main hypothesis made in the theory of each phenomenon.

As far as I know, the literature contains only one paper devoted to this problem—that of K. P. Stanyukovich on the formation of the moon's craters and on the determination of the momentum imparted by a falling meteorite. On the basis of his computation, Stanyukovich advances the hypothesis that as a ball drops, its kinetic energy is converted into potential energy of the gas into which it is converted by the impact; assuming further a few less clearly defined hypotheses, he arrives at the following conclusions:

1 The momentum acquired by the struck body is proportional to the energy of the incident body.

2 The volume of the crater is also proportional to the energy.

In the present note I propose an incompressible-medium model for which the calculations can be carried out to conclusion. My deductions do not agree with those of Stanyukovich.

1 One-Dimensional Case

We start with a consideration of the one-dimensional case, when the model is particularly simple. We consider impact between a plate of thickness a, flying at a velocity v_0, against the end of a cylinder (rod) of length l. The thickness a will be assumed much smaller than l. The problem consists of determining the momentum which the rod acquires as a result of the impact.

We assume the striking plate to be incompressible and absolutely hard. The rod is considered as a limiting case of a set of absolutely hard infinitesimally thin platelets, placed infinitely close to each other. During an inelastic impact between the striking plate and the first platelet of the rod, the momentum is conserved and kinetic energy will be lost as a result of the increase of the mass. This will continue as each succeeding platelet goes into motion. Let us now calculate, for the limiting case, the distribution of the kinetic energy loss in the system along the rod.

Thus, let a rod of length x be set into motion and let v be the velocity of this piece; as a plate of thickness dx is set into motion, the change in velocity dv should satisfy the relation

$$x dv + v dx = 0$$

from which we obtain after integration, noting that $v = v_0$ when $x = a$

$$v = v_0(a/x)$$

Let us calculate now the unknown kinetic energy loss

$$E = (1/2)xv^2$$

We have

$$dE = (1/2)v^2 dx + xv dv = -(1/2)v^2 dx = -(1/2)v_0^2 \left(\frac{a}{x}\right)^2 dx = -E_0 \frac{a}{x^2} dx$$

where

$$E_0 = -(1/2)av_0^2$$

is the initial energy of the striking plate. Assuming that the entire energy lost is converted into heat, we obtain the following distribution of heat along the rod

$$T = -\frac{dE}{dx} = E_0 \frac{a}{x^2}$$

Let us now denote by T_0 the minimum heat density necessary to vaporize the rod material. From this we find that the impact vaporizes the portion of the rod $0 < x < x_0$, where the unknown x_0 is found from the relation

$$T_0 = E_0(a/x_0^2)$$

As the vapor expands it separates from the rod, while the remaining portion of the rod acquires a momentum I. Let us calculate I, for the case of greatest interest, when

$$a \ll x_0 \ll l$$

and the energy going into vaporization is small compared with the initial energy of the striking plate. We can assume here that the entire energy of the gas goes into kinetic energy. We obtain for the velocity of the gas cloud

$$x_0 V^2 = av_0^2 \qquad V = \sqrt{(a/x_0)}v_0$$

Our problem has reduced to a purely gasdynamic problem. We confine ourselves now to only very rough calculations in two cases.

1 We make an additional assumption that all the scattered particles of the gas cloud acquire an identical velocity V, and then

$$x_0 V^2 = av_0^2 \qquad V = \sqrt{(a/x_0)}v_0$$

obtaining finally for the momentum

$$I = x_0 V = \sqrt{ax_0}v_0 = av_0^{3/2}$$

2 The second extreme case we consider is one in which each layer dx of the gas cylinder scatters (along the x direction) independently of the other elements. Then the gas element dx, located at a distance x from the end, yields a momentum

$$V dx = \sqrt{2T}\, dx = \sqrt{2E_0 a}\, (dx/x)$$

Translated from *Iskusstvennye Sputniki Zemli* ("Artificial Earth Satellites"), No. 3, USSR Acad. Sci. Press, Moscow, 1959, pp. 61–65.

From this we obtain for the unknown momentum

$$I = Sx_0 V dx = \sqrt{2E_0 a}\,\log\frac{x_0}{a} = \sqrt{2}\,av_0\log\frac{v_0}{\sqrt{T_0}}$$

2 Three-Dimensional Case

Let us now perform a calculation analogous to the preceding one for the case when a ball strikes a hemispherical plate of radius R. For this computation we must schematize the model still further. We assume that the action of the ball on the plate reduces to an impact of a spherical layer on the ball against a spherical cavity in the plate. All the velocities of the points of the striking layer are directed along the radii, and the velocity distribution coincides with the corresponding distribution in an incompressible liquid: The velocity v at a point located at a distance r from the center of the layer is determined from the formula

$$v = v_0(a/r)^2$$

where a is the radius of the internal cavity of the striker; v_0 the velocity of the points of this cavity. Let ka be the radius of the external surface of the striker. The medium is represented by a model similar to that considered in the linear formulation, namely that the medium is a set of infinitesimally thin spherical layers of an ideal incompressible liquid, located infinitesimally close to each other. As a result of the impact of the striker, its mass will start increasing as called for by the inelastic-impact scheme; as the mass increases, the momentum is conserved, and the kinetic energy of the system is converted into heat.

Let us perform the calculation. We determine first the radial momentum during the instant when the zone of motion in the medium is a hemisphere of radius r; let in this case the radial velocity of the internal surface of the striker be $\omega = \omega(r)$, then

$$\omega(ka) = v_0 \qquad [1]$$

Since the medium is incompressible, the velocity v at a point located at a distance x from the center will be

$$v = \omega(a/x)^2$$

From this we obtain for the momentum

$$I = \int_a^r 4\pi x^2\omega(a/x)^2 dx = 4\pi\omega a^2(r-a)$$

The condition that the momentum be constant yields

$$(r-a)d\omega + \omega dr = 0$$

$$\omega = C/(r-a)$$

where the constant C is determined from Equation [1]. Thus, finally

$$\omega = \frac{(k-1)a}{r-a}v_0 \qquad d\omega = -\frac{(k-1)a}{(r-a)^2}v_0 dr \qquad [2]$$

We now find the kinetic energy E under the same conditions

$$E = (1/2)\int_a^r 4\pi x^2\omega^2\left(\frac{a}{x}\right)^4 dx = 2\pi a^3\omega^2\left(1-\frac{a}{r}\right) \qquad [3]$$

From this we can obtain the distribution of heat T over the body. Then

$$T = -\frac{dE}{dr} = -4\pi a^3\omega\left(1-\frac{a}{r}\right)\frac{d\omega}{dr} - 2\pi a^4\frac{\omega^2}{r^2}$$

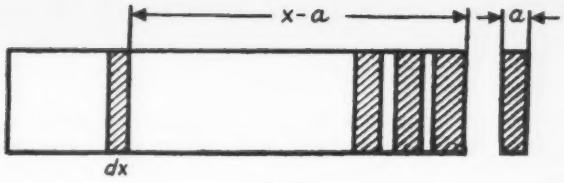

Fig. 1

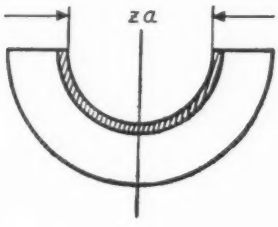

Fig. 2

or, taking Equation [2] into account

$$T = 4\pi a^3\omega\frac{r-a}{r}\cdot\frac{\omega}{r-a} - 2\pi a^4\frac{\omega^2}{r^2} = 4\pi a^5 v_0^2 \times \frac{(k-1)^2}{r(r-a)^2}\left[1-\tfrac{1}{2}\cdot\frac{a}{r}\right]$$

Denoting by E_0 the initial energy of the striker, we obtain

$$T = \frac{2(k-1)k}{r(r-a)^2}\left[1-(1/2)\cdot\frac{a}{r}\right]a^2E_0 \approx \frac{2k(k-1)}{r^2}a^2E_0$$

If we now assume that an amount of heat T_0 per unit volume is needed to vaporize the material, then as the ball strikes the body, there is formed in it a gas cavity of radius

$$\rho^3 = \frac{2k(k-1)}{T_0}a^2E_0 \qquad [4]$$

This cavity, defined by expression [4], will characterize the lower limit of the size of the funnel.

Let us now calculate the momentum acquired by the body. Again we consider the case when

$$a \ll \rho \ll R$$

and assume that a small part of the striker energy is consumed in vaporization of the foregoing mass of funnel. Denoting by V the velocity of the gas cloud that escapes from the funnel, we obtain

$$(2/3)\pi\rho^3V^2 = E_0 \qquad V = \sqrt{\frac{3E_0}{2\pi\rho^3}}$$

From this we obtain for the sought momentum I

$$I = (2/3)\pi\rho^3 V = AaE_0 \qquad A = \sqrt{\frac{4\pi}{3}\cdot\frac{k(k-1)}{T_0}}$$

It is interesting to note that in this scheme, the momentum depends greatly on the dimensions of the striking ball.

In analogy with the two-dimensional case, we can carry out the calculations in accordance with the second extreme scheme. Let us assume that each element dr of the spherical layer of gas scatters independently of the other elements and that the momentum imparted is directed along the normal to the spherical cavity.

The normal velocity V of the gas cloud due to an element dr of the spherical layer is determined from the energy balance

$$T = 2\pi r^2 V^2$$

If we now denote by α the angle between the symmetry axis and a line joining the center of the sphere with the element of the gas, then the component $J = dI/dr$ of the momentum along the symmetry axis due to the scattering of a ring of width $rd\alpha$, α = const, will be

$$dJ = 2\pi r^2 \sin \alpha \cos \alpha V d\alpha$$

Hence

$$J = \pi r^2 V = \pi r^2 \sqrt{\frac{T}{2\pi}} \cdot \frac{1}{r} = \sqrt{\frac{\pi T}{2}}\, r \approx \pi \sqrt{2(k-1)}\, \frac{a^{5/2} v_0}{r^{1/2}}$$

Integrating the latter expression with respect to r, along the thickness of the gaseous portion of the body, we obtain

$$I = B\,(k-1)^{4/3}\, T_0^{-1/6} a^{20/9} v_0^{4/3}$$

where B is a numerical constant.

Reviewer's Comment

Lavrent'ev has made a novel and useful contribution to the literature on theoretical prediction of hypervelocity cratering. He does not, however, compare his approach with that of Öpik (1), Grimminger (3), Rostoker (4), or Bjork (5); but notes simply that his results are different from those of Stanyukovich (2). A thorough review of cratering theories [of more ambitious scope than Allison's paper (6)], together with the correlation with experimental results, now abundantly available in the U. S. literature, would be most welcome at this time.

In the opinion of this reviewer, Bjork's treatment (5) of the hypervelocity impact process is the most satisfactory, having required the fewest assumptions. Bjork neglects the strength of the materials; but working with their equations of state at high pressures and densities, he applies the hydrodynamic equations to yield a complete picture of the positions of all particles and shock fronts at each instant in time during the cratering process. Correlation of his predictions with results of cratering experiments is good.

—MURRAY KORNHAUSER
General Electric Co.

[1] Öpik, E., "Researches on the Physical Theory of Meteor Phenomena," *Publications* de L'Observatoire Astronomique de L'Universite de Tartu, Tome XXVIII, no. 6, 1936.

[2] Stanyukovich, K. P., and Fedynskiy, V. V., "O Razrushitel'nom Deystvii Meteorituykh Udarov" (The Destructive Action of Meteorite Impacts), *Doklady Akad. Nauk SSSR*, vol. 57, nol 2, 1947, pp. 129–132; Technical Intelligence Translation ATIC-262907, ASTIA AD no. 24240.

[3] Grimminger, G., "Probability That a Meteroite Will Hit or Penetrate a Body Situated in the Vicinity of the Earth," *J. Appl. Phys.*, vol. 19, Oct. 1948, pp. 947–956.

[4] Rostoker, N., "The Formation of Craters by High-Speed Particles," *Meteoritics*, vol. 1, no. 1, 1953, pp. 11–27.

[5] Bjork, R. L., "Effects of a Meteorid Impact on Steel and Aluminum in Space," submitted to 10th Internatl. Astronaut. Congress, London, Aug. 28, 1959.

[6] Allison, F. E., "A Review of the Theories Concerning Crater Formation by Hypervelocity Impact," Proc. Third Symposium on Hypervelocity Impact, vol. 1, Feb. 1959.

Concerning the Problem of the Influence of Internal Degrees of Freedom of Particles on the Transport Coefficients of a Multicomponent Mixture of Gases

E. V. SAMUILOV

THE HEAT conduction coefficients of shear and bulk viscosity of gases can be calculated by the methods of kinetic theory. For monatomic gases the kinetic theory gives good agreement between the theoretical formulas and the experimental data. Subject to a suitably chosen potential of interaction between the molecules at ordinary temperatures, the theoretical results can also be applied successfully to the calculation of the coefficient of shear viscosity of polyatomic gases. However, the coefficient of heat conduction contains terms which cannot be obtained from the theory of monatomic gases. This was first demonstrated by Eucken. For monatomic gases the bulk viscosity is connected with the shear viscosity by the well-known Stokes equation. This equation does not hold for polyatomic gases. An analysis of the influence of the internal degrees of freedom of particles on the kinetic coefficients was carried out earlier by many investigators. Leontovich (1)[1] solved in general form the Boltzmann equation as applied to the propagation of small disturbances

Translated from *Fizicheskaya Gazodinamika* ("Physical Gasdynamics"), USSR Acad. Sci., pp. 59–69.

[1] Numbers in parentheses indicate References at end of paper.

in a gas at rest for the case $\omega \ll \tau$, where ω is the frequency of propagation of the disturbances in the gas and τ is the relaxation time for energy exchange between the translational and internal degrees of freedom of the particles. The solution was carried out by the Hilbert method for a continuous spectrum of the values of the internal energy. Wang Chang and Uhlenbeck (2), using the Enskog formalism, obtained the transport coefficients in general form, in terms of the effective scattering cross sections, for a discrete spectrum of values of the internal energy. However, they did not calculate the transport coefficients directly.

Pidduck (3) calculated the kinetic coefficients, using the model of "rough" spheres. Ishida (4) solved the Boltzmann equation for "solid ovaloids." Jeans (5) used "loaded spheres" as his molecule model. However, these papers have one common shortcoming. The diameters for elastic scattering, which can be strictly calculated on the basis of quantum-mechanical collision theory, were replaced by various artificial mechanisms for the transfer of energy from the internal degrees of freedom of the particles to the translational degrees of freedom.

In this paper we use the probabilities of various types of molecular collisions, obtained quantum-mechanically by various investigators. The system of generalized kinetic equations is solved by the Enskog method (6).

The system of integro-differential equations for the distribution function f_i of the components of the gas, with allowance for the internal degrees of freedom of the particles, has the following form

$$\frac{\partial f_i}{\partial t} + \mathbf{c}_i \cdot \frac{\partial f_i}{\partial \mathbf{r}} = \sum_{j,\ \epsilon_j,\ \epsilon'_i,\ \epsilon'_j} \int (f'_i f'_j - f_i f_j) K(\epsilon_i \epsilon_j \rightarrow \epsilon'_i \epsilon'_j) g_{ij} b db d\varphi d\mathbf{c}_j \quad [1]$$

where

f_i = $f_i(\mathbf{r}, \mathbf{c}_i, \epsilon_i, t)$
f'_i = $f'_i(\mathbf{r}, \mathbf{c}'_i, \epsilon'_i, t)$
$\mathbf{c}_i, \epsilon_i$ = velocity and internal energy of ith particle before collision
$\mathbf{c}'_i, \epsilon'_i$ = same values after collision
$\mathbf{r}$ = radius vector
t = time
$\mathbf{g}_{ij}$ = $\mathbf{c}_i - \mathbf{c}_j$
g_{ij} = $|\mathbf{g}_{ij}|$
b = collision parameter
φ = azimuth angle
$K(\epsilon_i, \epsilon_j \rightarrow \epsilon', \epsilon'_j)$ = probability of collision of two molecules with a change of the values of ϵ_i or ϵ_j to ϵ'_i or ϵ'_j

For given values of g_{ij}, ϵ_i, and ϵ_j, K satisfies the normalization condition

$$\sum_{\epsilon'_i,\ \epsilon'_j} K(\epsilon_i, \epsilon_j \rightarrow \epsilon'_i, \epsilon'_j) = 1$$

The equilibrium distribution functions $f_i^{(0)}$ have the following form

$$f_i^{(0)} = n_i \left(\frac{m_i}{2\pi kT}\right)^{3/2} e^{-\frac{m_i C_i^2}{2kT} - \frac{\epsilon_i}{kT}} \left(\sum_{\epsilon_i} e^{-\frac{\epsilon_i}{kT}}\right)^{-1} \quad [2]$$

where

n_i = number of particles of ith kind per unit volume
m_i = mass of ith particle
$\mathbf{C}_i$ = velocity of molecule of ith kind relative to local mean mass velocity of gas, $\mathbf{c}_0$.

$$\mathbf{C}_i = \mathbf{c}_i - \mathbf{c}_0$$

The local mean mass velocity is determined as follows

$$\mathbf{c}_0 = \frac{1}{\rho} \sum_i n_i m_i \bar{\mathbf{c}}_i$$

where

ρ = gas density, $\rho = \sum_i n_i m_i$
$\bar{\mathbf{c}}_i$ = mean velocity of the molecules of the ith kind in the laboratory system of coordinates

In agreement with the Enskog method, we assume that the distribution functions f_i do not depend explicitly on the time, but they are functionals of the macroscopic parameters of the medium, which vary with time. In the presence of small gradients of the macroscopic parameters, the distribution functions f_i at each point deviate slightly from the local equilibrium functions f_i^0. In the first approximation

$$f_i = f_i^{(0)}(1 + \Phi_i) \quad [3]$$

where Φ_i is a function of $\mathbf{C}_i$, ϵ_i and of the macroscopic parameters of the medium. In Equation [3], $f_i^{(0)}$ coincides with Equation [2] if the following normalization conditions are observed for the mean number of particles of each kind per unit volume, for the mean mass velocity, and for the temperature

$$n_i = \sum_{\epsilon_i} \int f_i^{(0)} d\mathbf{c}_i \quad [4]$$

$$\rho \mathbf{c}_0 = \sum_{j,\ \epsilon_j} \int m_j \mathbf{c}_j f_j^{(0)} d\mathbf{c}_j \quad [5]$$

$$\frac{3}{2} nkT + \sum_{j,\ \epsilon_j} \int n_j \epsilon_j e^{-\frac{\epsilon_j}{kT}} \left(\sum_{\epsilon_j} e^{-\frac{\epsilon_j}{kT}}\right)^{-1} = \sum_{j,\ \epsilon_j} \int E_j f_j^{(0)} d\mathbf{c}_j \quad [6]$$

Here

$$\sum_{j\epsilon_j} \int f_j^{(0)} \Phi_j d\mathbf{c}_j = 0 \quad [7]$$

$$\sum_{j,\ \epsilon_j} \int m_j \mathbf{c}_j f_j^{(0)} d\mathbf{c}_j = 0 \quad [8]$$

$$\sum_{j,\ \epsilon_j} \int E_j f_j^{(0)} \Phi_j d\mathbf{c}_j = 0 \quad [9]$$

In Equations [4 to 9] we have

$$n = \sum_i n_i \qquad E_i = \frac{m c_i^2}{2} + \epsilon_i$$

Inserting Equation [3] into [1] we obtain

$$f_i^{(0)} \left\{ \left[\frac{E_i}{kT} - \frac{\bar{E}_i}{kT} - 1 \right] \mathbf{C}_i \cdot \frac{\partial \ln T}{\partial \mathbf{r}} + \frac{n}{n_i} \mathbf{C}_i \cdot \mathbf{d}_i + \left[\frac{m_i}{kT} \mathbf{C}_i \mathbf{C}_i + \left(\frac{E_i}{kT} - \frac{\bar{E}_i}{kT} - 1 \right) \frac{kn}{\sum_j n_j C_{vj}} U \right] : \frac{\partial}{\partial \mathbf{r}} \mathbf{c}_0 \right\} = n_i \sum_j n_j I_{ij} (\Phi_i + \Phi_j) \quad [10]$$

where

$$n_i \sum_j n_j I_{ij} (\Phi_i + \Phi_j) \equiv - \sum_{j,\ \epsilon_j,\ \epsilon'_i,\ \epsilon'_j} \int f_i^{(0)} f_j^{(0)} (\Phi_i + \Phi_j - \Phi'_i - \Phi'_j) K dO_j$$

In the derivation of the left part of [10] we use the Maxwell transport equations, and also the condition that Φ_i is small. In Equation [10]

$$\bar{E}_i = \frac{3}{2} kT + \sum_{\epsilon_i} \epsilon_i e^{-(\epsilon_i/kT)} \left(\sum_{\epsilon_i} e^{-(\epsilon_i/kT)} \right)^{-1}$$

$$dO_j = g_{ij} b db d\varphi d\mathbf{c}_j$$

Here U is the unit tensor, $(\partial/\partial\mathbf{r})\mathbf{c}_0$ is the tensor whose components are the first row and first column, for example, are respectively

$$\frac{\partial u_0}{\partial x} \quad \frac{\partial v_0}{\partial x} \quad \frac{\partial w_0}{\partial x} \quad \text{and} \quad \frac{\partial u_0}{\partial x} \quad \frac{\partial u_0}{\partial y} \quad \frac{\partial w_0}{\partial z}$$

u_0, v_0 and w_0 are projections of $\mathbf{c}_0$ on the x, y and z axis respectively; $U\colon (\partial/\partial\mathbf{r})\mathbf{c}_0$ is the biscalar product of the tensors U and $(\partial/\partial\mathbf{r})\mathbf{c}_0$ and

$$\mathbf{C}_i \cdot \frac{\partial}{\partial \mathbf{r}} = U_i \frac{\partial}{\partial x} + V_i \frac{\partial}{\partial y} + W_i \frac{\partial}{\partial z}$$

$$\mathbf{d}_i = \frac{\partial}{\partial \mathbf{r}} \frac{n_i}{n} + \left\{\frac{n_i}{n} - \frac{n_i m_i}{\rho}\right\} \frac{\partial p}{\partial \mathbf{r}}$$

Also p is the thermodynamic pressure; p equals nkT.

The left half of the integral Equation [10] depends linearly on the gradients of the macroscopic parameters of the medium, and therefore Φ_i should have the form

$$\Phi_i = -\mathbf{A}_i \cdot \frac{\partial \ln T}{\partial \mathbf{r}} - B_i\colon \frac{\partial}{\partial \mathbf{r}} \mathbf{c}_0 + \frac{n^2}{\rho k T} \sum_{j \neq i} \frac{m_i m_j}{n_i} \mathbf{D}_{ij} \cdot \mathbf{d}_j \qquad [11]$$

where

$$\begin{aligned} \mathbf{A}_i &= \mathbf{C}_i A_i(C_i, \epsilon_j) \\ B_i &= \mathbf{C}_i{}^0\mathbf{C}_i B_i{}^{(1)}(C_i) + U B_i{}^{(2)}(C_i, \epsilon_i) \\ \mathbf{D}_{ij} &= \mathbf{C}_i D_{ij}(C_i) \end{aligned} \qquad [12]$$

In Equations [11 and 12], B_i is a tensor and $\mathbf{C}_i{}^0\mathbf{C}_i$ is a tensor with a vanishing sum of diagonal components. For example, the components of the first row of the tensor $\mathbf{C}_i{}^0\mathbf{C}_i$ are $U_i - (1/3)C_i{}^2$, U_iV_i, and U_iW_i. Inserting Equation [11] into [10] and equating the right and left side terms at $d \ln T/dr$, $(d/dr)c_0$, and d_j we obtain integral equations from which we can determine $\mathbf{A}_i$, B_i, and D_{ij}.

A total solution of the integral equations for $\mathbf{A}_i$, B_i, and D_{ij} can be obtained if detailed information is available on the probabilities of the various types of collisions of molecules; these probabilities are calculated from quantum-mechanical laws. Since the probabilities of the various types of collisions for the rotational degrees of freedom have still not been satisfactorily worked out, we shall consider here a gas with molecules that have only vibrational degrees of freedom in addition to the translational ones. It is known that as the temperature is increased, the first to be excited are the rotational levels of the molecules, and the vibrational levels follow. However, as will be explained below, certain results obtained for the vibrational degree of freedom can also be generalized to include the case of any internal degree of freedom and, in particular, for rotations. In addition, the results will be of practical interest if the magnitude of the kinetic coefficient is determined essentially by the translational-vibrational energy transitions in the collisions. Of the three kinetic coefficients mentioned in the foregoing, the bulk viscosity is indeed determined, under certain conditions, by these transitions.

We shall consider below the effect of the following type of molecule collisions on the kinetic coefficients:

1 Elastic collisions, occurring without a change in the vibrational quantum numbers v of the molecules. Elastic collisions of molecules will be described in terms of classical mechanics, using a spherically symmetrical interaction potential.

2 Elastic collisions, accompanied with a change in the numbers v by unity, i.e., collisions that lead to an exchange of vibrational energy quanta between molecules. This type of collision can occur only between molecules of the same kind. The probabilities of such collisions were calculated by Schwartz and Slawsky (7) who used the method of distorted waves, and are expressed in the following manner:

$$K(v, v_1 \to v'v'_1) = V^2(v_1 \to v')V^2(v_1 \to v'_1)(\pi m g_n/\alpha h)^2 \qquad [13]$$

where

$$V(v \to v \pm 1) = -\alpha h \left[\frac{v + (1/2) \pm (1/2)}{2\pi^2 m h \omega}\right]^{1/2}$$

$$V(v \to v) = 1$$

and

g_n = normal component of the colliding molecules
α = constant of the interaction potential between the molecules in the form $V_0e^{-\alpha r}$ (α can be chosen to fit the constants of the Lennard-Jones potential)

3 Inelastic collisions, accompanied by a change in the quantum numbers v of the molecules by unity. The probabilities of such types of collisions, according to Schwartz and Slawsky, are expressed in the following manner

$$K(v, v_1 \to v', v'_1) = V^2(v \to v')V^2(v_1 \to v'_1)[1/(16\pi^2)] \times (\theta^2 - \theta'^2)^2 \frac{(e^\theta - e^{-\theta})(e^{\theta'} - e^{-\theta'})}{(e^\theta + e^{-\theta} - e^{\theta'} - e^{-\theta'})^2} \qquad [14]$$

where

$$\theta = \frac{2\pi^2 m g_n}{\alpha h} \qquad \theta' = \frac{2\pi^2 m g'_n}{\alpha h}$$

Coefficient of Heat Conduction

The heat flux vector $\mathbf{q}$ is equal to

$$\sum_{j,\, v_j} \int f_j{}^{(0)} \Phi_j E_j \mathbf{C}_j d\mathbf{c}_j \qquad [15]$$

and is expressed in final analysis in terms of A_i and D_{ij}. The integral equation for A_i has the form

$$f_i{}^{(0)} \left(\frac{E_i}{kT} - \frac{\bar{E}_i}{kT} - 1\right) \mathbf{C}_i = ni \sum_{j,\, v_j} n_j I_{ij}(\mathbf{A}_i + \mathbf{A}_j) \qquad [16]$$

It can be shown that it is possible to solve Equation [16] by the Ritz variational method (8).

As is known, the Ritz method yields rapidly converging sequences of functions, and therefore when $\mathbf{A}_i$ is expanded in a series of known functions it is possible to retain merely the first terms of the expansion.

In accordance with the form of the left part of Equation [16], we rewrite $\mathbf{A}_i$ in the following form

$$\mathbf{A}_i = \left(a_i{}^{(1)} \frac{mC_i{}^2}{2kT} + a_i{}^{(2)} \frac{h\omega_i v_i}{kT} + a_i{}^{(3)}\right)\mathbf{C}_i$$

where the coefficients $a_i{}^{(k)}$ are determined, if Equation [16] is solved by the Ritz method, in the following manner. Inserting $\mathbf{A}_i$ into [16], taking the scalar product of the left and right halves of [16] successively with $(m_iC_i{}^2/2kT)\mathbf{C}_i$, $(h\omega_i v_i/kT)\mathbf{C}_i$ and $\mathbf{C}_i$, and summing and integrating the resultant equations over all possible v_i and $\mathbf{C}_i$, we obtain three linear equations for the coefficients $a_i{}^{(k)}$. We can obtain, analogously, $(3i–3)$ more equations. One of these is linearly dependent on the others. The lacking equation for the coefficients $a_i{}^{(k)}$ can be obtained from the normalization conditions [see Eq. 7 to 9]. Two of these [7 and 9], are automatically satisfied. The normalization Equation [8] establishes between the $a_i{}^{(k)}$ an additional dependence, which together with $(3i–1)$ equations obtained in the foregoing gives a complete system of equations for $a_i{}^{(k)}$.

To calculate

$$\sum_{vi} \int \mathbf{C}_i \cdot \frac{m_i C_i^2}{2kT} I_{ij}(\mathbf{A}_i + \mathbf{A}_j) d\mathbf{c}_i$$

$$\sum_{vi} \int \mathbf{C}_i \cdot \frac{\hbar\omega_i v_i}{kT} I_{ij}(\mathbf{A}_i + \mathbf{A}_i) d\mathbf{c}_i$$

$$\sum_{vi} \int \mathbf{C}_i I_{ij}(\mathbf{A}_i + \mathbf{A}_j) d\mathbf{c}_i$$

.....[17]

for the elastic collisions, we used the Lennard-Jones potential as the interaction potential. The elastic-collision integrals have also been tabulated for the Lennard-Jones function and are given in (9) in the form of effective temperature dependent scattering cross sections. These cross sections are denoted below by σ_i and $\sigma_{ij} = (\sigma_i + \sigma_j)/2$. For collisions of the second type, which give the correction terms in the expression for the heat conduction coefficient, we calculate the integrals of Equation [17] by using the model of a solid sphere with diameter σ_i and σ_{ij}. The terms that take into account the collisions of the third type in Equation [17] can be neglected, if the difference $\hbar\omega_i - \hbar\omega_j$ is not too small.

The system of $3i$ equations can be simplified by replacing the coefficients $a_i^{(3)}$ by $\delta_i^{(3)}$ in the following manner

$$a_i^{(3)} = \delta_i^{(3)} - \frac{5}{2} a_i^{(1)} - \frac{\bar{E}_{vi}}{kT} a_i^{(2)}$$

As a result of the substitution of $a_i^{(3)}$ the system of $3i$ equations for $a_i^{(k)}$ and $\delta_i^{(3)}$ assumes the following form

$$8n_iR_ia_i^{(1)} + \sum_{j \neq i} n_jR_{ij}\{Q_{ij}a_i^{(1)} + P_{ij}a_j^{(1)} + S_{ij}\delta_i^{(3)} + L_{ij}\delta_j^{(3)}\} = 15/4$$

$$a_i^{(2)}\left\{n_iR_i\left[1 - \frac{1}{\pi^2}\left(\frac{\alpha_i\hbar}{\hbar\omega_i}\right)^2 \frac{kT}{m_i}\right] + \sum_{j \neq i} n_jR_{ij}\right\} = \frac{3}{8}$$

$$\sum_{j \neq i} \{M_j^2 a_i^{(1)} + 2M_j\delta_i^{(3)} - M_i^2 a_j^{(1)} - 2M_i\delta_j^{(3)}\} = 0$$

$$\sum_j n_j\delta_j^{(3)} = 0$$

where

$$\begin{aligned}
R_i &= \sigma_i^2[(\pi kT)/m_i]^{1/2} \\
R_{ij} &= \sigma_{ij}^2[(2\pi kT)/(m_{ij}M_iM_j)]^{1/2} \\
Q_{ij} &= M_j(76M_iM_j + 55M_i^2 + 48M_j^2) - 5M_j(6M_j + 5M_i) \\
P_{ij} &= -M_i(87M_iM_j + 30M_i^2 + 30M_j^2) + 5M_i(5M_i + 6M_j) \\
S_{ij} &= 2M_i(6M_j + 5M_i) \\
L_{ij} &= -2M_i(5M_i + 6M_j) \\
M_i &= m_i/m_{ij} \\
M_j &= m_j/m_{ij} \\
m_{ij} &= m_i + m_j
\end{aligned}$$

In experiments one usually investigates the heat conduction of gases in the stationary state, i.e., for a zero average velocity of motion of the molecules of each kind. In order to calculate the value of the heat flux corresponding to the experimental conditions, we rewrite q in the following form

$$q = \sum_j n_j\bar{\mathbf{C}}_j[(5/2)kT - \bar{E}v_j) + \sum_{j,\,vj} \int f_j^0\Phi_j \times \left(E_j - \frac{5}{2}kT - \bar{E}_{vj}\right)\mathbf{C}_j d\mathbf{c}_j$$

Putting $\bar{C}_j = 0$, we get

$$\mathbf{q} = -\lambda \frac{\partial T}{\partial \mathbf{r}}$$

where $\lambda = \lambda_a + \lambda_b$ is the coefficient of heat conduction.

λ_a corresponds to the coefficient of heat conduction of a mixture of monatomic gases and is calculated in the ordinary manner (8).

λ_b is determined in terms of $a_i^{(j)}$

$$\lambda_b = \sum_i \frac{3}{8} n_i \frac{kT}{m_i} C^*_{vi}\left\{n_iR_i\left[1 - \frac{1}{\pi^2}\left(\frac{\alpha_i\hbar}{\hbar\omega_i}\right)^2 \frac{kT}{m_i}\right] + \sum_{j \neq i} n_iR_{ij}\right\}^{-1} \quad [18]$$

Here C^*_{vi} is the heat capacity of the internal degrees of freedom per molecule. The physical meaning of the terms that enter into the expression for λ can be readily interpreted using as an example a one-component gas, for which

$$\lambda = \frac{5}{2}\frac{\mu}{m}\frac{3}{2}k + nDC^*_v\left[1 + \frac{1}{\pi^2}\left(\frac{\alpha\hbar}{\hbar\omega}\right)^2 \frac{kT}{m}\right] \quad [19]$$

With

$$\lambda_a = \frac{5}{2}\frac{\mu}{m}\frac{3}{2}k$$

$$\lambda_b = mDC^*_v\left[1 + \frac{1}{\pi^2}\left(\frac{\alpha\hbar}{\hbar\omega}\right)^2 \frac{kT}{m}\right]$$

Here μ is the shear viscosity of the monatomic gas and D is the coefficient of self-diffusion (6). λ_a is determined only by elastic collisions of the first kind. Collisions of the second kind do not influence λ_a. The effect of inelastic collisions on the value of λ_a can be neglected because of the small probability of such collisions.

The value of λ_b, without the correction term, is determined only by the elastic collisions of the first kind and corresponds to the transfer of heat by self-diffusion of the excited molecules. The correction term in the expression for λ_b is due to elastic collisions of the second type. This correction is produced by the "relay" mechanism of heat transfer, through exchange of quanta of internal energy between the molecules during the collisions.

An equation similar to [19], without the correction for λ_b, was first given by Eucken in the following form

$$\lambda = \frac{5}{2}\frac{\mu}{m}\frac{3}{2}k + \mu\frac{C^*_v}{m} \quad [20]$$

Equation [20] differs from [19] without the correction for the mechanism of heat transfer by a constant factor in the second term

$$\frac{\rho D}{\mu} = 1.2.$$

Actually, Equation [20] was obtained under the assumption that the mean free paths of the molecule are the same for the transfer of momentum and internal energy. In the derivation of Equation [19] it is shown that when the collisions of the first and third types are neglected, the internal degrees of freedom contributes to λ through the diffusion mechanism of heat transfer. The correction term in λ_b in [19] retains its additive meaning when rotations of molecules are taken into account, provided the probabilities of inelastic collisions for rotations are small. Equation [18], without correction for the relay mechanism of heat transfer, represents a generalization of a formula of the Eucken type to include the case of a multicomponent mixture of gases, and can be used to calculate the coefficient of heat conduction with allowance for any arbitrary internal degrees of freedom, provided the probabilities of the collisions with change of internal state of particle are small.

Viscosity Coefficients

For a single component gas, the pressure tensor P equals

$$pU + \sum \int m\mathbf{CC}f^{(0)}\Phi d\mathbf{C} \qquad [21]$$

The correction term in Equation [21] is expressed in final analysis in terms of the tensor B. The integral equation for B has the form

$$f^{(0)}\left\{\frac{m}{kT}\,\mathbf{C^0C} = \left[\left(\frac{2}{3} - \frac{k}{C_v}\right)\frac{mC^2}{2kT} - \left(\frac{h\omega v}{kT} - \frac{\bar{E}_v}{kT}\right)\right]U\right\} = n^2 I(B) \qquad [22]$$

In accordance with the type of the left half of Equation [22], B can be written in the following manner

$$B = b_1\frac{m}{kT}\,\mathbf{C^0C} + \left(b_2\frac{mC^2}{2kT} + b_3\frac{h\omega v}{kT} + b_4\right)U$$

Using the normalization conditions [7 and 9], we can show that

$$B = b_1\frac{m}{kT}\,\mathbf{C^0C} + b_3\left[\left(\frac{h\omega v}{kT} - \frac{\bar{E}_v}{kT}\right) - \frac{C^*_v}{C_t}\left(\frac{mC^2}{2kT} - \frac{3}{2}\right)\right]U$$

To determine b_1, we insert B in Equation [22], take a biscalar product of the left and right halves of [22] with the tensor $(m/kT)\mathbf{C^0C}$, and sum and integrate the resultant equality over all v and $\mathbf{c}$. Since $\mathbf{C^0C}:U = 0$, the terms with b_3 drop out from the equation. The terms that take into account collisions of the second kind cancel each other out. Neglecting small corrections, which take into account collisions of the third type, we obtain

$$b_1 = \frac{15}{16}\frac{1}{n\sigma^2}\left(\frac{m}{\pi kT}\right)^{1/2}$$

To determine b_3 we multiply the tensor Equation [22] biscalarly with the unit tensor

$$\left[\left(\frac{h\omega v}{kT} - \frac{\bar{E}_v}{kT}\right) - \frac{C^*_v}{C_t}\left(\frac{mC^2}{2kT} - \frac{3}{2}\right)\right]U$$

and sum and integrate the expression term by term over all v and $\mathbf{c}$. Terms with b_1 drop out from the equation. The terms that take into account the collisions of the first and second type cancel each other out. As a result b_3 will be determined only by the inelastic collisions

$$b_3 = -\frac{1}{32\pi^{4.5}}\frac{C_t}{C_v}\left(\frac{1}{mkT}\right)^{1/2}\frac{1}{n\sigma^2}\left(\frac{\alpha^* h}{\hbar\omega}\right)^2\beta^{-1/2}\,e^{\beta - (h\omega/2kT)} \qquad [23]$$

where

$$\beta = 3\left[\frac{\pi^4(\hbar\omega)^2 m}{(\alpha^* h)^2 kT}\right]^{1/3} \qquad C_t = \frac{3}{2}k$$

α^* is a function of the temperature.

The expression for the pressure tensor, Equation [21], can be reduced to the form

$$P = nkTU - 2\mu\frac{\partial}{\partial\mathbf{r}}\mathbf{c}^0_0 - \zeta div\mathbf{c}_0 U$$

Here μ is the shear viscosity and ζ the bulk viscosity

$$\mu = nkTb_1 \qquad [24]$$

$$\zeta = -nkT(C^*_v/C_t)b_3 \qquad [25]$$

$(\partial/\partial\mathbf{r})\mathbf{c}^0_0$ is a symmetrical tensor, the sum of the diagonal components of which is zero.

The expression for μ coincides with the same expression as for a monatomic gas. Inasmuch as the probabilities of the collisions of third type are small up to dissociation temperatures, the influence of the vibrational degrees of freedom on the shear viscosity can be neglected. The rotational degrees of freedom, apparently, to modify Equation [24] to some degree at high temperatures.

The bulk viscosity ζ is determined only the elastic collisions. To explain the influence of rotations of molecules on the value of ζ at ordinary temperatures, it is possible to use the phenomenological theory of bulk viscosity, developed by Mandel'shtam and Leontovich (10). Since at ordinary temperatures the probabilities of inelastic collisions with simultaneous variation of both the vibrational and rotational state of the molecules are considerably less than the probabilities of inelastic collisions, in which either the vibrational or the rotational state of the molecule changes, we employ that part of the theory, in which the concepts developed by these authors are extended to include the case when the gas contains several relaxation processes, which are not interrelated to each other. It can be shown that when

$$\omega\tau_n \ll 1$$

where

τ_n = relaxation time of any relaxation process
ω = angular frequency of ultrasound

we have

$$\zeta = \frac{nk^2T}{C_t}\sum_n \tau_n\frac{C^*_n}{C_n} \qquad [26]$$

In Equation [26], C^*_n is the heat capacity of the internal degrees of freedom of the nth kind per molecule; C_n is equal to $C_t + C^*_n$.

It follows from Equation [26] that the bulk viscosity is made up additively of terms that characterize different relaxation processes. If the heat capacity of the vibrational degrees of freedom is not too small, and the relaxation time for the oscillations exceeds considerably the relaxation time for rotations, then ζ is determined in practice only by the inelastic collisions with change in the vibrational state of the molecules. At not too high temperatures, this holds for most gases.

The applicability of Equation [24] for different temperatures in addition to the foregoing remark, is restricted by the method with which the Boltzmann equation is solved and by the methods used to calculate the integrals through which b_3 is expressed.

The limits of applicability of Equation [25], from the point of view of the method used to solve the Boltzmann equation, are determined by the inequality

$$nkT \gg \zeta\, div\,\mathbf{c}_0 \qquad [27]$$

For the case of propagation of ultrasonic waves in a gas, condition [27] becomes

$$\zeta\omega \ll p$$

The limits of applicability of Equation [25] from the point of view of the methods used to calculate the integrals are determined as follows.

These integrals can be reduced to the form

$$J = \int_0^\infty\int_0^{\pi/2} e^{-(m/4kT)g^2}\varphi \pm (g_n)g^3\sin\psi\cos\psi d\psi dg$$

where

$$\varphi \pm = \frac{K(v, v_1 \rightarrow v \pm 1, v_1)}{V^2(v \rightarrow v \pm 1)}$$

After substituting x for $\cos\psi$ we obtain

$$J = \int_0^\infty \int_0^1 e^{-(m/4kT)g^2} \varphi \pm (gx) x dx dg$$

When going to the variables $y = gx$ and $x = t$, domain I of the (g, x) plane, bounded by the lines $g = g_1$, $g = g_2$, $x = 0$ and $x = 1$, is transformed into a domain in the (y, t) plane bounded by the rays $y = g_1 t$ and $y = g_2 t$ and the lines $t = 0$ and $t = 1$; we have

$$J_I = J_{II} + J_{III}$$

where J_I is the integral over domain I in the (y, x) plane; J_{II} is the integral in the region of the (y, t) plane bounded by the lines $y = g_1$, $x = 1$ and the ray $y = g_2 t$; J_{III} is the integral over the domain in the (y, t) plane bounded by the rays $y = g_2 t$, $y = g_1 t$, and the straight line $y = g_1$. Making the substitution $z = 1/t^2$ and $y = y$ in J_{II}, and going to the limits $g_1 \to 0$ and $g_2 \to \infty$, we obtain

$$J_{III} \to 0$$

$$J_{II} \to J = \frac{kT}{m} \int_0^\infty e^{-(m/4kT)y^2} \varphi \pm (y) dy$$

This integral was calculated by Schwartz (7) by the steepest descent method under the following assumption

$$e^{(2\pi^2 m)/(\alpha^* h)} \gg 1$$

$$\frac{m g_n^{*2}}{4} \gg h\omega \quad \text{or} \quad \frac{m g'^{*2}_n}{4} \gg h\omega \qquad \text{.....[28]}$$

where

$$g_n^* = \left(\frac{8\pi^2 kTh\omega}{\alpha^* hm}\right)^{1/3} \pm \frac{h\omega}{m}\left(\frac{8\pi^2 kTh\omega}{\alpha^* hm}\right)^{-1/3} \qquad [29]$$

$$\alpha^* = \frac{12}{r_0 D}\left[\frac{1}{2} + \frac{1}{2}(1 + D)^{1/2}\right]^{1/6} [1 + (1 + D)^{1/2} + D]$$

$$D = \frac{(m g_n^{*2}/4) + \epsilon}{\epsilon}$$

$$r_1 = r_0\left[\frac{1}{2} + \frac{1}{2}(1 + D)^{1/2}\right]^{-1/6} \qquad \text{.....[30]}$$

ϵ and r_0 are the constants of the Lennard-Jones potential. Conditions [28] determine the limits of applicability of Equation [25] from the point of view of the methods used to calculate the integrals.

Equation [25] gives the correct order of magnitude of ζ. Using the constants of the Lennard-Jones potential for CO_2, namely $\epsilon/k = 190$ and $r_0 = 3.996$ Å, we obtain $\alpha^* 4.98 \times 10^8$ cm for $T = 298$ K by successive approximations from Equations [29 and 30]. Assuming that σ equals r_1, where r_1 is the classical distance of the closest approach of the molecules, we obtain $\sigma = 3.54$ Å; $\zeta = 1.15$ g/cm-sec; $\nu/p \ll 0.1$ cm/atm; $\alpha_1\lambda = 17.5\nu/p$, where ν/p is in ms/atm; λ and α_1 are the wave length and the coefficient of absorption of ultrasound respectively. According to data by Fricke (11), we have $\alpha_1\lambda = 0.1$ when $p/\nu = 0.01$.

In conclusion, the author expresses his gratitude to Professor E. V. Stupochenko for useful remarks concerning the present work.

References

1 Leontovich, M., *J. Exptl. Theoret. Phys.* (USSR), Vol. 6, 1936, p. 561.
2 Wang Chang, C. S. and Uhlenbeck, G. E., University of Michigan Publication CM-681, 1951.
3 Pidduck, P., Proc. Roy. Soc., vol. A 101, 1922, p. 101.
4 Ishida, I., *Phys. Rev.*, vol. 10, 1917, p. 305.
5 Jeans, J. H., "Dynamical Theory of Gases," Cambridge University Press, 1904.
6 Chapman, S. and Cowling, T. G., "The Mathematical Theory of the Nonuniform Gases," Cambridge University Press, 1953.
7 Schwartz, R. N. and Slawsky, Z. R., *J. Chem. Phys.*, vol. 20, 1952, p. 1591.
8 Curtiss, C. F. and Hirschfelder, J., *J. Chem. Phys.*, vol. 17, 1949, p. 552.
9 Hirschfelder, J. O., Curtiss, C. F. and Bird, R. B., "Molecular Theory of Gases and Liquids," 1954.
10 Mandel'shtam, L. and Leontovich, M., *J. Exptl. Theoret. Phys.* (USSR) vol. 7, 1937, p. 438.
11 Fricke, E. F., *J. Acoust. Soc. Amer.*, vol. 12, 1940, p. 245.

Reviewer's Comment

The approach to the problem used in this paper is essentially the approach of Wang Chang and Uhlenbeck. The present authors, however, have carried the formal kinetic theory treatment somewhat further. The expression for the coefficient of thermal conductivity obtained by these authors is similar to that obtained by other methods by Hirschfelder (1). The authors use the phenomenological theory of bulk viscosity developed by Mandel'shtam and Leontovich. It is interesting that the expressions that they obtain are very similar in form to those obtained by the kinetic theory approach by Wang Chang and Uhlenbeck. In the introductory comments the authors refer to earlier studies of the effects of internal structure on the transport coefficients. The authors, however apparently were unaware of the formal treatment and evaluation of the transport coefficients for the idealized model of a gas made up of rigid ovaloids (2–4).

—C. F. Curtiss
University of Wisconsin

---

[1] Hirschfelder, J. O., "Heat Conductivity in Polyatomic or Electronically Excited Gases," *J. Chem. Phys.*, vol. 26, 1957, p. 282.
[2] Curtiss, C. F., "Kinetic Theory of Nonspherical Molecules," *J. Chem. Phys.*, vol. 24, 1956, p. 225.
[3] Curtiss, C. F. and Muckenfuss, C., "Kinetic Theory of Nonspherical Molecules. II," *J. Chem. Phys.*, vol. 26, 1957, p. 1619.
[4] Muckenfuss, C. and Curtiss, C. F., "Kinetic Theory of Nonspherical Molecules. III," *J. Chem. Phys.*, vol. 29, 1958, p. 1257.

Method of Calculation of the Transport Coefficients of Air at High Temperatures

E. V. STUPOCHENKO
B. V. DOTSENKO
I. P. STAKHANOV
E. V. SAMUILOV

THIS paper contains theoretical calculations of the transport coefficients of air—the viscosity and heat conduction—in the temperature range from 2000 to 8000 K and in the pressure range from 0.001 to 1000 atm. As in the case of the thermodynamic quantities, there are still no well-developed experimental methods available for the direct study of the transport properties of gases at such high temperatures. Yet, in solving the most important problems of modern engineering, particularly the problem of jet propulsion, it is essential to know the transport coefficients of the air at high temperatures and over a broad range of pressures. Therefore the theoretical approach, as in the case of the thermodynamic properties, becomes particularly important here. However, there is a great difference between problems in statistical thermodynamics and problems in kinetic theory. In the former (in the case of ideal gases) the mechanism of intermolecular (or interatomic) interactions does not play a substantial role, and all that need be known is the energy levels of the particles (molecules, atoms, etc.) and their statistical weights. In kinetic theory on the other hand, the laws of interaction between particles, the probabilities of transitions upon collision, play a decisive role; they enter in a substantial manner into the gas kinetic equation. The particular difficulties involved in the calculation of the transport coefficients are essentially due to this circumstance.

As is well-known, the statistical methods of calculating the transport coefficients, which Enskog and Chapman developed by extending and improving the method of Hilbert, were derived only for central forces diminishing with sufficient rapidity with increasing distance between molecules. Coulomb forces, and also inelastic collisions, particularly those accompanied by chemical reactions and ionization, entail certain complications. In a considerable portion of the investigated region of T and p in air, far-reaching dissociation and ionization processes take place, not to mention the excitation of the internal degrees of freedom. Therefore the calculation of transport coefficients is differently solved in different intervals of T and p.

The probability of molecule collisions accompanied by a reaction is relatively small. Equally small is the probability of transition of translational energy into vibrational energy, and vice versa. The transition of translational energy into rotational energy and vice versa is found to be more probable, but even these transitions do not affect the momentum transfer noticeably. Therefore, the viscosity can be calculated from the formulas for gas mixtures, neglecting the inelastic collisions even in the presence of substantial dissociation. The important problem in this case is that of choosing the form of the potential of interaction and the numerical values of the constants that enter into the expression for this potential.

Section I of this paper is devoted to the principles of calculating the viscosity of air under the conditions indicated in the foregoing. There are several known expressions for the intermolecular potential of the molecule interaction, and these expressions will be in good agreement with experiment if the constants are suitably chosen. However, the use of most of these expressions would not be correct for our calculations, for it would mean an excessive extrapolation of the experimental data to the region of very high temperature. For example, the term in the Lennard-Jones potential, proportional to r^{-12} (where r is the distance between molecules), which takes into account the repelling forces, is purely empirical in character. Yet, the role of repelling forces is large at high tempertures. These considerations have led us to choose the potential proposed by Buckingham, the form of which is theoretically justified from a quantum-mechanical examination of the problem of interaction between two molecules.

As regards the gas kinetic diameters of the atoms, the available data—experimental and theoretical—are quite scanty. The same atoms may interact with each other in accordance with entirely different laws, depending on the relative orientation of the spins of the outer electron shells of the colliding atoms. In particular, interactions of purely repulsive type or with a small potential well, may be realized. Since such interactions do not lead to the production of stable molecules, then naturally there are no spectral data that could be used to calculate the curve of the interaction potential. Yet most collisions do obey repulsive laws.

To obtain the necessary values of the nitrogen and oxygen atomic diameters, which were not measured experimentally, we used interpolation of the experimental data on the diameters of the atoms of other elements, based on the regularity of the periodic system.

An analysis of heat conduction is made complicated by the need of taking into account the excitation of the internal degrees of freedom as well as the chemical transformations occurring during the collisions between molecules. In Section 2 we analyze transport phenomena in a mixture of reacting gases. Recently many authors (Onsager, Haase, Eckert, Meixner, de Groot and others) have developed their own methods of investigating various macroscopic processes, such as diffusion, heat conduction, electric conduction, etc. These methods are known in the literature under the name of thermodynamics of irreversible processes. The most interesting and newest results are obtained by the thermodynamics of irreversible processes in which several processes interact, for example, heat conduction and diffusion, heat conduction and electric conduction, etc. In gases and liquids, where diffusion proceeds freely, heat transfer is always connected with a diffusion flow of matter. However, in the absence of a reaction, the fraction of the heat flow due to diffusion is insignificant and exists only until the establishment of a steady state, in which diffusion and thermal diffusion balance each other. In the presence of a reaction, the amount of heat transferred with the diffusing substance increases considerably (by the amount of the "energy of chemical affinity"), and, in addition, this component of the heat flow does not vanish with time, since there exists a nonvanishing diffusion flow of matter in the state of local chemical equilibrium.

Translated from *Fizicheskaya Gazodinamika* ("Physical Gasdynamics"), USSR Acad. Sci., pp. 39–58.

The problem consists of determining the specific type of law of heat transfer under conditions of local chemical equilibrium, and in finding the phenomenological coefficients that enter into this law. The first part of this problem is solved in the present paper by methods of the thermodynamics of irreversible processes. We succeed in expressing the law of heat conduction in terms of those transport coefficients that can be determined by methods of modern kinetic theory (5)[1], making it possible in turn to calculate these coefficients by means of one molecular model or another. In addition, no assumptions are made in this paper concerning the absence of a pressure gradient in the medium, as was done, for example, by Haase (4). This is necessary because heat exchange occurs in gasdynamics, as a rule, under nonisobaric conditions.

I Viscosity of Air in the Presence of Molecular Dissociation

1 Preliminary Remarks

In this chapter we report the results of an examination of the viscosity of air in the temperature range from 2000 to 8000 K, for pressures from 0.001 to 1000 atm. The viscosity of a gas in which no chemical reactions take place depends on the temperature and is almost entirely independent of the pressure. At high temperatures, on the order of several thousand deg K, the molecules of the air begin to dissociate into atoms, and consequently chemical reactions take place in the air and its viscosity becomes dependent on the pressure.

It is possible to obtain experimental values of the viscosity of the air only up to 2000 K. We are interested, on the other hand, in the viscosity of air in the temperature range from 2000 to 8000 K. We must therefore resort to theoretical methods of determining the viscosity. Among the papers devoted to this problem are those of Chapman and Enskog, who have derived approximate expressions for the viscosity and heat conduction of gas in terms of the so-called "collision integrals," which depend on the law of interaction between the gas particles.

The laws of interaction between atoms and between molecules are known only approximately, and this in turn makes for further inaccuracy in the expressions for the transport coefficients.

There are many equations for the dependence of the viscosity on the temperature, in accordance with the various representations concerning the character of the intermolecular interaction. Thus, the power law dependence of η on the temperature T

$$\eta \sim T^n \qquad n = \text{constant} \qquad [1]$$

corresponds to a power dependence of the interaction potential on the distance. However, when $T \lesssim 1000$ K, a better agreement with experiment is given by the Sutherland formula

$$\eta = \frac{aT^{1/2}}{1 + C/T} \qquad \begin{matrix} a = \text{constant} \\ C = \text{constant} \end{matrix} \qquad [2]$$

which takes into account the weak forces of attraction between molecules. But at high temperatures ($\sim$2000 K) it is possible to neglect the term C/T, since C is on the order of $\sim$100 K. Then Equation [2] becomes $\eta = aT^{1/2}$, which is in poorer agreement with experiment than the power law formula. Other empirical equations are also known (5).

The foregoing formulas were obtained from very simple concepts regarding the intermolecular forces, not corresponding to the present-day status of this problem. Therefore, to obtain a more accurate expression for this viscosity, we turn to later research data on intermolecular forces.

[1] Numbers in parentheses indicate References at end of paper.

It must be noted that at high temperatures the viscosity of air can be determined only with small accuracy, since at such temperatures free atoms appear in the air, and the laws of interaction between these atoms are still unknown. It can be considered established, however, that the gas kinetic diameters of the molecules of nitrogen and oxygen are close to those of the atoms of nitrogen and oxygen, and therefore in our approximate calculations of the transport coefficients we can assume that at such temperatures air represents a binary mixture of gas components: Molecular (N_2, O_2, NO) and atomic (N, O, A).

2 Interaction Between Molecules and Viscosity of the Molecular Component of the Mixture

A quantum mechanical analysis makes it possible to establish that at large distances (compared with the radius of the molecule) nonpolar molecules attract each other with a force, the potential of which can be represented in form of a series

$$U(r) = -\frac{C}{r^6} - \frac{C'}{r^8} - \cdots \qquad [3]$$

Obviously, at large distances the first term is the only one of importance. Without any theoretical justification, the repulsion forces were also expressed by means of a power law, with a suitable choice of the power exponent. A well-known potential for the intermolecular interaction is the Lennard-Jones potential

$$U = 2\epsilon[(1/2)\xi^{-12} - \xi^{-6}] \qquad [4]$$

where

ϵ = depth of potential minimum
$\xi = r/r_m$
r_m = distance between centers of molecules

For the molecules O_2 and N_2, the value of ϵ/k (where k is the Boltzmann constant) is approximately on the order of 100 K, r_m is approximately 4 Å, and ϵ and r_m can be determined from the experimental data, both from the transport coefficients and—independently—from the values of the virial coefficients. It is important to note here that the values of r_m and ϵ determined by such independent methods were found to be practically equal (Table 1).

Table 1[a]

	ϵ/k, K		r_m, Å	
Gas	Viscosity	Virial coefficients	Viscosity	Virial coefficients
air	97.0	99.2	3.617	3.692
O_2	91.46	95.9	3.681	3.72
N_2	113.2	117.5	3.433	3.58

[a] See (6).

"Collision integrals" for the Lennard-Jones potential were tabulated by Hirschfelder, Bird and Spotz (6). The values of the viscosity, calculated from the data of these calculations, are in good agreement with the experiment. It turns out, however, that at high temperatures the dependence of the viscosity so calculated on the temperature obeys a power law

$$\eta \sim T^n \qquad [5]$$

where $n = 0.666$.

This is explained by the fact that at high temperatures the principal role is assumed by the repulsion forces, corresponding in the Lennard-Jones formula to the term $\sim r^{-12}$, which does not reflect correctly the nature of these forces. Consequently, the use of the Lennard-Jones potential in the calcu-

lation of the viscosity is not reliable at high temperatures. It can be considered as proved (7) that the repulsion forces depend on the distance exponentially. One of the most useful expressions for the law of intermolecular interaction, with account of this character of repulsion forces, is the modified Buckingham potential

$$U = \frac{\epsilon}{1 - 6/\alpha}\left[\frac{6}{\alpha}e^{\alpha(1-\xi)} - \xi^{-6}\right] \qquad [6]$$

Here α is a dimensionless parameter. Depending on the type of molecule, α may range from 12 to 17 or higher. The values of α, r_m and ϵ can be obtained by comparing the results of theoretical calculation with experimental data on viscosity, the second virial coefficient and the interaction of molecules in crystals at temperatures near 300 K.

Table 2[a]

Gas	α	r_m, Å	ϵ, erg
Ne	14.5	3.147	38
A	14	3.866	123.2
Kr	12.3	4.056	158.3
Xe	13.0	4.450	231.2
CH_4	14.0	4.206	152.1
N_2	16.2	4.040	113.2
	17.0	4.011	101.2
CO	17	4.10	132
	17	3.937	119.1

[a] See (8).

The discrepancy between the values of the parameters obtained from different experiments for the same diatomic molecules is due to the fact that, strictly speaking, the potential of Equation [6] is applicable only to spherically symmetrical molecules. Diatomic molecules can be considered spherically symmetrical only approximately. The nonsphericity influences least of all the equilibrium properties, i.e., the second virial coefficient.

The error introduced by nonsphericity into the viscosity of N_2 is found to be on the order of 2 per cent at temperatures above 600 K; i.e., it is fully within the permissible accuracy.

As yet we have no corresponding data for O_2 molecules but, using the similarity between the Lennard-Jones potential and the potential of Equation [6] at not too small values of $r(r \geq 0.3r_m)$, we can determine these parameters. The viscosity (η), calculated by the Enskog-Chapman method and Equation [6], has the following form

$$\eta = \frac{5}{16}\left(\frac{mkT}{\pi}\right)^{1/2}\frac{f_\eta}{r_m^2\Omega^{(2,2)}(T^*)} \qquad [7]$$

where

m = mass of molecule
k = Boltzmann's constant
T = absolute temperature
T^* = (kT/ϵ)
ϵ = same meaning as in Equation [4]

The functions $\Omega^{2,2}$ and f_η are not expressed analytically. They were tabulated by Mason (7), and by Mason and Rice (5). It can be seen from Equation [7] that the ratio

$$\eta(T^*)/\eta(T_0^*) = \Psi(T^*)$$

where T_0^* is a certain fixed value of T^*, is the same function of the reduced temperature T^* for all gases. If we calculate a similar function $\Psi(T^*)$ for the model of elastic solid spheres, then at high temperatures ($T \geq 4000$ K) its values will be 1.5 or 2 times as small as the corresponding values of $\Psi(T^*)$, calculated with the use of the Buckingham potential.

3 Gas Kinetic Diameters of Atoms and Viscosity of the Atomic Component of Air

There are only few known expressions for the interaction forces between atoms, from which to calculate the transport coefficients. Only those inert gases have been studied for which the interaction forces between atoms and their gas kinetic diameters[2] are known with sufficient accuracy. See Table 3.

Table 3

Gas	T, K	σ_T, Å
He	273	2.19
Ne	293	2.59
A	273	3.66
Kr	273	4.18
Xe	273	4.93
Kn	288	5.2

The outer shell of the atom of an inert gas is closed, and this facilitates considerably the theoretical and experimental investigations. In particular, the attraction forces between the atoms are inversely proportional, in first approximation, to the sixth power of the distance.

The total interaction between the atoms of inert gases is in good agreement with the Lennard-Jones potential, making it possible to determine the parameters ϵ and r_m for these gases with satisfactory accuracy.

The situation is quite different for atoms with an unfilled electron shell. The energy of the interaction between such atoms either has a very strong minimum or corresponds to pure repulsive forces, depending on the relative orientation of the spins of the external electrons. For an interaction with a minimum, the dependence of the interaction energy on the distance is sufficiently well known from spectroscopic data. Several empirical formulas have been obtained, such as the Morse function, the Hulbert-Hirschfelder function, etc.

However, spectroscopic data make it possible to determine the behavior of the curve only near the minimum, and only by extrapolation can one obtain information on the behavior of the curve at large distances (compared with r_m) or in the repulsion part. As to curves of purely repulsive type, there are as yet neither experimental nor reliable theoretical data, since in spectroscopy one deals with interactions that correspond to a curve with a minimum. The interaction energy was calculated theoretically for hydrogen; for more complicated atoms, the calculations entail considerable difficulties connected with solving many electron problems.

Consequently, in calculating the coefficients for the atoms it becomes necessary to forego any dependence of the interaction energy on the distance and to use the model of elastic rigid spheres. However, even in this formulation of the problem we find that no reliable experimental data are as yet available for the solution of this problem.

The effective cross sections for the viscosity can be determined if one knows the effective cross sections for scattering, since a definite connection exists between the cross section for the viscosity and the cross section for scattering (see, for example, Mott and Massey, "Theory of Atomic Collisions"). Specifically, if we denote by $I\vartheta d\omega$ the probability of scattering of a particle within a solid angle $d\omega$ at an angle ϑ to the initial direction, then the total effective scattering cross section Q is determined as follows

$$Q = 2\pi\int_0^\pi I(\vartheta)\sin(\vartheta)d\vartheta \qquad [8]$$

[2] The gas kinetic diameter σ_T at a temperature T is given by

$$\sigma_T = \sqrt{0.998[(mkT)^{1/2}/\pi^{3/2}\eta(T)]}$$

where $\eta(T)$ is the viscosity at the temperature T.

and the effective cross section for the viscosity is

$$Q = 2\pi \int_0^{\pi} I(\vartheta) \sin^3 \vartheta d\vartheta \qquad [9]$$

The angle ϑ depends on the law of interaction between the atoms. Since there is still no exact theoretical expression for this law, it becomes necessary to resort to experimentally determined effective scattering cross sections.

However, the presently available experimental data are scanty, and furthermore it is found that the values of the diameters of the same atoms differ greatly from each other when scattered by different gases.

We need more reliable information, in the form of data on viscosity and diffusion. Data on viscosity, for example, yield the diameters of atomic hydrogen [9] [cited in (6)]

$$\sigma_T = 2.52 \text{ Å} \quad \text{at} \quad T = 273 \text{ K}$$

$$\sigma_T = 2.48 \text{ Å} \quad \text{at} \quad T = 373 \text{ K}$$

The diameter of deuterium was found to equal the diameter of ordinary hydrogen. If the temperature dependence of σ_T is presented in the form

$$\sigma_T^2 = \sigma_\infty^2(1 + C/T) \qquad [10]$$

we obtain for different atoms the values of σ_∞ and C shown in Table 4.

Table 4

Gas	σ_∞, Å	C, K
He	1.82	173
Ne	2.52	128
A	2.99	142
Kr	3.22	188
Xe	3.55	252
H	2.39	31
D	2.39	31

From experiments on diffusion we know the gas kinetic diameter of sodium atoms

$$\sigma_T = 3.7 \text{ Å} \quad \text{at} \quad T = 291 \text{ K}$$

In calculating this value it was also assumed that

$$\sigma_{12} = (1/2)(\sigma_1 + \sigma_2)$$

In addition, there is available information on the diameters σ for atoms of zinc, cadmium and hydrogen. Thus, the information on gas kinetic diameters is extremely scanty. Consequently, one can speak only of an approximate estimate of this quantity for the oxygen and nitrogen atoms, which are of interest to us.

The meager data cited show that the gas kinetic diameters of the atoms are definitely related to the number of the atoms in the periodic system of the element. The most important fact is that as the atomic number increases, we have not a monotonic increase in the atom diameter, but a periodic variation. Furthermore, the diameter does not increase with increasing atomic number within each period, but, on the contrary, decreases. Thus, the diameter of the hydrogen atom at $T = 273$ K is 2.52 Å, which is noticeably greater than the diameter of helium (2.19 Å) and is approximately equal to the diameter of neon (2.59 Å at 293 K), in spite of the fact that the latter has 10 electrons as opposed to the single electron of hydrogen. Furthermore, σ_∞ of hydrogen is 2.39 Å, whereas that of helium is 1.82 Å and neon 2.25 Å.

The diameter of the sodium atom, the first in the third period of the periodic system, is 3.7 Å at 291 K, considerably greater than the diameter of neon which has the next lower atomic number, and is somewhat greater than the diameter of argon (3.66 Å), which is at the end of the third period. Finally, the diameter of lithium, located vertically between hydrogen and sodium, should also be intermediate between the two, i.e., approximately 3 Å, considerably in excess of the gas kinetic diameter of neon (2.52 Å), with which the second period ends.

The foregoing data indicate that, at least in the first periods, the gas kinetic diameter of the atoms decreases somewhat from the start to the end of the period, and then, in going from the inert gas which ends the period, to the alkali metal which begins the new period, the diameter increases sharply.

There is another physical quantity which also depends on the atomic number of a given atom in the periodic table. This is the ionization potential, with which the atomic radius is directly connected (quantum mechanically). The values of the ionization potential have been well investigated for almost all gases. The ionization potential increases with the atomic number within the period and decrease sharply in going to the next period. It is particularly significant to us that the change in potential within the period is practically monotonic, which apparently indicates a monotonic variation in the gas kinetic diameter, too.

In connection with this, one must note the following fact. The products of the gas kinetic radii σ_T of the atoms of inert gases times the ionization potentials V_i of the same atoms are nearly equal to each other (Table 5). We can therefore assume that for each group (more accurately, subgroup) of elements in the periodic system, the products of the gas kinetic radii of the atoms times the values of the ionization potentials of the same atoms are nearly equal to each other, i.e., that this product is practically constant for a given group (subgroup) of the periodic table. An indirect confirmation of this group

Table 5

Gas	V_i, volts[a]	σ_T(Å)	$\sigma_T V_i$
He	24.46	2.19	53.6
Ne	21.47	2.59	55.6
A	15.68	3.66	57.4
Kr	13.93	4.18	58.3
Xe	12.08	4.93	59.5
Rn	10.7	5.2	55.7

[a] Hodgeman, Ch. D., "Handbook of Chemistry and Physics" 1951.

is the fact that the magnitude of the ionization potential—the energy necessary to remove an electron from the atom—is inversely proportional to the distance between the given electron and the nucleus of the atom, and this distance, or the quantum-mechanical radius, should be directly proportional to the gas kinetic radius of the atom. One can assume furthermore that this product changes over the period as a function of the number of the electrons on the outer orbit or as a function of the total spin of the outer electron shell of the atom.

However, since the changes in the collision diameter over the period are not very large, we shall not introduce a large error if we assume them to be linear within each of the periods. To find the diameter σ_{Li} we can take the arithmetic mean of the diameters of hydrogen and sodium, between which lithium is located

$$\sigma_{Li} = \frac{2.39 + 3.7}{2} \text{ Å} = 3.05 \text{ Å}$$

We next locate the diameter of neon at high temperatures. The value of σ_∞ from Table 4 cannot be used, since Equation [10] cannot be applied at such high temperatures. Nor are there any experimental data for temperatures from 3000 to 10,000 K.

However, since the electron shell of the neon atom is filled, we can apply to it the Buckingham molecular potential.

Therefore the gas kinetic diameter of neon can be determined at the required temperatures from a knowledge of the "collision integrals" and of the transport coefficients for neon at the same temperatures. The gas kinetic diameter obtained in this manner is

$$\sigma_{Ne} = 1.8 \text{ Å}$$

If we assume that the gas kinetic diameter of the atom varies linearly along the period we obtain for the oxygen atom $\sigma_O = 2.16$ Å, and for the nitrogen atom $\sigma_N = 2.3$ Å. It is obvious that within the limits of the presently attainable accuracy, one can assume for the general gas kinetic diameter for the atomic component

$$\sigma_1 = 2.2 \text{ Å (or } 2.3 \text{ Å)} \qquad [11]$$

Knowing the gas kinetic diameter, we can calculate the viscosity by the Chapman formula

$$\eta = 0.998[(m_1 kT)^{1/2}/\pi^{3/2}\sigma_1^2] \qquad [12]$$

where m_1 is the mass of the atom.

4 Viscosity of Air

To calculate the viscosity of air, which is a mixture of the atomic and molecular components, it is necessary to know the law of interaction between the atoms and molecules. Information on this interaction is also practically nonexistent, and consequently we must again use the model of elastic spheres. The collisions between the molecule and the atom are considered here as collisions between elastic spheres with effective diameter

$$\sigma_{12} = (1/2)(\sigma_1 + \sigma_2) \qquad [13]$$

where

σ_1 = diameter of atoms as determined in the foregoing

σ_2 = diameter of the molecules, calculated from the relation

$$\sigma_2(T) = \sqrt{0.998[(m_2 kT)^{1/2}/\pi^{3/2}\eta_2(T)]} \qquad [14]$$

$\eta_2(T)$ = viscosity of the molecuarl component at temperature T

Obviously, the diameter of the molecule depends on the temperature.

Expressions for the viscosity of a binary mixture of gases were derived by Chapman and Enskog, but since the viscosity of the atomic component has been calculated thus far with low accuracy, it is logical to employ the earlier formula derived by Enskog on the basis of an examination of the transport processes in a gas consisting of molecules, with an interaction that diminishes rapidly with distance (10)

$$\eta = \frac{\eta_1}{1 + \alpha_{12}(x_2/x_1)} + \frac{\eta_2}{1 + \alpha_{21}(x_1/x_2)} + \frac{2d(\eta_1\eta_2)^{1/2}}{[1 + \alpha_{12}(x_2/x_1)][1 + \alpha_{21}(x_1/x_2)]} \Big/ \left(1 - \frac{d^2}{[1 + \alpha_{12}(x_2/x_1)][1 + \alpha_{21}(x_1/x_2)]}\right) \qquad [15]$$

where

η_1 = viscosity of the atomic component

η_2 = viscosity of the molecular component

x_1, x_2 = relative molar fractions of the first and second components

$$\sigma_{12} = \frac{1}{3}\left(\frac{\sigma_{12}}{\sigma_1}\right)^2 \left[\frac{2m_2}{m_1 + m_2}\right]^{1/2} \frac{5m_1 + 3m_2}{m_1 + m_2}$$

$$\sigma_{21} = \frac{1}{3}\left(\frac{\sigma_{12}}{\sigma_2}\right)^2 \left[\frac{2m_1}{m_1 + m_2}\right]^{1/2} \frac{3m_1 + 5m_2}{m_1 + m_2}$$

$$d = \left(\frac{8}{9}\right)^{1/2} \frac{(m_1 m_2)^{3/4}}{(m_1 + m_2)^{3/2}}$$

σ_1 = effective diameter of atom

σ_2 = effective diameter of molecule

σ_{12} = effective diameter for collisions between atoms and molecules

m_1, m_2 = masses of atom and molecules

We note that if we calculate the viscosity of air with the aid of the exact Chapman-Enskog formula, which has been derived for elastic spheres, the result deviates from that calculated by the approximate formula [15] by approximately 2 or 3 per cent which obviously includes the inaccuracy in the calculation of the viscosity of the atomic component.

Data on the composition of air at high temperatures, which are essential for the calculation of x_1 and x_2, can be found in the report of the Laboratory for the Physics of Combustion, the Power Institute for 1955 (5). This report contains data on the composition and thermodynamic properties of air at temperatures from 2000 to 8000 K and pressures from 0.001 to 1000 atm. It is seen from these data that total dissociation of the molecules of air occurs only at pressures less than 1 atm. For higher pressures at 8000 K a certain amount of undissociated molecules still remain; at pressures of several hundred atmospheres, approximately 50 per cent of the molecules remain undissociated.

It must be noted further that at temperatures near 8000 or 10,000 K, and for very low pressures even somewhat earlier, the degree of ionization becomes so substantial, that further calculation of the transport coefficients without allowance for ionization becomes meaningless.

The results of the calculations of the viscosity of air in the corresponding temperature intervals and pressure intervals are contained in the reports of the Laboratory for the Physics of Combustion, the Power Institute, for 1955 (5 and 11), devoted to calculation of the transport coefficients (Fig. 1).

II Heat Conduction in a Binary Mixture of Chemically Reacting Gases

1 Heat Flow in a Binary Mixture of Gases

Unlike the viscous stress tensor, which always depends only on the velocity gradient tensor, heat flow in liquids and gases in which diffusion is possible is closely related with the diffusion flow of the material, and depends therefore not only on the temperature gradient, but also on the gradient of the chemical potential. In the presence of a chemical reaction, the role of those heat flow components, which arise as a result of diffusion of molecules, increases greatly.

To investigate the problem of heat conduction under conditions of chemical reactions it is necessary first to agree on the definition of the concept "heat flow." The heat flow is determined by the form of the energy equation employed. In this paper we shall write the energy equation in the form

$$\rho \frac{\partial E}{\partial t} + pu_k \frac{\partial E}{\partial x_k} - \pi_{ik} \frac{\partial u_i}{\partial x_k} + \frac{\partial I_k^{(q)}}{\partial x_k} = 0 \qquad [1]$$

where

E = internal energy per unit mass of mixture

π_{ik} = stress tensor

u_k = hydrodynamic velocity

ρ = density of the mixture

$I^{(q)}$ = heat flow vector

Repetition of an index denotes summation over this index. In a binary mixture of A_1 and A_2

$$E = \eta_1 E_1 + \eta_2 E_2 \qquad [2]$$

where

$\eta_i = \dfrac{\rho_i}{\rho_1 + \rho_2} = \dfrac{\rho_i}{\rho}$

η_1, η_2 = mass fractions of components A_1 and A_2 in mixture

ρ_1, ρ_2 = densities of components A_1 and Z_2

E_1, E_2 = internal energies per unit masses of A_1 and A_2

The diffusion flux $\mathbf{I}^{(1)}$ of the component A_1 is defined as

$$I^{(1)} = \rho_1(u^{(1)} - u) = \frac{\rho_1\rho_2}{\rho}(u^{(1)} - u^{(2)}) = -I^{(2)} \qquad [3]$$

where

u = hydrodynamic velocity, determined from the relation

$$u = \eta_1 u^{(1)} + \eta_2 u^{(2)} \qquad [4]$$

$u^{(1)}$, $u^{(2)}$ = velocities of the components A_1 and A_2

$I^{(2)}$ = diffusion flux of component A_2

We obtain from the thermodynamics of irreversible processes (1 and 2)

$$I^{(q)} = -L_{q1}\frac{1}{T}\nabla\left(\frac{\varphi^{(1)} - \varphi^{(2)}}{T}\right) - L_{qq}\frac{1}{T}\nabla T \qquad [5]$$

$$I^{(1)} = -I^{(2)} = -L_{11}\frac{1}{T}\nabla\left(\frac{\varphi^1 - \varphi^2}{T}\right) - L_{q1}\frac{1}{T}\nabla T \qquad [6]$$

where

L_{q1}, L_{11}, L_{qq} = phenomenological coefficients

$\varphi^{(1)}$, $\varphi^{(2)}$ = partial specific thermodynamic potentials of components A_1 and A_2

T = absolute temperature

∇ = grad $= \dfrac{\partial}{\partial x_1} + \dfrac{\partial}{\partial x_2} + \dfrac{\partial}{\partial x_3}$

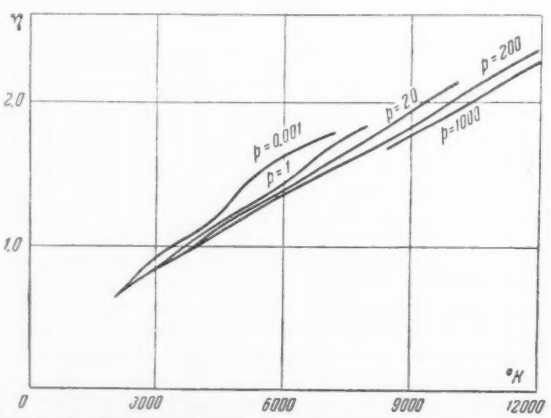

Fig. 1 Coefficient of viscosity in millipoise (1 poise = gm/cm-sec) as a function of the temperature for various pressures p, atm

Equations [5 and 6] have been derived assuming no mass forces.

Onsager's principle of the symmetry of the kinetic coefficients was taken into account in the derivation of Equations [5 and 6].

The coefficients L_{qq}, L_{11} and L_{q1} determine fully the heat flow and the diffusion flow and consequently all other coefficients introduced for the description of diffusion, and heat conduction should be expressible only in terms of these three coefficients.

Let us introduce a new phenomenological coefficient of "heat transfer" [see (1 and 2) for more details]

$$L_{q1} = L_{11}Q^* \qquad [7]$$

We then have instead of [5 and 6]

$$I^{(1)} = L_{11}\left\{-\frac{1}{T}\nabla\left(\frac{\varphi^{(1)} - \varphi^{(2)}}{T}\right) - Q^*\frac{1}{T}\nabla T\right. \qquad [8]$$

$$I^{(q)} = Q^*J^{(1)} - \left\{L_{qq} - L_{q1}Q^*\right\}\frac{1}{T}\nabla T \qquad [9]$$

or, denoting

$$(L_{pp} - L_{q1}Q^*)/T = \lambda \qquad [10]$$

we obtain the following expression for the heat flow

$$I^{(q)} = Q^*I^{(1)} - \lambda\nabla T \qquad [11]$$

The stationary state, in the absence of a chemical reaction, is determined by the condition

$$I^{(1)} = 0 \qquad [12]$$

Thus we have in the stationary state

$$I^{(q)} = -\lambda\nabla T \qquad [13]$$

and consequently λ is the coefficient of heat conduction in the stationary state.

Next, assuming that $\varphi = \varphi(T, p, \eta_1)$, and employing the Gibbs-Duhem equation

$$\eta_1\frac{\partial\varphi^{(1)}}{\partial\eta_1} + \eta_2\frac{\partial\varphi^{(2)}}{\partial\eta_2} = 0 \qquad [14]$$

we obtain from Equation [8] the following expression for $I^{(1)}$

$$I^{(1)} = L_{11}\left\{-(v_1 - v_2)\nabla p - \frac{1}{\eta_2}\left(\frac{\partial\varphi^{(1)}}{\partial\eta_1}\right)_{p,T} \times \right.$$
$$\left. \nabla\eta_1 - (Q^* - h_1 + h_2)\frac{\nabla T}{T}\right\} \qquad [15]$$

where

p = hydrostatic pressure

h_1, h_2 = specific enthalpies of A_1 and A_2

v_1, v_2 = specific volumes of A_1 and A_2

Comparing Equations [11 and 15] we find that even in the absence of a temperature gradient the heat flux does not vanish if the concentration gradient or the pressure gradient does not vanish. Inserting [15] into [11], we find that the coefficient of ∇T is

$$\kappa = \lambda + L_{11}Q^*(Q^* - h_1 + h_2)(1/T) \qquad [16]$$

κ is the coefficient of heat conduction, which determines the heat flow in the state of uniform mixing, i.e., when $\nabla p = 0$ and $\nabla\eta_1 = 0$; it is obvious that κ does not equal λ. If there is no reaction, the initial levels from which the energies of the molecules of A_1 and A_2 are reckoned can be chosen independent of each other. In particular, we can reckon the energy of each molecule from the lowest energy level of the corresponding molecule. Then the difference $h_1 - h_2$ is small. Then, as seen from theoretical calculations based on kinetic

theory and from experiment, the second term in Equation [16] is small compared with the first, and only one term, $-\lambda \text{ grad } T$, need be retained in Equation [11]. The calculations for this case are known from the kinetic theory of gases (3), and lead to the expression

$$I^{(q)} = pk_T(\bar{C}_2 - \bar{C}_1) - \lambda \nabla T \qquad [17]$$

where

k_T = thermal diffusion ratio
$\bar{C}_1, \bar{C}_2$ = mean thermal velocities of A_1 and A_2

Inasmuch as $\bar{C}_1 - \bar{C}_2$ equals $u^{(1)} - u^{(2)}$, we can rewrite Equation [11] with the aid of Equation [3] in the form

$$I^{(q)} = Q^*(\rho_1\rho_2/\rho)(\bar{C}_1 - \bar{C}_2) - \lambda \nabla T \qquad [18]$$

Comparing [17 and 18] we see that the coefficient of heat conduction, calculated in the Enskog-Chapman theory for a binary mixture of gases, coincides with the coefficient of heat conduction for the stationary state, Equation [10].

2 Heat Flux in a Reacting Mixture of Gases at Equilibrium

We consider the case when a chemical reaction takes place. From the molecular-kinetic point of view, the heat flux in the reacting mixture contains additional terms, over and above those contained in the absence of reaction. Indeed, the heat flux is expressed as

$$n_1\overline{E_1\mathbf{C}^{(1)}} + n_2\overline{E_2\mathbf{C}^{(2)}}$$

where

$$E_1 = (1/2)m_1C^{(1)2} + U^{(1)}$$
$$E_2 = (1/2)m_2C^{(2)2} + U^{(2)} + \epsilon$$

and are the energies of the molecules A_1 and A_2 respectively; $U^{(1)}$ and $U^{(2)}$ are the energies of the internal degrees of freedom of molecules A_1 and A_2; ϵ is the difference in the lowest energy levels of molecules A_1 and A_2.

We shall assume henceforth that equilibrium exists between the translational and internal degrees of freedom of the molecule.

In the absence of a reaction, the initial levels from which the energy is reckoned can be chosen independently, and consequently we can assume $\epsilon = 0$. This cannot be done in the presence of a chemical reaction, which leads to the appearance of an additional heat flux term $\epsilon\bar{C}^{(2)}$, which can also be written in more symmetrical form as $\epsilon_1\bar{C}^{(1)} + \epsilon_2\bar{C}^{(2)}$.

The physical meaning of these terms is obvious: In the presence of reaction, the heat flux includes also the transfer of chemical-affinity energy, caused by the thermal motion of the molecules. The mechanism of the transfer of this energy, like the mechanism of transfer of the internal energy, is of the diffusion type.

Assume that the reaction begins at $t = 0$ and there was no reaction before that time. If τ is the relaxation time of the reaction, then at $t \ll \tau$ the reaction does not influence the heat flow or any other macroscopic process. Let us examine what takes place at $t \gg \tau$. The presence of a reaction does not change the form of the general thermodynamic equations for the heat flux, Equations [5 and 11]. This is due to the fact that the reaction is determined by scalar quantities (the speed of reaction and the chemical activity), whereas the heat flux is a vector. A vector can be linearly related with a scalar only if the coefficient of proportionality is a vector. Thus, the phenomenological coefficient that characterizes the connection between the heat flux and the chemical reaction should be a vector. But, on the other hand, this coefficient should be isotropic, since it pertains to an isotropic medium. The only isotropic vector is a null vector, and this indeed explains the absence of a direct connection between the heat flux and chemical reaction.

However, the presence of reaction leads to a change in the stationary state. If the stationary state is defined by the condition $I^{(1)} = 0$, in the absence of reaction, then, in the presence of reaction, if $t \gg \tau$, the stationary state is a state of local chemical equilibrium, determined by the condition

$$\nu_1\tilde{\varphi}^{(1)} - \nu_2\tilde{\varphi}^{(2)} = \nu_1^0\tilde{\varphi}^{(1)} - \nu_2^0\tilde{\varphi}^{(2)} = 0 \qquad [19]$$

where

$\tilde{\varphi}^{(1)}, \tilde{\varphi}^{(2)}$ = partial molar thermodynamic potentials of components A_1 and A_2
ν_1, ν_2 = stoichiometric coefficients of reaction in a binary mixture of gases

$$\nu_1A_1 - \nu_2A_2 = 0 \qquad [20]$$

Finally

$$\nu_1^0 = \nu_1\mu_1 \qquad \nu_2^0 = \nu_2\mu_2 \qquad [21]$$

where μ_1 and μ_2 are the molecular weights of A_1 and A_2.

Since Equation [19] holds at each point, then

$$\nabla(\nu_1^0\varphi^{(1)} - \nu_2^0\varphi^{(2)}) = 0 \qquad [22]$$

thus, in the case of a chemical reaction, the diffusion flux does not vanish in the stationary state.

To calculate the heat flux and the conditions of local chemical equilibrium, we make use of Equations [11 and 15]. Inserting $I^{(1)}$ from Equation [15] into [11] we find

$$I^{(q)} = -L_{11}Q^*(v_1 - v_2)\nabla p - L_{11}Q^* \times \frac{1}{\eta_2}\left(\frac{\partial\varphi^{(1)}}{\partial\eta_1}\right)_{p,T}\nabla\eta_1 - \left\{L_{11}Q^*\frac{Q^* - h_1 + h_2}{T} + \lambda\right\}\nabla T \qquad [23]$$

We can use Equation [19] to rewrite the conditions of local equilibrium [22] as

$$v_R\nabla p - h_R\frac{\nabla T}{T} + \frac{\nu_1^0\eta_2 + \nu_2^0\eta_1}{\eta_2}\left(\frac{\partial\varphi^{(1)}}{d\eta_1}\right)_{p,T}\nabla\eta_1 = 0 \qquad [24]$$

where we introduce the symbols

$$v_R = \nu_1^0v_1 - \nu_2^0v_2 \qquad [25]$$

$$h_R = \nu_1^0h_1 - \nu_2^0h_2 \qquad [26]$$

After obtaining $\nabla\eta_1$ from Equation [24] and substituting into [23], we find

$$I^{(q)} = -L_{11}Q^*v\frac{\nu_2^0 - \nu_1^0}{\nu_1^0\eta_2 + \nu_2^0\eta_1}\nabla p - \left\{L_{11}Q^*\frac{Q^* - h_1 + h_2}{T} + L_{11}Q^*\frac{h_R}{\nu_1^0\eta_2 + \nu_2^0\eta_1}\frac{1}{T} + \lambda\right\}\nabla T$$

where $v = \eta_1v_1 + \eta 2v_2$ is the specific volume. Since, because of the conservation of mass, $\nu_1\mu_1$ equals $\nu_2\mu_2$, or

$$\nu_1^0 = \nu_2^0 = \nu^0 \qquad [27]$$

we have

$$h_R = \nu^0(h_1 - h_2) \qquad [28]$$

$$\nu_1^0\eta_1 + \nu_2^0\eta_2 = \nu^0 \qquad [29]$$

that is

$$I^{(q)} = -\left\{\frac{L_{11}Q^{*2}}{T} + \lambda\right\}\nabla T \qquad [30]$$

Thus, if the stationary state, under the conditions of a chemical reaction in a binary mixture of gases, is the state of local chemical equilibrium, then the term proportional to grad p drops out of the expression for the heat flux (exactly as the stationary state without a reaction). Equation [30] is the simplest expression for the heat flux under conditions of chemical equilibrium, but the coefficients L_{11} and the heat transfer Q^* are still not in general use. In connection with this, it is advantageous to obtain an expression for the heat

flux in terms of the better known coefficients of diffusion and thermal diffusion. We introduce the coefficient of ordinary diffusion D_{12} by means of the equation

$$I^{(1)} = -\rho D_{12} \nabla \eta_1 \qquad [31]$$

at $\nabla T = 0$ and $\nabla p = 0$, and a coefficient of thermal diffusion D_{12}^T

$$I^{(1)} = -\rho D_{12}^T \eta_1 \eta_2 \nabla T \qquad [32]$$

at $\nabla p = 0$, $\nabla \eta_1 = 0$.

Then the coefficients L_{11} and Q^* are expressed in terms of D_{12} and D_{12}^T in the following manner

$$L_{11} = \frac{\rho \eta_2 D_{12}}{(\partial \varphi^{(1)}/\partial \eta_1)_{p,\,T}} \qquad [33]$$

$$Q^* = \frac{D_{12}^T}{D_{12}} \eta_1 T \left(\frac{\partial \varphi^{(1)}}{\partial \eta_1}\right)_{p,\,T} + h_1 - h_2 \qquad [34]$$

From Equations [30, 33 and 34] we find

$$I^{(q)} = -\left\{\lambda + \rho \frac{(D_{12}^T)^2}{D_{21}} \eta_2 \eta_1^2 T \left(\frac{\partial \varphi^{(1)}}{\partial \eta_1}\right)_{p,\,T} + \frac{\rho \eta_2 D_{12} (h_1 - h_2)^2}{(\partial \varphi^{(1)}/\partial \eta_1)_{p,\,T} T} + 2\rho \eta_1 \eta_2 D_{12}^T (h_1 - h_2)\right\} \nabla T = -\lambda_0 \nabla T \qquad [35]$$

This expression for the heat flux is equally useful for a reacting binary mixtures of liquids or of gases. Let us consider next the case when the reacting mixture can be considered as a mixture of ideal gases and then

$$\varphi^1 = \varphi_0^{(1)}(T) + \frac{RT}{\mu_1} \ln \frac{p(\eta_1/\mu_1)}{(\eta_1/\mu_1) + (\eta_2/\mu_2)} \qquad [36]$$

$$\left(\frac{\partial \varphi^{(1)}}{\partial \eta_1}\right)_{p,\,T} = \frac{RT}{\eta_1} \frac{1}{\eta_1 \mu_2 + \eta_2 \eta_1} \qquad [37]$$

From this we obtain, for a binary mixture of reacting gases, the following expression for the heat conduction

$$\lambda_0 = \lambda + \frac{(D_{12}^T)^2}{D_{12}} \eta_2 \eta_1 \frac{\rho RT}{\eta_1 \mu_2 + \eta_2 \mu_1} + D_{12} \eta_1 \eta_2 (\eta_1 \mu_2 + \eta_2 \mu_1) \frac{\rho (h_1 - h_2)^2}{RT^2} + 2\rho \eta_1 \eta_2 D_{12}^T (h_1 - h_2) \qquad [38]$$

or, introducing

$$k_T = D_{12}^T T / D_{12} \qquad [39]$$

the thermal diffusion relation, and

$$\bar{\mu} = \frac{\mu_1 \mu_2}{\mu_2 \eta_1 + \mu_1 \eta_2} \qquad [39a]$$

the mean molecular weight, we obtain finally

$$\lambda_0 = \lambda + k_T^2 \frac{\eta_1 \eta_2 \bar{\mu}^2}{\mu_1 \mu_2} D_{12} \frac{p}{T} + \eta_1 \eta_2 \mu_1 \mu_2 \frac{p}{T} D_{12} \left\{\left(\frac{h_1 - h_2}{RT}\right)^2 + 2k_T \frac{\bar{\mu}}{\mu_1 \mu_2} \left(\frac{h_1 - h_2}{RT}\right)\right\} \qquad [40]$$

This expression determines the coefficient of heat conduction of a reacting binary mixture of gases in the state of local equilibrium. The thermal flux is then expressed as

$$I^{(q)} = -\lambda_0 \nabla T \qquad [41]$$

The coefficient λ_0 is expressed in terms of the following transport coefficients

λ = coefficient of heat conduction of stationary state of the nonreacting gases

D_{12} = coefficient of ordinary diffusion, defined by Equation [31]

k_T = thermal diffusion ratio, see Equation [39]

The definition of k_T includes also the coefficient of thermal diffusion D_{12}^T, which is defined by Equation [32].

If the number of inelastic collisions accompanied by the reaction is small compared with the total number of collisions, then all these coefficients can be calculated by the ordinary techniques of modern kinetic theory of gases (the Chapman-Enskog method). The coefficient λ includes corrections for the heat conduction of the internal degrees of freedom (i.e., corrections of the same type as introduced by Euken).

Inasmuch as $[(h_1 - h_2)/RT]\mu$ is a large quantity, and k_T is a small one, the second term of Equation [40] is small compared with the remaining terms. Consequently, the third term is greater than the fourth, but not enough so as to permit the neglecting of the latter in calculating the heat conduction. The third and fourth terms are comparable with the value of λ, and in some cases exceed it considerably.

The problem of heat conduction in a binary mixture of reacting gases was the subject of a paper by Nernst at the beginning of this century [this work is mentioned in (4)]. Nerst considered a mixture of ideal gases and did not take thermal diffusion into account; he therefore obtained only one of the three terms that supplement the ordinary heat conduction (λ), namely, a term proportional to the square of $(h_1 - h_2)/RT$. This problem was analyzed by modern thermodynamic methods by Haase (4). Haase arrived at an expression similar to that obtained in this paper, but without the first correction term (proportional to k_T^2). This difference is due apparently to the difference in the definition of the concept "heat flux." In addition, Haase considered a case in which the reaction occurs in a mixture without a pressure gradient, i.e., a case having little interest in hydrodynamics.

We note that the transport coefficients for a binary mixture, calculated in (3), are related to the coefficients in Equation [40] by the relations

$$\lambda^1 = \lambda \qquad [42]$$

$$D_{12}^1 = D_{12} \qquad [43]$$

$$D_{12}^{T1} = D_{12}^T T \xi_1 \xi_2 \qquad [44]$$

$$k_T^1 = k_T \xi_1 \xi_2 \qquad [45]$$

where

λ^1 = heat conduction coefficient for a binary mixture of gases, after Chapman

D_{12}^1 = diffusion coefficient, after Chapman

D_{12}^{T1} = coefficient of thermal diffusion, after Chapman

k_T^1 = thermal diffusion ratio, after Chapman

ξ_1, ξ_2 = molar fractions of the components A_1 and A_2

The connection between the molar (ξ) and mass (η) fractions is given by the equations

$$\xi_i = \frac{\eta_i/\mu_i}{(\eta_1/\mu_1) + (\eta_2/\mu_2)} = \frac{\eta_i}{\eta_1 + \eta_2 \nu} \qquad [46]$$

$$\eta_i = \frac{\mu_i \xi_i}{\mu_1 \xi_1 + \mu_2 \xi_2} = \frac{\xi_i}{\xi_1 + (\xi_2/\nu)} \qquad [47]$$

where $\nu = \nu_1/\nu_2$ is the ratio of the stoichiometric coefficients of the reaction.

To solve any hydrodynamic problem it is necessary to write also, in addition to the energy equation, the continuity equation and the equation of motion. Neither equation changes in the presence of a reaction. Under conditions of local equilibrium, in order to make this a closed system of equations it is enough to supplement it with the system of equations of chemical equilibrium, which, in the case of a reaction in the binary mixture of gases, reduces to one equation,

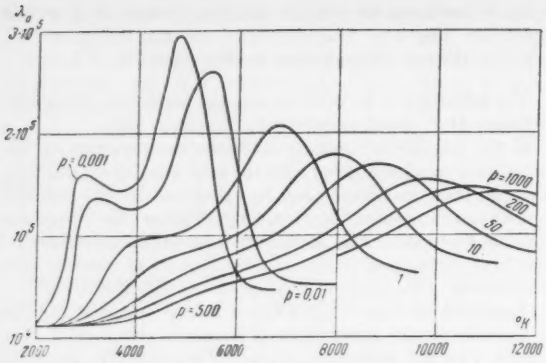

Fig. 2 Coefficient of heat conduction in erg/cm-sec-deg as a function of the temperature for various pressures p, atm

expressing the law of effective masses. Consequently, the resultant system of equations includes the following kinetic parameters: L_{q1}, L_{qq}, ν' and ν''; here ν' and ν'' are shear and bulk viscosities, respectively, which enter into the expression for the stress tensor. In the general case the heat flow depends on two transport coefficients L_{q1} and L_{qq}, but on the basis of the foregoing discussion it can be expressed, in the case of local equilibrium, in terms of one coefficient λ_0 from Equation [40].

In the case of a boundary layer, the stress tensor terms proportional to the bulk viscosity drop out of the equations, and the system of the phenomenological equations then depends only on two transport coefficients: The shear viscosity ν' and the coefficient of heat conduction of equilibrium reacting mixture λ_0.

Calculations of the coefficient of heat conduction in a reacting binary mixture of gases (λ_0) in equilibrium, performed on the basis of formula [40] are given in the 1955 report of the Laboratory of Physics of Combustion, Power Research Institute (11). See Fig. 2.

References

1 de Groot, S. R., "Thermodynamics of Irreversible Processes," Interscience Publishers, Inc., N. Y., 1951.

2 Denbigh, K. G., "The Thermodynamics of the Steady State," John Wiley & Sons, Inc., N. Y., 1951.

3 Chapman and Cowling, "The Mathematical Theory of Non-Uniform Gases," Cambridge University Press, 1953.

4 Haase, *Zeits. f. Naturforschung*, 1953.

5 Report, Laboratory for Physics of Combustion, Power Scientific Research Institute, 1955.

6 Hirschfelder, Bird and Spotz, *J. Chem. Phys.*, vol. 16, 1948, p. 968; vol. 17, 1949, p. 1343.

7 Mason, *J. Chem. Phys.*, vol. 22, no. 2, 1954.

8 Hirschfelder, Curtiss and Bird, "Molecular Theory of Gases and Liquids," New York, 1954.

9 Amdur, *J. Chem. Phys.*, vol. 4, 1936, p. 339.

10 Report, Laboratory for Physics of Combustion, Power Scientific Research Institute, 1954.

11 Report, Laboratory for Physics of Combustion, Power Scientific Research Institute, 1955.

Reviewer's Comment

A calculation of the coefficients of viscosity and thermal conductivity of air in the temperature range 2000 to 8000 K and the pressure range 0.001 to 1000 atm is discussed in this paper. Clearly, the problem is one with important technical applications. It is disappointing that the present paper presents only rough results obtained some time ago (1955), and these results are given only in graphical form.

The treatment is based on a model in which air is idealized as a binary mixture of "atoms" and "molecules." The problem of predicting the three intermolecular potentials is discussed at some length. In the actual calculations the molecule-molecule interaction is taken to be of a modified Buckingham form and, because of a lack of information, the atom-atom in atom-molecule interactions are taken to be of the simple rigid sphere form. The choice of the rigid sphere diameters is made by an interesting interpolation in the periodic table based on a few known values.

The transport of energy in a reacting gas mixture is discussed from the point of view of the thermodynamics of irreversible processes. It is concluded that, if the reaction rates are sufficiently rapid, the transport of energy is described by a single effective coefficient of conductivity. The calculation of this effective coefficient of conductivity is discussed and the results are given graphically.

—C. F. Curtiss
University of Wisconsin

Methods of Combatting Interfering Currents That Arise at the Input of an Electrostatic Fluxmeter Operating in a Conducting Medium

I. M. IMYANITOV and
YA. M. SHVARTZ

ONE of the authors (3)[1] proposed the use of an electrostatic rotary-type fluxmeter to measure the charge acquired by a satellite through a variety of processes, starting with diffusion charging due to difference in thermal velocities of the ions and electrons in the plasma of the ionosphere, and ending with charging due to ultraviolet rays.

The operation of an electrostatic fluxmeter mounted on an insulated body in a plasma can be briefly reduced to the following. The stator of the fluxmeter, a detailed description of which can be found in the monograph (1) by one of the authors, is a section of the surface of the body, but electrical contact with the remaining surface (the outer shell of the body) is through resistor R, which serves as the input resistance for the instrument. It is obvious that under steady state conditions when the rotor is stationary, the surface of the stator has the same potential and the same surface-charge density as would be possessed by that part of the surface which the stator replaces. Because of the periodic screening of the stator by the rotor, which is very close to the stator, the space charge, which always surrounds a charged surface in a plasma, causes periodic flow of surface charge to and from the stator. This displacement current flowing through the resistance R produces a voltage drop, which is measured with the vacuum-tube circuit.

However, along with this displacement current, produced as noted by changes in charge as the stator is being screened, additional currents can flow to this plate in a plasma and thus distort the measurement. These currents result from the fact that the medium in which the meter is placed is conducting.

Such conduction currents can be caused by the following factors.

1 The satellite may move with a speed comparable to the thermal velocities of the ions and electrons; this causes current to flow to the satellite surface.

2 The potential of the satellite at the place where the electrostatic fluxmeter is located may deviate from the equilibrium value, i.e., from the potential that an isolated body placed in the plasma would acquire at rest. This is caused by the motion of the satellite in the magnetic field, by the flow of displacement current in the input resistance, or by a forced change of potential in some section of the satellite surface.

3 The satellite surface may be exposed to ultraviolet, x-rays, and other types of radiation capable of producing photoemission.

4 Current may be produced by motion through the ionosphere.

The major distinguishing feature of the conduction current is that its instantaneous value is proportional to the area of the exposed portion of the stator. It is therefore 90 deg out of phase with the displacement current, if the fluxmeter itself can be considered an active load (1). An estimate of the order of magnitude of the conduction current shows that for a charged particle concentration $N = 10^6/\text{cm}^3$, the limiting value of the current density does not exceed 10^{-7} amp/cm^2. At the same time, the photocurrent density does not exceed 10^{-8} amp/cm^2.

The appearance of conduction current (3) at the input of the measuring circuit of the electrostatic fluxmeter raises the lower limit of the electrostatic field measured by this fluxmeter, and consequently also the lower limit of the measured satellite charge. A way must therefore be found of combatting the conduction current.

The fact that the conduction current is 90 deg out of phase with the displacement current when the fluxmeter operates as an active load (1) affords an opportunity of greatly reducing the influence of the conduction current by using a synchronous detector at the output of the fluxmeter measuring circuit.[2] (See Fig. 1.)

In fact

$$U_{out} = U_{in} \cdot k \cdot \cos\varphi$$
$$U'_{out} = U'_{in} \cdot k \cdot \cos(\varphi + 90 \text{ deg}) = |U'_{in} \cdot k \cdot \sin\varphi| \quad \ldots\ldots [1]$$

where

U_{in} = effective value of the displacement signal input voltage
U_{out} = signal voltage at the output of the synchronous detector
U'_{in} = effective value of the conduction input voltage
U'_{out} = conduction voltage at the output of the synchronous detector
k = gain of the measuring circuit
φ = phase shift between the reference (commutator) voltage of the synchronous detector and the signal voltage of the detector, due to the operation of the measuring circuit

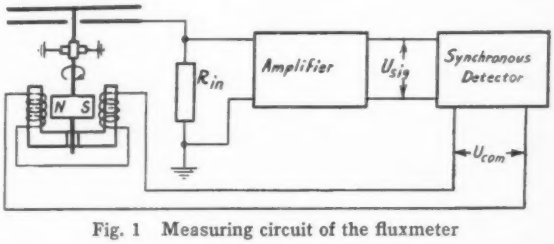

Fig. 1 Measuring circuit of the fluxmeter

Translated from *Iskusstwennye Sputniki Zemli* ("Artificial Earth Satellites"), No. 3, USSR Acad. Sci. Press, Moscow, 1959, pp. 77–83.

[1] Numbers in parentheses indicate References at end of paper.

[2] The problem of the use of synchronous detectors in electrostatic-fluxmeter circuits is considered in detail in (1).

In the ideal case, when $\varphi = 0$ deg, the use of the synchronous detector would permit complete elimination of the conduction voltage. In an actual circuit, however, it is impossible to obtain a zero phase shift in the measuring circuit over the entire operating frequency range; furthermore, variation in the temperature characteristics of the components used in the circuit also prevents a zero phase shift to be maintained over the entire temperature range. Finally, difficulties lie also in the fact that the actual wave forms of the input voltages (Fig. 2) contain higher harmonics, as a result of which it is impossible to suppress the conduction voltage completely.

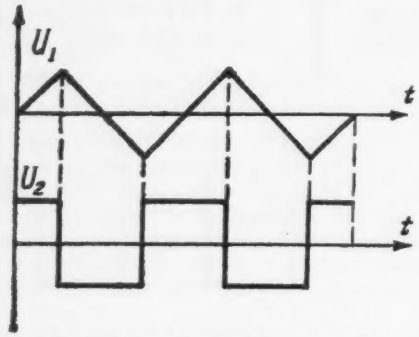

Fig. 2 Wave forms of input voltages

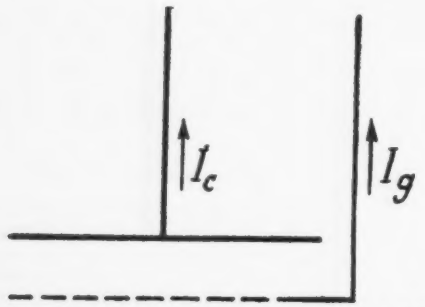

Fig. 3 Diagram of experiment on the determination of the ratio of the currents flowing on the grid and on the collector

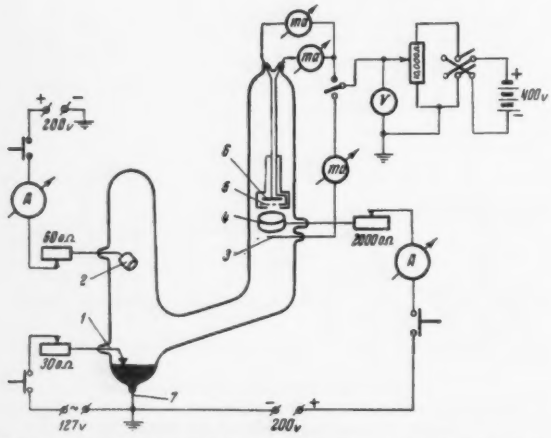

Fig. 4 Overall diagram of the experiment: 1—ignitor, 2—main anode, 3—probe, 4—auxiliary anode, 5—grid, 6—collector, 7—cathode

Let us dwell on another method of reducing the conduction current. We recall that in ordinary electrostatic fluxmeters a-c amplifiers are usually employed. Therefore the conduction current is amplified only when it is modulated by the rotation of the rotor. This brings to mind the following method of reducing the conduction current—construct the rotor and stator plates in such a way as to reduce, on the one hand, the modulation of the flux of charged particles incident on the stator and on the other hand, the absolute magnitude of the current incident on the surface of the stator. This can be done by making the rotor and stator in the form of metallic grids of certain electrical and optical transparency.

To verify the ability of a grid to transmit charged particles without stopping them, we determined experimentally the ratio I_g/I_c of the electric currents flowing in the grid and collector of a mercury gas discharge (Fig. 3). The general experimental setup is illustrated in Fig. 4. The parameters of the plasma were determined from the probe characteristics and were as follows for the condition of the experiment: Electron temperature, 20,000 K; electron concentration, 10^9 to 10^{10} cm^{-3} at a mercury vapor pressure of 1.3×10^{-3} to 5×10^{-4} mm mercury.

Fig. 5 shows the dependence of I_g/I_c on the thickness d of the space charge layer near the grid (calculated theoretically as a function of the potential applied to the grid and to the collector). In the experiment we used a metal grid with square (0.5×0.5 mm) meshes made of 30 μ wire. As seen from Fig. 5, at space charge layer thicknesses considerably in excess of the linear dimensions of the grid cells, the grid current is several times smaller than the collector current, meaning that the charged particles pass through the grid meshes without being stopped. This results from the fact that when the space charge layer is considerably thicker than the dimensions of the individual mesh, the distribution of the electric field at the grid has approximately the same character as in a parallel-plate capacitor. Consequently the particles entering the plane of the grid have a velocity component directed perpendicular to the plane of the grid, and therefore penetrate freely

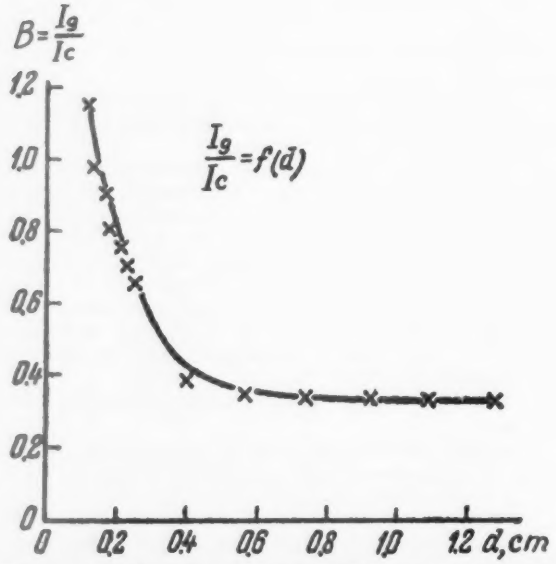

Fig. 5 Dependence of I_g/I_c on the thickness of the space charge layer near the grid

into the space behind the grid where they are trapped by the collector.

The use of a grid instead of a solid rotor reduces the modulation of the charged-particle current, and the use of a grid-like stator reduces the absolute magnitude of the current. However, the parameters of the grid, the dimension of their meshes and the diameter of the wires should be chosen such that the electric field produced by the space charge at the surface does not penetrate beneath the grid; in other words, the grid must be equivalent to a metal plane as regards the distribution of the electric field at the surface. There are known formulas for the calculation of the electric constant of grids in a vacuum (2), which can be used in the first approximation to calculate the grids of the rotor and stator for the case when the space charge layer is considerably thicker than the linear dimensions of the grid meshes.

The construction of the receiving part of the electrostatic fluxmeter is shown schematically in Fig. 6, where 1 is the rotor, 2 is the stator and 3 is the collector. Parts 1 and 2 are made, as usual, in the form of multisector plates. The collector serves to trap the charged particles passing through the grids of the stator and the rotor.

Rotor 1, made of wire mesh, should have a lower electric penetration factor than stator 2, which in turn should have a lower penetration factor than collector 3. Let us denote the distance between the rotor and stator by x_{12} and that between the stator and the collector by x_{23} (naturally, the spacing between the mesh wires should be chosen less than x_{12} or x_{23}).

To calculate the electric penetration factor of the rotor (assuming the stator to be a metallic surface) we use the formula

$$a_1 = \frac{C_{a_2}}{C_{a_1}} = \frac{\ln \coth \pi\sigma}{2\pi x_{12} Lg - \ln \cosh \pi\sigma} \qquad [2]$$

where

σ = filling factor of the grid
$Lg = (2/p)[1 - (dg/p)]$ for a square-mesh grid

To calculate the electric penetration of the stator we used the following formula

$$a_2 = \frac{C_{a_2}}{C_{a_3}} = \frac{\ln \coth \pi\sigma}{2\pi x_{23} Lg - \ln \cosh \pi\sigma} \qquad [3]$$

The values of a_1 and a_2 determine the fraction of the source field that penetrates through the grids.

Let us note that the formulas underestimate somewhat the values of a_1 and a_2, since the formulas can be used only when the source is located at a distance greater than the dimension of the grid mesh (2). The field produced by the space charge located near the grid, at distances less than the spacing of the grid, will penetrate much more strongly than indicated by the foregoing formulas. However, in view of the fact that at ion concentrations and temperatures observed in the plasma of the ionosphere the thicknesses of the space charge layers at negatively charged values will be on the order of a centimeter, it is possible to select the wire spacing in the grid such as to make the error, due to disregarding the space charge near to the grid, less than 10 per cent.

By way of an example, let us perform calculations based on formulas [2] and [3] for $x_{12} = 0.3$ cm, $x_{23} = 1$ cm, and grids with square meshes and the following parameters: Spacing 0.5 and 1 mm, wire diam 30 μ. The calculation data are given in the following

Spacing, mm	σ	a_1	a_2
0.5	0.12	0.01	0.002
1	0.06	0.05	0.01

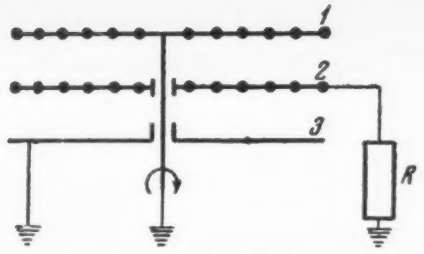

Fig. 6 Diagram showing receiving portion of the electrostatic fluxmeter

These calculations show that the grids, while almost completely shielding the electric field, permit the passage of the charged particles, trapping only a small fraction of the latter. If the electric data are available on the circuit actually employed, and if the coefficients a_1, a_2 and b are determined (see material which follows), it is possible to choose the necessary combination of grid and collector parameters.

The method proposed for combatting the conduction current due to the charged particles is equally applicable for combatting photocurrent, since the use of a rotor in the form of a grid greatly attenuates the modulation of the radiation fluxes that create the photocurrents. The coefficient of attenuation in this case is equal to σ, the filling factor. In addition, the use of a stator in the form of a grid reduces greatly the area subjected to the action of the radiation, and consequently decreases the magnitude of the photocurrent by a factor $1/\sigma_{eff}$. However, since the collector is close to the stator, photoelectrons may strike the latter and consequently σ_{eff} may increase. In general, however, the conduction current J'_{phot} produced at the input by a photocurrent J_{phot} is $J'_{phot} = J_{phot} \cdot \sigma \cdot \sigma_{eff}$.

Let us consider still another way of combatting conduction current—the use of negative feedback proportional to the conduction voltage.

Indeed, by using two detectors in parallel at the output of the measuring circuit, one tuned to the displacement signal voltage and the other to the conduction voltage, and by feeding back the detected conduction voltage to the input (4), it is possible to reduce greatly the amplitude of the a-c conduction voltage at the input of the synchronous detector. The effectiveness of such negative feedback depends greatly on the extent to which the wave form of the input a-c voltage, produced by the feedback, coincides with the wave form of the input conduction voltage, i.e., it will depend on the purity of the wave form of the input conduction voltage.

In concluding the survey of the methods that can be used to combat conduction current at the input of the fluxmeter, let us estimate the minimum value of the electrostatic field intensity, determined by the charge density on the surface of the satellite, which could be measured with an electrostatic fluxmeter without the use of additional data on its orientation.

Let us introduce the following notation

$$n = \frac{u'}{u''} \qquad [4]$$

where

u' = value of minimum measurable signal voltage at output
u'' = value of the conduction voltage at the output

$$u' = u'_{in} \cdot k \cdot \cos\varphi$$
$$u'' = u''_{in} \cdot k \cdot \sin\varphi \qquad [5]$$

u'_{in} = effective value of the minimum measurable signal voltage at the input
u''_{in} = effective value of the input conduction voltage

The remaining symbols are indicated in connection with Equation [1].

From the theory of the electrostatic fluxmeter it follows that

$$u'_{in} = \frac{E_{min} \cdot f \cdot R}{2\pi} \qquad u''_{in} = \frac{j_a \cdot bR}{2} \qquad [6]$$

where

E_{min} = minimum measurable value of the electric field intensity
f = commutation frequency
R = input resistance
j_a = maximum density of conduction current per unit surface
b = attenuation coefficient, equal to the product $b_1 b_2$
b_1 = coefficient of attenuation of the modulation of the charged-particle current by the rotor grid
b_2 = coefficient of attenuation of the charged-particle current by the stator grid

In Equation [6], the area of the stator S is taken to be unity, and the entire calculation is carried out for the first voltage harmonic.

Inserting the values of u'_{in} and u''_{in} into Equation [4] we obtain

$$n = \frac{E_{min} f}{\pi j_a b_1 \cdot b_2 \cdot \tan \varphi} \qquad [7]$$

Putting $n = 1$, we obtain for the value of the minimum measurable current, E_{min}

$$E_{min} = \frac{\pi j_a \cdot b_1 \cdot b_2 \cdot \tan \varphi}{f} \qquad [8]$$

Using $f = 1500$ cps, $j_a = 10^{-7}$ amp/cm^2, and $\tan \varphi = 0.03$, i.e., $\varphi = 2$ deg, we obtain several values for E_{min} as functions of the product $b_1 b_2$

$b_1 \cdot b_2$	0.1	0.04	0.01
E_{min} (v/cm	0.54	0.22	0.05

We emphasize that E_{min} is the minimum measurable electrostatic field intensity at the surface of the satellite, caused by its own charge, and determined under the conditions of maximum possible conduction current to the surface of the satellite. Inasmuch as the magnitude of the conduction current depends greatly on the orientation of the given portion of the surface relative to the satellite course, the values of E_{min} also depend on the same parameters.

For comparison with E_{min}, we list the values of the intensity of the electric field on the surface of a stationary sphere, produced by its own charge under the following plasma parameters: $N = 10^6$ and 10^5 cm^{-3}, $T_i = 1000$ K, $T_e = 5000$ and 10,000 K (we assume that the radius of the sphere is considerably greater than the thickness of space charge layer around it).

	$T_e = 5000$ K	$T_e = 10{,}000$ K
$N = 10^6$	1.0	1.2
$N = 10^5$	0.32	0.38

References

1 Imyanitov, I. M., "Pribory i metody dlya izucheniya atmosfernovo elektrichestva" (Instruments and Methods for the Investigation of Atmospheric Electricity), M. Gostekhisdat, 1957.

2 Katsman, Yu. A., "Osnovy rascheta radiolamp" (Principles of Design of Vacuum Tubes).

3 Imyanitov, I. M., *Uspekhi Fiz. Nauk* (*Progress in Physical Sciences*), vol. 63, no. 1B, 1957, p. 267 (translation published by International Physical Index, New York).

4 Imyanitov, I. M. and Mikhailovskaya, V. V., *Trudy GGO* (*Transactions, Main Geophysical Observatory*), no. 018, 1949, p. 64.

Reviewer's Comment

The senior author of this excellent article has been associated with the USSR program in atmospheric electricity for more than a decade. He is the leading Soviet proponent of the use of the rotating electrostatic fluxmeter, or electric field meter, to measure the electrical charge acquired by a satellite in the ionosphere.

The description of the operation of the fluxmeter is concise and conventional. The 90-deg phase displacement between the conduction and displacement currents was also recognized by American scientists in the upper atmosphere rocket research program at least as early as 1947 [Clark, 1949 (2)], although no detailed description of the theory of operation of this mechanical-commutator instrument was published. Later versions of this American device [Clark, 1957 (3)] used an electromagnetic commutator and synchronous detector very similar to the Soviet system. British workers have utilized the same quadrature phase relationship to eliminate precipitation current effects from measurements of the electric field strength at the Earth's surface [Mapleson and Whitlock, 1955(4)].

For some unaccountable reason, Imyanitov and Shvartz apparently do not use a variable phase adjustment in their commutator voltage source. This American technique gains a factor of about 10 below the USSR value of 0.03 for tan φ.

But the core of the present Soviet contribution is the ingenious metallic mesh construction of both the rotor and stator assemblies, which simultaneously decreases the photocurrent, the ion current, and the modulation of both currents, while maintaining high efficiency for the electric field measurement. As shown on the table following Equation [8], the factor of improvement varies from 10 to 100, depending on the percentage of open area of the mesh.

Combining these two factors, one favorable and the other unfavorable to the USSR, we find that the best Soviet fluxmeter is capable of measuring an electric field from six to ten times smaller than that which can be measured by the best solid-plate American model, for the same magnitude of interfering conduction current.

It should also be noted, from a comparison of the last two Soviet tables, that their best instrument is capable of measuring an electric field strength some six times smaller than that expected to occur at the satellite surface. This means that the American device is still adequate to make the measurement under these worst possible assumptions of electron density, satellite orientation and conduction current density [Bourdeau and others, 1960 (1)]. However, there is little doubt that the Soviet fluxmeter is at present potentially the best available for its purpose.

—John F. Clark
NASA
Washington, D. C.

1 Bourdeau, R. E., Jackson, J. E., Kane, J. A. and Serbu, G. P., "Ionospheric Measurements Using Environmental Sampling Techniques," presented at the First International Space Science Symposium, Jan. 12, 1960.

2 Clark, J. F., *Instruments*, vol. 22, 1949, p. 1007.

3 Clark, J. F., *J. Geophys. Research*, vol. 62, 1957, p. 617.

4 Mapleson, W. W. and Whitlock, W. S., *J. Atmos. Terr. Phys.*, vol. 7, 1955, p. 61.

Some Results of the Determination of the Structural Parameters of the Atmosphere Using the Third Soviet Artificial Earth Satellite

V. V. MIKHNEVICH
B. S. DENILIN
A. I. REPNEV
V. A. SOKOLOV

The problem of measuring the pressure and density of high layers of the atmosphere using an artificial Earth satellite was discussed in (1).[1] An analysis is given in this work of the state of the ideas held prior to 1957 regarding the structural parameters of the upper atmosphere. By that time the mean distributions of pressure, density and temperature up to a height of 100 km were known (2–4), and it had been established that at heights up to 90 km the atmosphere is intermixed, and that oxygen dissociates above 90 km (5). Up to 1956, direct measurements of the density, pressure and composition of the atmosphere above 100 km were very few in number, and therefore the ideas concerning the atmosphere at these altitudes were not well defined. In recent years experiments have been carried out on the determination of the density of the atmosphere at great altitudes (6–8). A particularly large contribution to the study of the upper layers of the atmosphere resulted from the investigations made with Soviet artificial Earth satellites, which made it possible to determine the density of the atmosphere both from measurements with manometers installed on the third Soviet Earth satellite (9) and from the drag on the satellites (10–11). The present article is devoted to an analysis of a part of the results of the determination of the density of the atmosphere obtained from manometer measurements on the third Soviet artificial satellite.

I Apparatus

THE APPARATUS (Fig. 1) used on the artificial Earth satellite to determine the density of the atmosphere included two ionization manometers (M_1 and M_2) and one magnetic electric discharge manometer (M_3).[2] The command for switching on the apparatus was transmitted from the program timing mechanism (PTM) to the switching-connecting device (SCD). The current between the electrodes of the manometer, proportional to the number of particles per unit volume, was fed to the input of a direct current amplifier (DCA). The output of the amplifier, which depended on the size of the input signal, was transmitted to Earth by a radiotelemetry system (RTS).

The position of the manometers on the satellite is shown in Fig. 2. The manometers were installed in conical recesses in the head part of the satellite, in so-called sockets. The manometers were secured in the sockets with the aid of panels equipped with hermetic contacts, through which the electrodes of the manometers were connected with the amplifiers and power supplies inside the satellite.

To eliminate the effect of atmospheric ions and electrons on the manometer readings, special traps were installed at their inputs (1,9). Besides this, a screen in electrical contact with the body of the satellite was placed at the edge of the socket protecting the collecting outlet of the manometer from incident charged particles.

To decrease the effect of desorbed molecules on the manometer readings, the outer shell of the satellite was made of materials having a maximum rate of desorption and a minimum vapor pressure. In addition, the manometers installed in the satellite were first outgassed and evacuated. The manometers were uncapped with the aid of a breaking device during the separation of the protective cone from the satellite after it was in orbit.

II Method

The density and pressure within a manometer chamber are not equal to their values in the atmosphere, owing to the high satellite velocity, temperature differences between the gas in the satellite and the free atmosphere, as well as changes of the orientation of the inlet aperture of the satellite relative to the velocity vector of the satellite.

At the altitudes of interest to us, the mean free path is very much greater than the characteristic dimension of the apparatus (the satellite). Under these conditions there are no collisions between particles in the inflowing stream and the particles that remain in the manometer. If the velocity of a body u is significantly larger than the mean thermal velocity of the particles in the medium, then $NSu \sin\theta$ particles will pass in a unit time through a manometer opening of area S (N is the number of particles per unit volume of the atmosphere, and θ is the angle between the velocity vector and the plane of the aperture). Undergoing a series of collisions with the walls of the manometer, the particles attain a most probable velocity v_1, which is determined by the wall temperature T_1. In one unit of time $(N_1\gamma_1/2\sqrt{\pi})S$ particles flow out of the manometer aperture. At equilibrium both particle fluxes are equal. From the equality of the fluxes, the concentration of particles N at a given point in the atmosphere is given by the formula

$$N = \frac{N_{A_v} \cdot P_i}{\sqrt{2\pi M R^* T_1 u \sin\theta}} \qquad (\theta \geq 7\text{–}8 \text{ deg})$$

Translated from *Iskusstvennye Sputniki Zemli* ("Artificial Earth Satellites"), No. 3, USSR Acad. Sci. Press, Moscow, 1959, pp. 84–97. Translation provided by the U. S. Joint Publication Research Service.

[1] Numbers in parentheses indicate References at end of paper.

[2] The construction and operating principle of the manometers are described in detail in (9, 12 and 13).

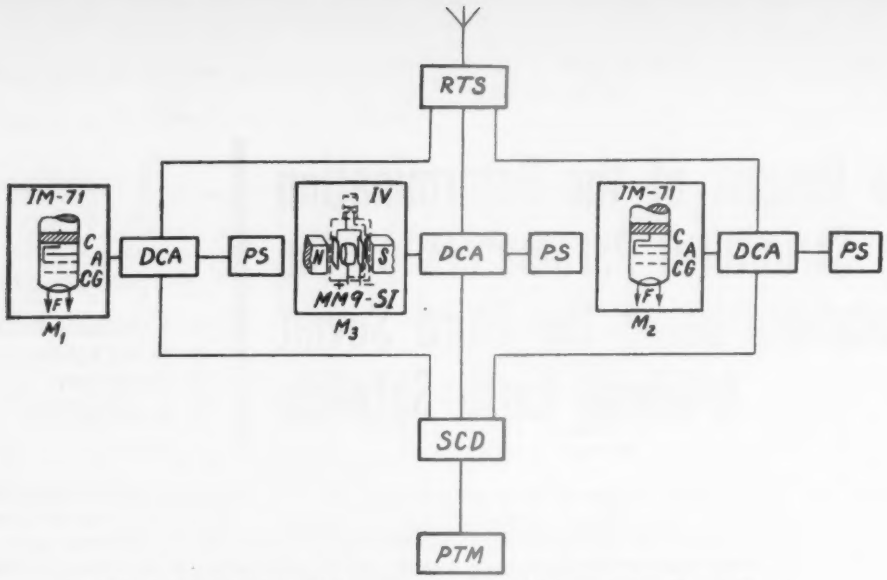

Fig. 1 Block diagram of the manometric apparatus mounted on the satellite

provided the manometer is graduated not in particle concentration N, but in pressure $P_1 = N_1 k T_1$. Here M is the molecular weight of the gas, R is the universal gas constant, and N_A is Avogadro's number.

The velocity u, which is needed for the calculation of N, is known with great accuracy from observations of the orbit. T_1 is measured directly on the satellite and is telemetered together with the manometer reading P_1.

The molecular weight was taken equal to that given in (14); see Table 1. The value of M above 600 km was obtained by extrapolation.

As is seen from the formula presented, a possible change in the molecular weight does not lead to a significant error in the determination of N. For example, a change of M from 18 to 24 gm/mole causes N to decrease less than 20 per cent.

The orientation of the inlet aperture of the manometer relative to the velocity vector of the satellite ($\sin\theta$) was determined from a method established in (15)

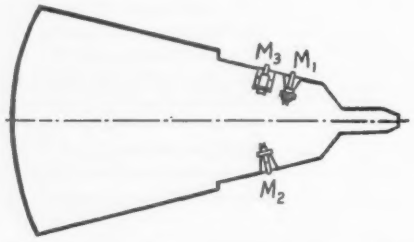

Fig. 2 Placement of the manometers on the satellite

$$\sin\theta = m\{\nu[A_1a + B_1b + C_1c] + \mu[A_2a + B_2b + C_2c] + \xi[A_3a + B_3b + C_3c]\} + n\{\nu[-A_1a' + B_1b' + C_1c'] + \mu[-A_2a' + B_2b' + C_2c'] + \xi[-A_3a' + B_3b' + C_3c']\} + k\{\nu[A_1a'' - B_1b'' + C_1c''] + \mu[A_2a'' - B_2b'' + C_2c''] + \xi[A_3a'' - B_3b'' + C_3c'']\}$$

where

$$\begin{aligned} a &= \cos\phi\cos\varphi - \sin\phi\sin\varphi\cos\theta_0 \\ b &= \sin\phi\cos\varphi + \cos\phi\sin\varphi\cos\theta_0 \\ c &= \sin\varphi\sin\theta_0 \\ a' &= \cos\phi\sin\varphi + \sin\phi\cos\varphi\cos\theta_0 \\ b' &= -\sin\phi\sin\varphi + \cos\phi\cos\varphi\cos\theta_0 \\ c' &= \cos\varphi\sin\theta_0 \\ a'' &= \sin\phi\sin\theta_0 \\ b'' &= \cos\phi\sin\theta_0 \\ c'' &= \cos\theta_0 \end{aligned}$$

Here ϕ, φ and θ_0 are the Eulerian angles; ν, μ and ξ are the direction cosines of the velocity vector in an absolute system of coordinates (the Z axis is directed toward Polaris, the X axis toward the vernal equinox, and the Y axis completes a right-handed coordinate system) as in Fig. 3; A_i, B_i and C_i ($i = 1, 2,$

Table 1 Variation of molecular weight with height

Height, km	Molecular weight, gm/mole	Height, km	Molecular weight, gm/mole	Height, km	Molecular weight, gm/mole	Height, km	Molecular weight, gm/mole
225	21.28	295	18.63	365	17.25	435	16.53
230	21.04	300	18.50	370	17.18	440	16.50
235	20.80	305	18.37	375	17.12	445	16.46
240	20.57	310	18.25	380	17.06	450	16.43
245	20.36	315	18.14	385	17.00	455	16.40
250	20.15	320	18.03	390	16.94	460	16.37
255	19.94	325	17.92	395	16.89	465	16.34
260	19.75	330	17.82	400	16.84	470	16.31
265	19.56	335	17.73	405	16.79	475	16.30
270	19.40	340	17.64	410	16.74	480	16.27
275	19.22	345	17.55	415	16.70	485	16.24
280	19.07	350	17.47	420	16.65	490	16.22
285	18.91	355	17.39	425	16.61	495	16.19
290	18.77	360	17.32	430	16.57	500	16.16

Table 2 Structural parameters of the atmosphere at heights of 225–500 km

Height, km	N, cm^{-3}	P, gm/cm^3	H, km	T, K	P, dyne/cm^2	P, mm Hg
225	$6.01 \cdot 10^9$	$2.12 \cdot 10^{-13}$	40.0	936	$7.76 \cdot 10^{-4}$	$6.25 \cdot 10^{-7}$
230	5.31	1.79	40.6	938	6.88	5.54
235	4.7	1.7	41.3	941	6.1	4.92
240	4.17	1.42	42.0	946	5.44	4.4
245	3.71	1.25	42.8	952	4.88	3.94
250	3.3	1.1	43.5	958	4.36	3.54
255	2.94	$9.73 \cdot 10^{-14}$	44.3	964	3.91	3.17
260	2.64	8.66	45.2	971	3.54	2.88
265	2.36	7.77	46.0	979	3.19	2.6
270	2.12	6.83	47.0	987	2.89	2.35
275	1.91	6.1	47.9	996	2.63	2.14
280	1.72	5.44	48.8	1005	2.39	1.95
285	1.55	4.87	49.7	1015	2.17	1.78
290	1.4	4.36	50.7	1026	1.98	1.62
295	1.27	3.93	51.7	1037	1.82	1.49
300	1.15	3.53	52.7	1048	1.66	1.37
305	1.07	3.26	53.7	1059	1.56	1.29
310	$9.57 \cdot 10^8$	2.9	54.5	1072	1.42	1.17
315	8.73	2.63	55.9	1084	1.31	1.008
320	7.98	2.39	57.0	1097	1.21	1.0
325	7.31	2.17	58.1	1110	1.12	$9.28 \cdot 10^{-6}$
330	6.7	1.98	59.2	1124	1.04	8.62
335	6.17	1.82	60.3	1138	$9.69 \cdot 10^{-5}$	8.06
340	5.68	1.66	61.5	1153	9.04	7.52
345	5.22	1.52	62.8	1169	8.96	7.46
350	4.82	1.4	64.8	1185	7.88	6.58
355	4.46	1.29	65.2	1200	7.39	6.18
360	4.13	1.19	66.7	1219	6.95	5.82
365	3.86	1.1	68.1	1237	6.59	5.53
370	3.56	1.02	69.5	1257	6.18	5.19
375	3.31	$9.41 \cdot 10^{-15}$	70.9	1276	5.83	4.9
380	3.08	8.72	72.4	1295	5.51	4.64
385	2.92	8.24	73.9	1305	5.26	4.44
390	2.69	7.56	75.2	1335	4.96	4.19
395	2.52	7.07	76.7	1353	4.71	3.98
400	2.36	6.6	78.9	1373	4.47	3.79
405	2.21	6.16	79.7	1393	4.25	3.6
410	2.08	5.78	81.2	1417	4.07	3.46
415	1.95	5.41	82.9	1440	3.88	3.3
420	1.84	5.09	84.6	1465	3.72	3.17
425	1.73	4.79	86.3	1489	3.56	3.04
430	1.64	4.51	88.1	1514	3.43	2.93
435	1.55	4.25	90.0	1539	3.29	2.82
440	1.47	4.03	91.7	1563	3.17	2.72
445	1.39	3.8	93.6	1589	3.05	2.62
450	1.32	3.6	95.5	1614	2.94	2.53
455	1.25	3.4	98.6	1643	2.84	2.44
460	1.19	3.23	99.9	1675	2.75	2.37
465	1.13	3.06	102.0	1709	2.66	2.3
470	1.08	2.92	104.5	1745	2.6	2.25
475	1.03	2.79	107.0	1781	2.53	2.19
480	$9.82 \cdot 10^7$	2.65	109.3	1810	2.45	2.13
485	9.4	2.53	111.5	1845	2.39	2.08
490	8.97	2.42	113.9	1880	2.33	2.02
495	8.61	2.31	116.5	1917	2.28	1.98
500	8.24	2.21	119.0	1953	2.22	1.94

3) are constants for a given loop

$A_1 = \cos\rho_0 \cos\gamma_0$ $\quad A^2 = -\sin\rho_0$ $\quad A_3 = \cos\rho_0 \sin\gamma_0$

$B_1 = \sin\gamma_0$ $\quad B_2 = 0$ $\quad B_3 = -\cos\gamma_0$

$C_1 = \sin\rho_0 \cos\gamma_0$ $\quad C_2 = \cos\rho_0$ $\quad C_3 = \sin\rho_0 \sin\gamma_0$

ρ_0 and γ_0 are angular coordinates of the angular momentum vector; m, n and k are the direction cosines of the manometer axes relative to the principal axes of the satellite.

After determining N (the number of particles per unit volume), the density ρ was calculated and also the height H of the homogeneous atmosphere[3]

Here N'' and N' are the number of particles per unit volume of the atmosphere at two points differing in altitude by $\Delta h = 10$ km.

Next were calculated the temperature

$$T = MGH/R^*$$

and the atmospheric pressure

$$P = k\,NT$$

when k is the Boltzmann constant.

[3] The value of H determined with this formula leads to an error of about 30 per cent compared with calculations based on the formula

$$H = -\frac{\Delta h}{2.3\,(\log N''/N' - \log T''/T')} \qquad H = -\frac{\Delta h}{2.3\,(\log N'' - \log N')}$$

It should be noted that in the determination of the density of the atmosphere we did not use the hypothesis that the local distribution of the particle velocities is Maxwellian at great heights. The height of the homogeneous atmosphere, the temperature and the pressure were calculated under the assumption that the usual barometric formula is appplicable to the rarefied gas in the presence of temperature gradients.

III Results

The third Soviet Earth satellite was launched on May 15, 1958. In accordance with the plan of the experiment, from the moment that the manometers were uncovered their discharge currents (corresponding to the density measurements) were continuously recorded, and periodic calibration of the

Table 3 Values of the density (in gm-cm^{-3}) at various heights from manometer measurements on rockets and from the drag on satellites

	Rocket data			Drag data	
Height, km	Containers and rockets. Mean latitude of European USSR	Viking-7 33° N lat.	Aerobee-Hi 59° N lat.	1957 a_1 1957 a_2 1957 B_1 1958 a 1958 B_2 1958 γ (10, 11)	1957 a_1 1957 a_2 1957 B_1 1958 a 1958 B_2 1958 γ (19–25)
100	$4 \cdot 10^{-10}$	$2.5 \cdot 10^{-10}$	$7 \cdot 10^{-10}$	...	...
110	$9.8 \cdot 10^{-11}$	$5 \cdot 10^{-11}$	$1.5 \cdot 10^{-10}$	...	...
120	$2.2 \cdot 10^{-11}$	$1.2 \cdot 10^{-11}$	$2 \cdot 10^{-11}$	...	$6.9 \cdot 10^{-11}$
130	$7.4 \cdot 10^{-12}$	$3.3 \cdot 10^{-12}$	$6 \cdot 10^{-12}$	...	$3.01 \cdot 10^{-11}$
140	$3.2 \cdot 10^{-12}$	$1.2 \cdot 10^{-12}$	$3 \cdot 10^{-12}$	...	$1.49 \cdot 10^{-11}$
150	$1.6 \cdot 10^{-12}$	$6.6 \cdot 10^{-13}$	$2 \cdot 10^{-12}$	...	$8.07 \cdot 10^{-12}$
160	$9.5 \cdot 10^{-13}$	$4.3 \cdot 10^{-13}$	$1.3 \cdot 10^{-12}$	...	$4.70 \cdot 10^{-12}$
170	$6.4 \cdot 10^{-13}$	$3.0 \cdot 10^{-13}$	$1 \cdot 10^{-12}$	...	$2.89 \cdot 10^{-12}$
180	$4.4 \cdot 10^{-13}$	$2.3 \cdot 10^{-13}$	$8 \cdot 10^{-13}$	...	$1.87 \cdot 10^{-12}$
186	...	...	...	...	$6.7 \cdot 10^{-13}$
190	$3.3 \cdot 10^{-13}$	$1.8 \cdot 10^{-13}$	$7.5 \cdot 10^{-13}$	...	$1.25 \cdot 10^{-12}$
197 ± 1	...	...	...	...	$7.0 \cdot 10^{-13}$
200	$2.7 \cdot 10^{-13}$	$1.4 \cdot 10^{-13}$	$7 \cdot 10^{-13}$	...	$(3\text{–}8.63) \cdot 10^{-13}$
201 ± 4	...	...	...	...	$6.7 \cdot 10^{-13}$
202 ± 4	...	...	...	...	$7.37 \cdot 10^{-13}$
206 ± 4	...	...	...	...	$5.4 \cdot 10^{-13}$
210	$2.0 \cdot 10^{-13}$	$1.1 \cdot 10^{-13}$	$6.0 \cdot 10^{-13}$	...	$6.04 \cdot 10^{-13}$
211 + 4	...	...	...	...	$4.6 \cdot 10^{-13}$
212	...	...	...	...	$(4.4\text{–}4.8) \cdot 10^{-13}$
215	...	...	...	...	$4.7 \cdot 10^{-13}$
220	$1.6 \cdot 10^{-13}$	$9.0 \cdot 10^{-14}$	...	...	$(3.5\text{–}5.7) \cdot 10^{-12}$
225	...	...	...	$(2.9\text{–}4.1) \cdot 10^{-13}$	...
228	...	...	...	$(2.4\text{–}3.2) \cdot 10^{-13}$	...
230	$1.25 \cdot 10^{-13}$	...	...	...	$3.32 \cdot 10^{-13}$
232	...	...	...	...	$1.5 \cdot 10^{-13}$
233	...	...	...	...	$2.2 \cdot 10^{-13}$
240	$1.1 \cdot 10^{-13}$	...	...	...	$2.51 \cdot 10^{-13}$
241	...	...	...	...	$2.5 \cdot 10^{-13}$
250	$9 \cdot 10^{-14}$	...	...	$(1.5\text{–}1.6) \cdot 10^{-13}$	$(1.1\text{–}1.9) \cdot 10^{-13}$
260	$6.9 \cdot 10^{-14}$	...	...	...	$1.51 \cdot 10^{-13}$
270	...	...	...	$(9.4\text{–}10) \cdot 10^{-14}$	$1.19 \cdot 10^{-13}$
275	...	...	...	...	$8.5 \cdot 10^{-14}$
280	...	...	...	...	$9.51 \cdot 10^{-14}$
290	...	...	...	$(5.8\text{–}7.0) \cdot 10^{-14}$	$7.68 \cdot 10^{-14}$
300	...	...	...	...	$(5\text{–}6.27) \cdot 10^{-14}$
310	...	...	...	$(3.8\text{–}4.7) \cdot 10^{-14}$	$5.16 \cdot 10^{-14}$
320	...	...	...	...	$4.29 \cdot 10^{-14}$
330	...	...	...	$(2.6\text{–}3.2) \cdot 10^{-14}$	$3.58 \cdot 10^{-14}$
340	...	...	...	...	$3.02 \cdot 10^{-14}$
350	...	...	...	$(1.8\text{–}2.2) \cdot 10^{-14}$	$(2.1\text{–}3) \cdot 10^{-14}$
360	...	...	...	...	$2.18 \cdot 10^{-14}$
368	...	...	...	$(1.4\text{–}1.5) \cdot 10^{-14}$	$(1.4\text{–}1.5) \cdot 10^{-14}$
370	...	...	...	...	$1.87 \cdot 10^{-14}$
400	...	...	...	...	$1.5 \cdot 10^{-14}$
					$9.3 \cdot 10^{-15}$
405	...	...	...	...	$(9^{+8}_{-4}) \cdot 10^{-15}$
450	...	...	...	...	$(1.0\text{–}4.5) \cdot 10^{-15}$
500	...	...	...	...	$(2.3\text{–}6) \cdot 10^{-15}$
550	...	...	...	...	$(2.2\text{–}4) \cdot 10^{-15}$
600	...	...	...	...	$2 \cdot 10^{-15}$ $6.8 \cdot 10^{-16}$
650	...	...	...	...	$1 \cdot 10^{-15}$ $3.8 \cdot 10^{-16}$
700	...	...	...	...	$7 \cdot 10^{-16}$
720	...	...	...	...	$(1.2 \pm 0.3) \cdot 10^{-16}$

Conventional designations of the satellites: 1957 a_1—Carrier rocket of the first Soviet satellite (launched Oct. 4, 1957); 1957 a_2—First Soviet artificial satellite (launched Oct. 4, 1957); 1957 a_3—Nose cone of first Soviet satellite (launched Oct. 4, 1957); 1957 B_1—Record Soviet artificial satellite (launched Nov. 3, 1957); 1957 B_2—Nose cone of record Soviet satellite (launched Nov. 3, 1957); 1958 a—Explorer satellite (launched Feb. 1, 1957); 1958 B_1—Carrier rocket of Vanguard (launched March 17, 1958); 1958 B_2—Vanguard I satellite (launched March 17, 1958); 1958 V—Explorer III satellite (launched March 26, 1958).

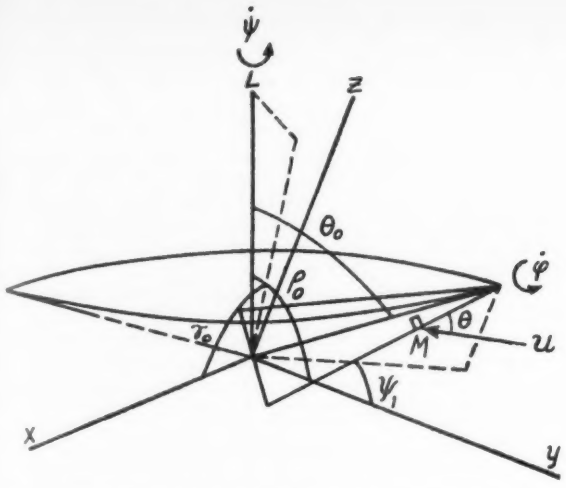

Fig. 3 Illustration of the orientation of the manometer in space

amplifiers was made, as were checks of the emission current and the manometer wall temperature.

The results obtained provide a description of the atmosphere at altitudes of 225–500 km for May 16, 1958. Measurements at various altitudes refer to different times of day (13:00–19:00 local time) and different geographical latitudes (57 deg N–65 deg N).

The values of the density obtained in the present experiment practically agree, in the region of perigee of the Soviet satellites (225–230 km), with the density values found from observation of the change of orbit (see Fig. 4a and Table 3).

At the same time, the values of density and pressure obtained are about 1.5–10 times greater than the values proposed by numerous models (14,16,17), with the exception of the model introduced in (18). See Figs. 4b and 5. In the majority of cases the models were based on generalizations of a very few observations on the upper layers of the atmosphere, obtained by various means, at different times of day and season, at different latitudes, etc. The experimental investigations of the upper layers of the atmosphere were isolated. The assumptions used in the construction of various models were distinct and often contradictory, for instance, the use of diffusion separation in some and intermixing in others. All this causes the models to be noticeably different from each other, so that they neither characterize the actual state of the atmosphere (since recent investigations indicate the pres-

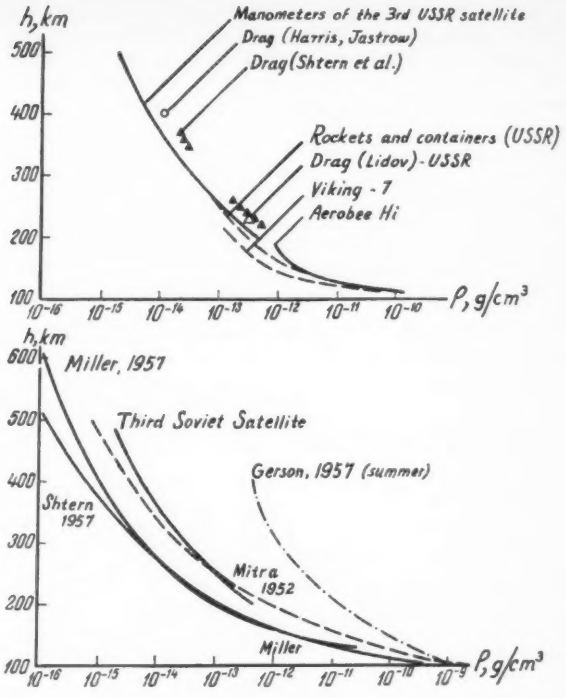

Fig. 4 Variation of density with altitude. (a) Experimental data; (b) based on several models.

ence of seasonal, daily, latitude and other variations, and indicate that it is incorrect to unify obtained data) nor yield statistical average values of the parameters, since the amount of data is insufficient for this.

Some of the differences in the data obtained from the manometer readings and from the satellite drag can be explained, obviously, by the presence of regular daily, seasonal and latitude variations as well as variations associated with solar disturbances.

It is known that the drag of the second and third Soviet satellites was not constant (27–30). In January 1958 the

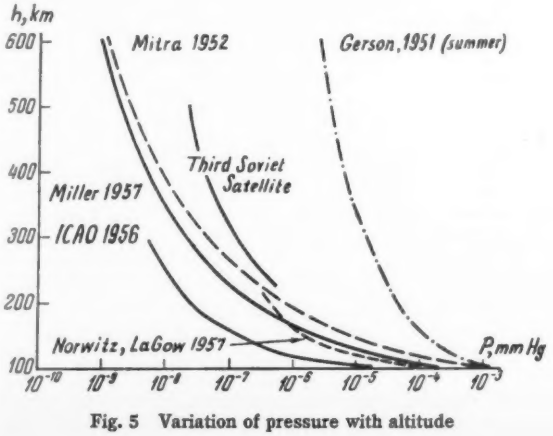

Fig. 5 Variation of pressure with altitude

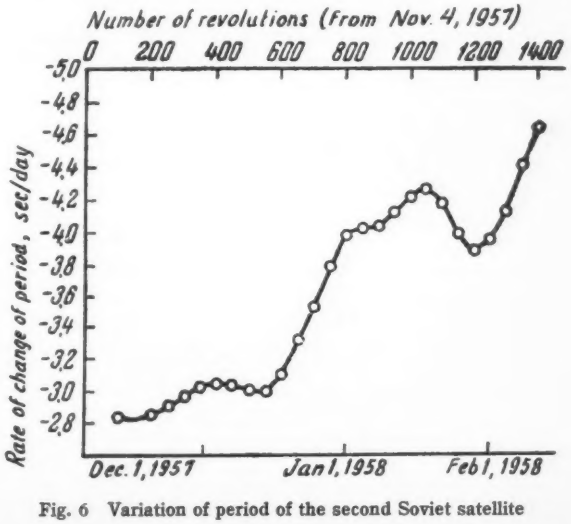

Fig. 6 Variation of period of the second Soviet satellite

rate of decrease of the period of the second satellite fluctuated between 4.4 and 3.9 sec per day (Fig. 6). In February an increase of from 3.9 to 5 sec per day alternated with a decrease of as much as 4.5 sec per day. The probable error in the determination of the period was found to be about 0.03 sec per day (27).

In the first days of the existence of the third satellite, the decrease in the period of rotation amounted to 0.97 sec per day, and after 450 revolutions (June 17) to only 0.59 sec per day (30). A retardation in the decrease of the period is also noticeable in a curve of the change of period with time (Fig. 7). Each point represents an average taken over 54 revolutions. It is noted in (30) that in the period from May 15 to July 17 the atmosphere contracted so to speak by an amount equal to 25 km.

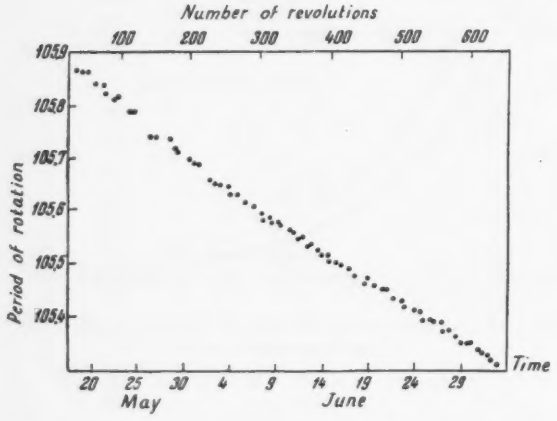

Fig. 7 Change of the period of rotation of the third Soviet satellite

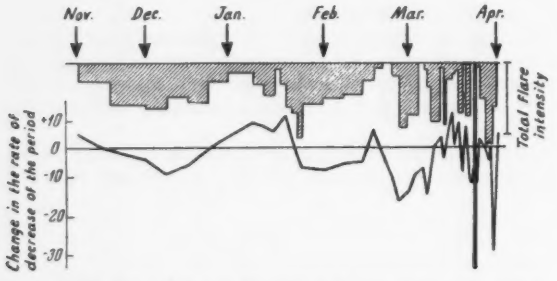

Fig. 8 Correlation between the rate of change of the period of rotation of the second satellite and the intensity of stellar flares

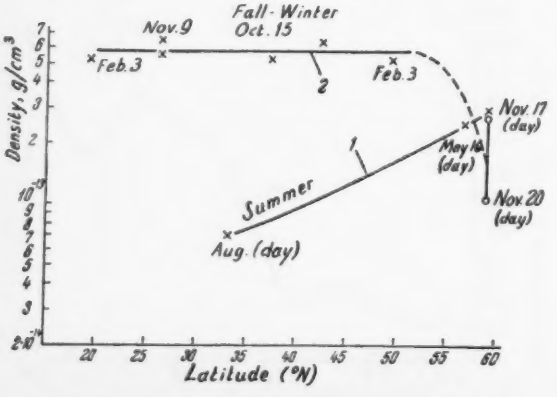

Fig. 9 Variation of density of atmosphere with latitude

In addition, during observations of solar activity and of the change of the period of rotation of the second Soviet satellite, it was observed that the strong magnetic storm in the middle of February 1958 and the 10 deg extension of the zones of the aurorae toward the Equator were accompanied by an increase in the change of the period of the satellite from 3.9 to 5 sec per day (31). Changes in the intensity of flares on the sun (i.e., the product of the area of a flare by its duration) also exhibit a correlation with the rate of change of the period of the satellite (32). See Fig. 8.

The results of rocket investigations point to the existence of daily, seasonal and latitude variations (33,8). Thus, according to the data of these articles, at a height of 200 km (Fort Churchill, 59 deg N) the summer daytime value of the density $(6.7 \pm 2.0) \times 10^{-13}$ gm/cm³ is approximately twice as high as the corresponding winter value

$$\left(3.6 \begin{matrix} +3.0 \\ -1.5 \end{matrix}\right) \times 10^{-13} \text{ gm/cm}^3$$

and five times larger than the winter night-time value of the density $(1.3 \pm 0.6) \times 10^{-13}$ gm/cm^{-3}. At the same height the density at latitudes 33 and 59 deg N on a summer day proved to be equal to $(1.4 \pm 0.5) \times 10^{-13}$ and $(6.7 \pm 2.0) \times 10^{-13}$ gm/cm³, respectively. The presence of a latitude effect is also shown by the results of investigations made with meteorological rockets (34), by the method of falling spheres (35), and in other ways.

The available experimental data are insufficient to provide the hoped-for determination of the functional dependence of density on latitude in the upper layers of the atmosphere (Fig. 9). However, all the results of rocket density measurements made with manometers on summer days (curve 1) display an

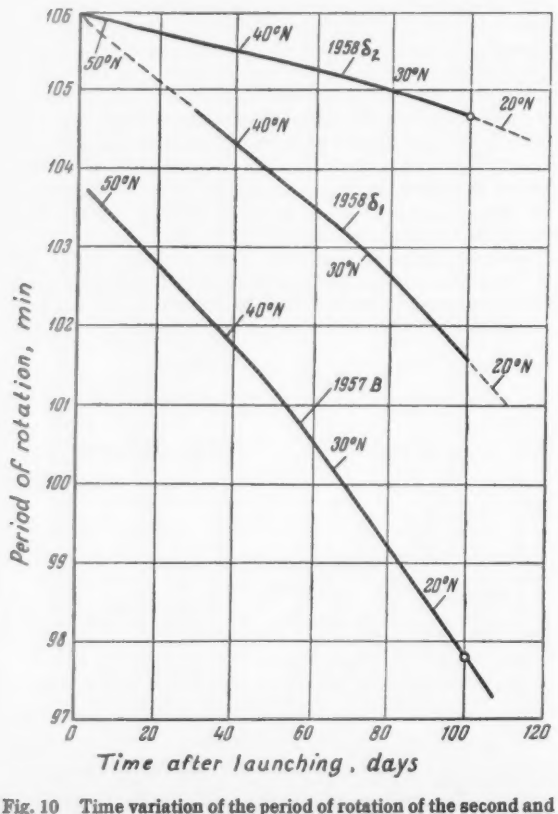

Fig. 10 Time variation of the period of rotation of the second and third satellites and the rocket of the third satellite with time

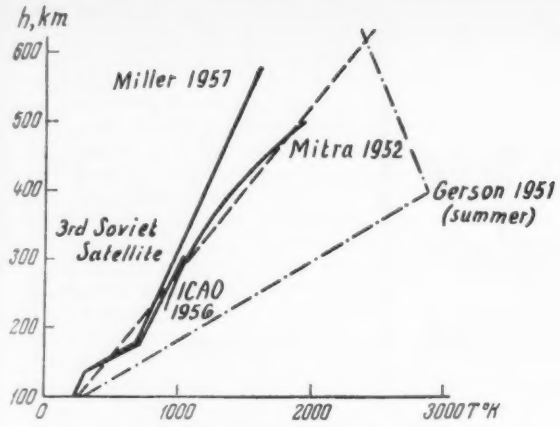

Fig. 11 Temperature of the atmosphere

increase in density with increasing latitude in the range 33–59 deg N. For winter days, however, there is observed a somewhat less pronounced increase of density with latitude [see (33) and Table 3, column 2].

The latitude effect on density in the fall and winter season, as gathered from observations of the change in orbit of the first and second Soviet satellites, is much weaker [see curve 2 in Fig. 9 and (36,37)], possibly because the same value for the height of the homogeneous atmosphere, $H = 30$ km, was used for all latitudes in extrapolation of the data to 206 km. In addition, it is possible that these data refer to different times of the day.

The observed kink in the curves of the periods of rotation of the second and third satellites and the carrier rocket of the third satellite vs. time as the latitude 30 deg is approached probably indicates an increase in density on approaching the Equator, owing to the equatorial bulging of Earth.

The facts enumerated attest to the fact that the state of the upper atmosphere may vary markedly and that it depends both on external effects on the atmosphere and also on the season, time of day and geographical latitude.

Values obtained from measurements on the third Soviet artificial Earth satellite, which give the density, height of the homogeneous atmosphere, temperature and pressure, characterize the state of the atmosphere at altitudes of 225–500 km for the daytime hours on May 16, 1958 at latitudes of 57–65 deg N. In particular, on May 16, 1958 the temperature of the atmosphere appeared to be relatively high (Fig. 11).

As a result of further reduction of all the experimental data, additional material will be obtained on the density, pressure and other parameters of the atmosphere, which will enable a clearer explanation of the dependence of the structural parameters on the latitude and time of day.

References

1 Danilin, B. S., Mikhnevich, V. V., Repnev, A. I. and Shvidkovskii, Ya. G., *Usp. Fiz. Nauk* (Progress in the Physical Sciences), vol. 63, 1957, no. 1b. (Transl. by International Physical Index Inc., N. Y.)

2 Mikhnevich, V. V. and Khvostikov, I. A., *Izv. AN USSR* (News of the USSR Acad. of Sciences), Geophysical Series, 1957, no. 11.

3 Mikhnevich, V. V., *Usp. Fiz. Nauk* (Advances in the Physical Sciences), vol. 63, 1957, no. 1b.

4 Alekseyev, P. P., Besyadovskiy, Ye. A., Golyshev, E. I., Izakov, M. N., Kasatkin, A. M., Kokin, G. A., Livshits, N. S., Masanova, N. D. and Shvidkovskiy, Ye. G., *Meteorologiya i gidrologiya* (Meteorology and Hydrology), 1957.

5 Mirtov, B. A., *Usp. Fiz. Nauk* (Advances in the Physical Sciences), vol. 63, 1957, no. 1b.

6 Mikhnevich, V. V., *Priroda* (Nature), 1958, no. 5.

7 Horowitz, R., La Gow, H. E., *Geophys. Res.*, vol. 62, no. 1, 1957.

8 La Gow, H. E., Horowitz, R., Ainsworth, J., *Ann. de Geoph.*, vol. 14, no. 2, 1958.

9 Mikhnevich, V. V., *Iskusstvennye sputniki Zemli* (Artificial Earth Satellites), 1959, no. 2. (To be published by Plenum Press, N. Y.)

10 Lidov, M. L., *ibid.*, no. 1.

11 El'yasberg, P. Ye., *ibid.*, no. 1.

12 Pen'chko, Ye. A. and Khavkin, L. P., *Pribory i tekhnika eksperimenta* (Apparatus and Technique of Experiment), 1959, no. 1.

13 Grigor'yev, A. M. and Volkov, G. P., *Elektronika* (Electronics), 1958, no. 12.

14 Miller, J., *Geophys. Res.*, vol. 62, no. 3, 1957.

15 Veletskiy, V. V. and Zonov, Yu. V., in press.

16 Mithra, S. K., *Verkhnyaya atmosfera* (The Upper Atmosphere) *Izd-vo inostr. lit.*, 1955.

17 Sterne, T. E., *Astron. J.*, vol. 63, no. 3, 1958.

18 Gerson, N. C., *Adv. in geophys.*, vol. 1, 1952.

19 Paetzold, H. K., *Raketentechn. u. Raumfahrtforsch.*, vol. 2, no. 2, 1958.

20 Sterne, T. E., *Science*, vol. 127, no. 3308, 1958.

21 Whipple, F., *Science*, 128, no. 3316, 1958.

22 Jacchia, L. G., "IGY Satellite Report," series no. 4, 1958.

23 Schilling, B. F., Sterne, T. E., "IGY Satellite Report," series no. 4, 1958.

24 Harris, I. and Jastrow, R., *Science*, vol. 128, no. 3321, 1958.

25 Harris, I., Jastrow, R., Report to the 5th Assembly of the CSAGI, Moscow 1958.

26 Sterne, T., *Science*, vol. 128, no. 3321, 1958.

27 Jacchia, L. G., *Sky and Telescope*, vol. 17, no. 6, 1958.

28 King-Hele, D. G. and Merson, R. H., *J. Brit. Interplanet. Soc.*, vol. 16, no. 8, 1958.

29 King-Hele, D. G. and Walker, D. M., *Nature*, vol. 182, no. 4639, 1958.

30 Hergenhahn, G., *Naturwissenschaften*, vol. 45, no. 18, 1958.

31 Bartels, J., *Naturwissenschaften*, vol. 45, no. 8, 1958.

32 Nonweiler, T., *Nature*, vol. 182, no. 4633, 1958.

33 La Gow, H. E., Horowitz, R. and Ainsworth, J., IGY World Data center A, "IGY Rocket Report Series," no. 1, 30 July 1958, Nat. Acad. Sci., Washington, D. C.

34 Shvidkovskii, E. G., *Iskusstvennye sputniki Zemli* (Artificial Earth Satellites), 1958, no. 2 (translated in ARS JOURNAL, vol. 29, no. 10, pp. 733–736.)

35 Jones, L. M., Fischbach, F. F. and Peterson, J. W., IGY World Data Center A., "IGY Rocket Report Series," no. 1, 30 July 1958, Nat. Acad. Sci., Washington, D. C.

36 Groves, G. V., *Nature*, vol. 181, no. 4615, 1958.

37 Priester, W. and Sterne, T., vol. 34, nos. 3–4, 1958.

Reviewer's Comment

This article is a competent account of experimental procedures and results obtained by USSR scientists in the measurement of upper atmosphere densities, using manometers in Sputnik III as well as in the analysis of the drag on the Sputniks. The discussion of Soviet work is completed by a general review of density determinations by rockets and satellites, and their theoretical interpretation, both in the U. S. and in the USSR.

The values of density and pressure quoted in the USSR paper agree with the results of other investigations in their indication that upper atmosphere densities are greater by an order of magnitude than the values predicted in earlier atmospheric models. Among the interesting aspects of the USSR results is the indication for a significant latitude dependence of density in rocket manometer measurements.

Mikhnevich et al. also report the detection of a latitude effect by the measurement of the drag on Sputniks I and II, although most U. S. and British analyses of satellite drag have not shown a significant latitude variation. It is clear that additional data, preferably obtained in situ by gages rather than by study of satellite orbits, will be required for the resolution of this very interesting question regarding the degree of latitude variations in the upper atmosphere. This reviewer is in agreement with the position taken by the USSR investigators, who conclude that the "state of the atmosphere may vary markedly and that it depends on external effects on the atmosphere and also on the season, time of day, and geographical latitude."

—ROBERT JASTROW
NASA
Washington, D. C.

Motion of a Slender Blunted Body in the Atmosphere With High Supersonic Speed

V. V. LUNEV

WE CONSIDER the question of the influence on the distribution of pressure over a thin blunted body (i.e., a body with a longitudinal dimension much greater than the dimension of the blunted edge) of the strong increase in entropy of the gas behind the nose shock wave arising from the blunted leading edge. The question of the effect of the blunted edge on the distribution of pressure, without allowance for the foregoing phenomenon, was considered by G. G. Chernyi (1,2).[1]

1 Let p $\rho_\infty V_\infty^2$, $\rho\rho_\infty$, iV_∞^2 and wV_∞ be the pressure, density, enthalpy and absolute velocity of the gas. The subscript ∞ refers to dimensional quantities in the fore stream. With a constant adiabatic exponent κ on the streamlines which intersect the shock wave at an angle φ, and with $M \sin \varphi \gg 1$, the flow parameters will be connected with p by means of the following relations[2]

$$\rho = \left(\frac{p}{\theta}\right)^{1/\kappa} \qquad i = \frac{\kappa}{\kappa - 1}\,\theta^{1/\kappa} p^{(\kappa-1)/\kappa} \qquad w = \sqrt{1 - 2i}$$

$$\theta = \frac{2}{\kappa + 1}\sin^2\varphi\left(\frac{\kappa - 1}{\kappa + 1}\right)^{\kappa} \qquad \text{[1.1]}$$

In our case the angle φ will range from $\pi/2$ to small values of the order of the relative slenderness of the body. At a distance of the order of the diameter of the blunted edge, downstream of the nose of the body, the pressure between the surface of the body and the shock wave is of the same order of magnitude as the pressure behind the shock, and $p \ll 1$ for slender bodies. From this we obtain from Eq. [1.1]

$$\frac{\rho}{\rho_0} \sim (\sin\varphi)^{-2/\kappa} \qquad \frac{i}{i_0} \sim (\sin\varphi)^{2/\kappa} \qquad \frac{1 - w}{1 - w_0} \sim \frac{i}{i_0} \qquad \text{[1.2]}$$

The subscript 0 refers to the flow quantities which have passed through the normal portion of the shock. The relations [1.2] show that at the surface of the blunted slender body there is formed a high entropy layer of gas,[3] in which the flow quantities have a different order of magnitude from those in the remaining region of flow, where $\sin\varphi \ll 1$. Near the surface of the body the condition $w \approx 1$, which holds in hypersonic flow for sharp slender bodies (law of plane sections), is not satisfied.

For flight in the atmosphere with $M \gtrsim 10$, the air in the high entropy layer is in a dissociated state. For qualitative deductions we can use here the visual constant adiabatic exponent formulas

$$i_0 = \frac{\kappa_0}{\kappa_0 + 1}\left(\frac{2}{\kappa_0 + 1}\right)^{1/\kappa_0} p^{(\kappa_0-1)^2/\kappa_0} \approx 0.5\, p^{(\kappa-1)/\kappa_0}$$

etc. ($p \approx 1$ at the critical point) with a smaller adiabatic exponent

$$\kappa_0 = 1.15 + 1.3$$

On a blunted cone of half-angle $\alpha = 10$ deg at $M = \infty$, at a large distance from the nose and with $\kappa_0 = 1.4$, 1.3 and 1.2, the values of i_0 and w_0 are 0.186, 0.224, 0.28 and 0.79, 0.745 and 0.665 respectively. Thus, as κ_0 is decreased, an ever-increasing part of the work done by the motion of the blunted nose will remain in the high entropy layer in the form of irreversible thermal energy and in the form of kinetic energy of the translational motion of the gas in the direction of the flight of the body. In accordance with the principal premises of references (1, 2 and 4) it follows from the foregoing arguments that the dissociation of the air in the high entropy layer should decrease the effect of the blunting on the distribution of pressures along the lateral surface of the body.

2 We shall confine ourselves henceforth to a consideration of axisymmetric bodies. Let r_0 be the radius from the axis

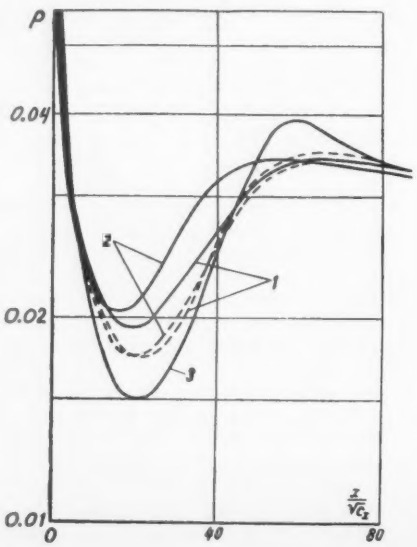

Translated from *Izvestiia Akademii Nauk SSSR, Otdelenie Tekhnicheskikh Nauk, Mekhanika i Mashinostroenie* (*Bull. USSR Acad. Sci., Div. Tech. Sci., Mechanics and Machine Building*), no. 4, 1959, pp. 131–133.

[1] Numbers in parentheses indicate References at end of paper.

[2] The limitation $M \sin\varphi \gg 1$ is used here only for simplicity; the phenomenon discussed in the following takes place for slender bodies even for $M \gtrsim 4$.

[3] A detailed examination of the flow in a high entropy layer for constant κ and variable flight conditions is given in (3).

of the blunt nose; xr_0 and yr_0 the Cartesian coordinates along and normal to the axis of the body, with the origin of the coordinates at the nose; r_0r, r_0R and r_0y_0 the shape (in the meridian plane) of the surface of the body, of the shock wave, and of the boundary of the high entropy layer respectively; and $V_\infty u$ the velocity component in the direction of the x axis.

At large values of M the shock wave has a large inclination only at points which lie opposite points of the surface with large slope. Therefore, by virtue of the remarks made previously, we can assume that the mass flow of gas in the high entropy layer equals the mass flow of the incident stream passing through an area equal to the area of the blunted portion from the axis, and that outside of this layer $u \approx 1$, i.e., $y = y_0$ is the line of contact discontinuity. Outside the high entropy layer we consider the gas to be perfect with a constant κ. As in (2) we assume that the pressure in the disturbed region, with the exception of a negligibly small region adjacent to the shock wave, is approximately equal to the pressure $p = p(x)$ on the surface of the body, and that the velocity of the gas in the direction of the y axis equals its value behind the shock wave

$$v(x) = 2R'(M^2R'^2 - 1)/[(\kappa + 1)M^2R'^2]$$

Such a rough approximate formulation of the problem is fully justified in estimating the influence of the foregoing effect. Applying the momentum and energy theorems to a layer of unit width fixed in space (perpendicular to the direction of motion), and taking into account the added work done by the pressure forces, mass transfer, momentum and energy transfer through this layer due to the longitudinal velocity of the gas, $1 - u$, we obtain the following system of equations for the motion of the gas

$$\frac{1}{\kappa + 1}\left(1 - \frac{1}{M^2R'^2}\right)R'R^2 = I + \int_0^x \left(p - \frac{1}{\kappa M^2}\right)Rdx \qquad [2.1]$$

$$2\left(\frac{1}{\kappa + 1}\right)^2\left(1 - \frac{1}{M^2R'^2}\right)^2 R'^2R^2 + \frac{p}{\kappa - 1}(R^2 - r^2) =$$

$$E - E_1(p) + \frac{R^2}{\kappa(\kappa - 1)M^2} + 2\int_0^x r'rpdx$$

$$E = (1/2)c_x)\,E_1 = \int_0^1 \left[\frac{(1 - u)^2}{2} - \frac{p}{\rho}\frac{1 - u}{u} + \frac{1}{u}\left(i - \frac{\kappa}{\kappa - 1}\frac{p}{p}\right)\right]d\psi$$

$$d\psi = 2\rho uydy$$

.....[2.2]

Here E and I are the dimensionless energy and momentum (per unit angle) along the y axis, imparted to the gas by the blunt nose (2), and c_x is the drag coefficient of resistance of the blunt nose.

Equations [2.1 and 2.2] differ from the corresponding equations obtained by G. G. Chernyi (2) in the inclusion of the term $E_1(p)$ which, as shown by analysis, is always positive. The value of $E_1(p)$ is comparable with the value E if the air in the high entropy layer is dissociated, and is negligibly small if the gas is assumed to be everywhere polytropic with $\kappa = 1.4$.

In order to make the system [2.1 and 2.2] closed at $x = 0$, we assume that the density of the gas in the regon $y_0 \leq y \leq R$ is equal to the density behind the shock ρ_1 at $x = 0$. Then

$$R^2 - y_0^2 = \frac{1}{\rho_1}(R^2 - 1) \qquad \rho_1 = \frac{(\kappa + 1)M^2R'^2}{2 + (\kappa - 1)M^2R'^2}$$

$$y_0^2 - 1 = \int_0^1 \frac{d\psi}{\rho u} \qquad [2.3]$$

From [2.1 to 2.3] we determine the initial values of p, R and R' at $x = 0$.

The figure shows the results of calculations of the pressure distribution p over cones with $\alpha = 10$ deg, blunted in the form of a hemisphere (curve 1) or flatly truncated (curve 2), flying at $M = 30$ at an altitude of the order of 40 km (solid lines) and in a constant property gas with $\kappa = 1.4$ (dotted). The values $c_x = 0.92$ and 1.8 were taken for the spherically blunted and flat faced nose respectively. The same figure shows curve 3, obtained at $M = \infty$ by G. G. Chernyi by a somewhat different formulation (2). We note that almost the same results are obtained by solving the system [2.1 + 2.2] at $M = 30$ and at $M = \infty$.

In the determination I, E_1 and y_0, the form of the shock wave arising from the blunted leading edge and the form of the blunt surface are assumed parallel. The distance between the shock and the body was determined from the formulas of (5), and the pressure was determined assuming a Newtonian pressure distribution. The values of the parameters for dissociated air were taken from the tables of (6).

The results given are evidence of the fact that in the atmosphere at very large flight velocities with thin blunt bodies ($M > 20$, for $\alpha = 10$ deg, as shown by calculations) the increase in entropy behind the shock wave arising from the blunted leading edge noticeably affects the pressure distribution at large distances downstream.

The author expresses his sincere gratitude to T. G. Korchikova and A. G. Kuz'mina for much help in the performance of the calculations.

References

1 Chernyi, G. G., "Flow Around Slightly Blunted Bodies," *Doklady Akad. Nauk SSSR (Trans. Acad. Sci.* USSR) vol. 114, no. 4, 1957.

2 Chernyi, G. G., "Flow Around a Slender Blunted Cone at High Supersonic Speeds," *Doklady Akad. Nauk SSSR (Trans. Acad. Sci. USSR)*, vol. 115, no. 4, 1957.

3 Moeckel, "Some Effects of Bluntness on Boundary-Layer Transition and Heat Transfer at Supersonic Speeds," NACA Rep. 1312.

4 Cheng and Pallone, "Leading-Edge Effect in Hypersonic Flow," *J. Aeronaut. Sci.*, no. 7, 1956.

5 Serbin, "Supersonic Flow Around Blunt Bodies," *J. Aeron. Sci.*, no. 1, 1958.

6 Predvoditelev, A. S., et al., "Tablitsy termodinamicheskikh funktsii vozdukha" (Tables of Thermodynamic Functions of Air), USSR Acad. Sci. Press, Moscow, 1957.

Original received February 4, 1959

Reviewer's Comment

The problem treated in the present translation is that of determining the pressure distribution on a thin blunted body in a hypersonic flow. In the United States, Cheng (1), and in Russia, Chernyi (2), have shown that with small blunting the hypersonic equivalence principle [or hypersonic similitude; see Hayes and Probstein (3)] can be applied, provided an additional similitude parameter which depends on the bluntness is invariant. In Russia the equivalence principle is referred to as the "law of plane sections." However, with blunting the equivalence principle fails in the vicinity of the blunt nose itself, as well as in a layer of fluid of high entropy near the surface of the body. Previous works have used the equivalence principle [e.g., Lees and Kubota (4), and (1, 2 and 4) of the present translation] in order to apply one-dimensional nonsteady inviscid solutions to the calculation of steady hypersonic flows over slender bodies with small nose blunting. In so doing the influence on the solution of the high entropy layer near the surface in which the equivalence principle fails was neglected. The importance of this entropy layer has previously been pointed out by Hayes and Probstein (5).

Lunev in his paper has investigated the effect of this entropy layer by assuming the shock layer to be divided into two regions by a discontinuous surface across which the longitudinal velocity can be discontinuous. The region between this contact surface and the body surface is termed a "high entropy layer." This layer results from the high entropy which arises behind the normal portion of the shock wave generated by the the blunt nose. Lunev assumes that in the region outside of the entropy layer, between the contact surface and the shock wave, that the flow variables are constant and have values equal to their values just behind the shock wave. He further assumes that the pressure and normal velocity are constant across the entire shock layer. The only question which arises here is that if the normal velocity is constant across the shock layer and depends only on the longitudinal coordinate, then if there is a discontinuity in the longitudinal velocity across the edge of the entropy layer one is led to the conclusion that there should be also a discontinuity in flow direction at the edge of the entropy layer. It would therefore seem that one should also take into consideration the normal velocity change across the shock layer. However, it is possible that this effect may turn out to be small.

Under Lunev's assumptions he derives the appropriate momentum and energy integrals for the flow taking into account the energy contained in the entropy layer. Using rough estimates for the shock shape, for the detachment distance at the nose, for the pressure distribution on the nose, and for the mass flow in the entropy layer he calculates a modified pressure distribution along the body surface which differs considerably from that obtained without consideration of the entropy layer. This reviewer believes these results to be very interesting and important.

—Ronald F. Probstein
Brown University

[1] Cheng, H. K., "Similitude of Hypersonic Real-Gas Flows Over Slender Bodies With Blunted Noses," *J. Aeron. Sci.*, vol. 26, 1959, pp. 575–585.
[2] Chernyi, G. G., "Gas Flow of High Supersonic Speeds," (in Russian), Gosizdat, Fiz-Mat. Lit., Moscow, 1959, pp. 205–209.
[3] Hayes, W. D. and Probstein, R. F., "Hypersonic Flow Theory," Academic Press, New York, 1959, pp. 30–52.
[4] Lees, L. and Kubota, T., "Inviscid Hypersonic Flow Over Blunt-Nosed Slender Bodies," *J. Aeron. Sci.*, vol. 24, 1957, pp. 195–202.
[5] Hayes, W. D. and Probstein, R. F., *J. Aeron. Sci.*, vol. 24, 1957, p. 64.

Investigation of a Stationary Discontinuity Surface in an Electromagnetic Field With a Gas Conductivity Jump

G. A. LYUBIMOV

THE PROPERTIES of discontinuity surfaces in ordinary gasdynamics have by now been thoroughly investigated. The conditions on such surfaces have been derived and their structure and stability have been investigated. Likewise, the discontinuity surfaces in an infinitely conducting medium have been investigated in magnetogasdynamics. This paper treats a stationary discontinuity surface, on which, along with discontinuities existing in the thermodynamic parameters (flow and velocity), the conductivity of the gas also experiences a discontinuity. The analysis discloses certain new properties of the discontinuity surfaces, which have no analogies in ordinary gasdynamics.

1 We consider a plane, stationary discontinuity surface, on which is incident a stream of nonconducting gas ($\sigma_1 = 0$). The external electric and magnetic fields are considered parallel to the discontinuity surface and perpendicular to each other. We assume the parameters of the incident stream and the intensities of the electric and magnetic fields in front of the discontinuity surface to be specified. The conductivity of the gas behind the discontinuity surface is considered infinite ($\sigma_2 = \infty$). The laws of conservation of mass, momentum, energy and tangential component of the electric field are written in this case in the following form (5)[1]

$$\rho_1 v_1 = \rho_2 v_2 \qquad p_1 + \rho_1 v_1^2 + \frac{H_1^2}{8\pi} = p_2 + \rho_2 v_2^2 + \frac{H_2^2}{8\pi}$$

$$\rho_1 v_1 \left(\frac{v_1^2}{2} + i_1\right) - \frac{c}{4\pi} E_1 H_1 = \rho_2 v_2 \left(\frac{v_2^2}{2} + i_2\right) - \frac{c}{4\pi} E_2 H_2$$

$$E_1 = E_2 = -(1/c) v_2 H_2 \qquad \text{.....[1.1]}$$

The same relations connect the parameters of the stream and the field on the boundaries of a certain transition region, which separates two moving streams, if $\sigma_1 = 0$, $\sigma_2 = \sigma_0 \neq \infty$, and the motion in the transition region is one-dimensional. If the width of this region is much less than the characteristic length of the problem, it can be considered as a discontinuity surface with a finite jump in conductivity. Upon going through such a discontinuity surface, the parameters of the stream and of the field are related by Equation [1.1].

Translated from *Izvestiia Akademii Nauk SSSR, Otdelenie Tekhnicheskikh Nauk, Mekhanika i Mashinostroenie* (*Bull. USSR Acad. Sci., Div. Tech. Sci., Mechanics and Machine Building*), no. 5, 1959, pp. 9–15.

[1] Numbers in parentheses indicate References at end of paper.

If the stream and field parameters are specified in front of the discontinuity surface, relations [1.1] determine the values of all the parameters of the stream and the field behind it. Using the density ratio $\epsilon = \rho_1/\rho_2$, we obtain for the parameters behind the discontinuity surface

$$v_2 = \epsilon v_1 \qquad H_2 = -(cE_1/\epsilon v_1)$$

$$p_2 = p_1 + \rho_1 v_1^2(1-\epsilon) + \frac{1}{8\pi}\left(H_1^2 - \frac{c^2E_1^2}{\epsilon^2 v_1^2}\right)$$

We can determine ϵ from the cubic equation

$$\epsilon^3 - \frac{2\gamma}{\gamma+1}\left(\eta + 1 + \frac{\kappa^2}{2}\right)\epsilon^2 + \frac{2(\gamma-1)}{\gamma+1} \times$$
$$[(1/2) + \frac{\gamma}{\gamma-1}\eta - \xi\kappa]\epsilon + \frac{\gamma-2}{\gamma+1}\xi^2 = 0 \quad [1.2]$$

where

$$\eta = p_1/\rho_1 v_1^2$$

$$\xi = cE_1/v_1^2\sqrt{4\pi\rho_1}$$

$$\kappa = H_1/v_1\sqrt{4\pi\rho_1}$$

Here, as everywhere else, the gas is considered perfect with a constant ratio of specific heats, $\gamma = c_p/c_v$.

Eliminating the velocities from [1.1], we arrive at a relation analogous to the Hugoniot adiabat in ordinary gasdynamics

$$i_2 - i_1 - \frac{p_2 - p_1}{2}(V_1 + V_2) - \frac{1}{16\pi}(H_2^2 - H_1^2) \times$$
$$(V_1 + V_2) - \frac{H_2 V_2}{4\pi}(H_1 - H_2) = 0 \quad [1.3]$$

and when $H_1 = H_2$ [1.3] goes into the ordinary Hugoniot adiabat.

Let us investigate the curves obtained by plotting [1.3] in the p-V plane ($V = 1/\rho$).

a Case $E_1 = 0$. Relation [1.3] assumes the following form

$$i_2 - i_1 - \frac{p_2 - p_1}{2}(V_1 + V_2) + \frac{H_1^2}{16\pi}(V_1 + V_2) = 0 \quad ([1.4]$$

We note that unlike ordinary gasdynamics, the adiabat [1.4] does not pass through the point of the original state p_1V_1, but passes below it

$$p_2 = p_1 - \frac{H_1^2}{8\pi}(\gamma - 1) \qquad \text{for} \qquad V_1 = V_2$$

This is caused by the fact that in this formulation we cannot have surfaces of discontinuity of infinitesimally small intensity, since by assuming an infinite conductivity jump we imply a finite discontinuity in the intensity of the magnetic field.

The adiabat [1.4] has the following asymptotes in the p-V plane

$$V = \frac{\gamma-1}{\gamma+1}V_1 = V \text{ deg} \qquad p = -\frac{\gamma-1}{\gamma+1}\left(1 + \frac{H_1^2}{8\pi p_1}\right)p_1$$

Let us investigate the character of curve [1.4] and its location relative to the Poisson adiabat

$$p_2 V_2^\gamma = p_1 V_1^\gamma \qquad [1.5]$$

Since we have at the points of the adiabat [1.4]

$$\frac{dp_2}{dV_2} = -\left[\frac{\gamma}{(\gamma-1)^2}p_1V_1 - \frac{\gamma}{\gamma-1}V_1\frac{H_1^2}{16\pi}\right] \times$$
$$\left[\frac{\gamma+1}{2(\gamma-1)}V_2 - \frac{V_1}{2}\right]^{-1} \qquad [1.6]$$

$$\frac{d^2p_2}{dV_2^2} = \frac{\gamma+1}{\gamma-1}\frac{dp_2}{dV_2}\left[\frac{\gamma+1}{2(\gamma-1)}V_2 - \frac{V_1}{2}\right]^{-1} \qquad [1.7]$$

then

$$\frac{dp_2}{dV_2} < 0 \qquad \text{for} \qquad H_1 < \frac{16\pi p_1}{\gamma-1} \qquad [1.8]$$

$$\frac{dp_2}{dV_2} > 0 \qquad \text{for} \qquad H_1 > \frac{16\pi p_1}{\gamma-1} \qquad [1.9]$$

From this, and also from the condition $p_2 > 0$, it follows that condition [1.8] gives rise to a branch of [1.4] located to the right of the line $V = V_1(\gamma-1)/(\gamma+1)$, while condition [1.9] produces a branch of [1.4] located to the left of line $V = V_1(\gamma-1)/(\gamma+1)$. Relation [1.7] shows that in both cases the curve [1.4] is concave upwards. It is easy to show that adiabats [1.4] and [1.5] have only one point of intersection.

The relative placement of the Poisson adiabat and of [1.4] subject to condition [1.8] is shown in Fig. 1, and that subject to condition [1.9] is shown in Fig. 2 (1 is the Poisson adiabat; 2 is the adiabat [1.4]).

According to Figs. 1, the only shocks possible when condition [1.8] and the condition of increasing entropy are satisfied are those for which

$$p_2 > p^* \qquad V_2 < V^*$$

Thus, unlike in ordinary gasdynamics, not only rarefaction jumps are forbidden, but also condensation jumps with small increase in pressure $p_2 - p_1 < p^* - p_1$.

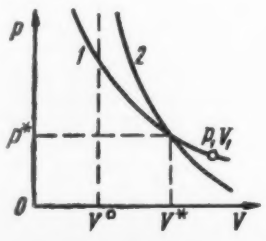

Fig. 1

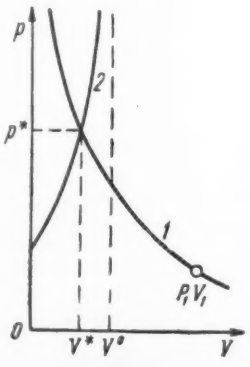

Fig. 2

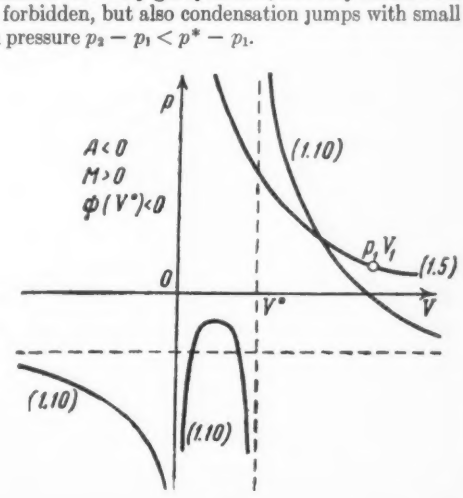

Fig. 3

When conditions [1.9] are satisfied, the possible discontinuity surfaces are shocks with properties that are not encountered in ordinary gasdynamics of nonconducting gases. These shocks are characterized by a larger density increase than the maximum possible ones in ordinary gasdynamics, $(\gamma + 1)\rho_1 < (\gamma - 1)\rho_2$, and are also characterized by the fact that their density rise decreases with increasing pressure jump.

b Case $E_1 \neq 0$. Relation [1.3] can be converted, with the aid of the expression for H_2, from [1.1] to the following form

$$\frac{1}{\gamma - 1}(p_2V_2 - p_1V_1) + \frac{p_2 + p_1}{2}(V_2 - V_1) - \frac{1}{16\pi} \times \left(k^2\frac{V_1^2}{V_2^2} - H_1^2\right)(V_1 + V_2) - \frac{kV_1}{4\pi}\left(H_1 - k\frac{V_1}{V_2}\right) = 0 \qquad \left(k = -\frac{cE_1}{v_1}\right)$$

.....[1.10]

Henceforth we shall retain the name adiabat for the curve [1.10] in p-V plane even though the parameter k includes the velocity of the incident stream.

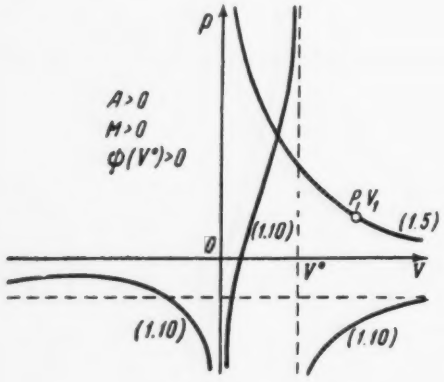

Fig. 4

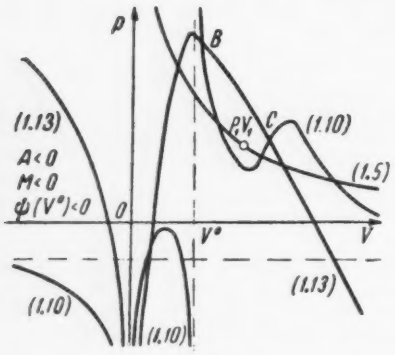

Fig. 5

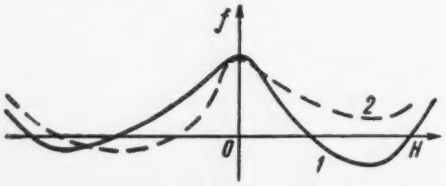

Fig. 6

Let us write down the derivative

$$\frac{dp_2}{dV_2} = \frac{\psi(V_2)}{V_2^3}\left[\frac{\gamma + 1}{2(\gamma - 1)}V_2 - \frac{V_1}{2}\right]^{-2} \qquad [1.11]$$

where

$$\psi(V_2) = \left(-\frac{\gamma}{\gamma - 1}p_1V_1 + \frac{\gamma}{\gamma - 1}\frac{H_1^2V_1}{16\pi} - \frac{\gamma + 1}{\gamma - 1}\frac{H_1kV_1}{8\pi}\right)V_2^2 + \frac{\gamma + 1}{\gamma - 1}\frac{3k^2V_1^2V_2^2}{16\pi} - \frac{\gamma}{\gamma - 1} \times \frac{3k^2V_1^2V_2}{16\pi} + \frac{k^2V_1^4}{16\pi} = AV_2^3 + BV_2^2 + CV_2 + D \qquad [1.12]$$

By specifying an initial point p_1, V_1, the intensity of the magnetic field in front of the discontinuity surface, and also the parameter k, we define the unique adiabat [1.10] in the p-V plane.

This curve has the following asymptotes

$$p = -\frac{\gamma - 1}{\gamma + 1}\left(p_1 + \frac{H_1^2}{8\pi}\right) \qquad V = \frac{\gamma - 1}{\gamma + 1}V_1 = V \text{ deg} \qquad V = 0$$

It is seen from [1.12] that for any values of the parameters ahead of the discontinuity surface we have $D > 0$ and $\psi(0) > 0$. The form of the curve [1.10], for specific values of the parameters in front of the discontinuity surface, depends on the signs of the coefficient A and of the discriminant M of the equation $\psi(V_2) = 0$. Different cases are possible here, some of which are shown in Figs. 3–5. On the same figures are plotted the curves for the Poisson adiabat and those bounding the region of discontinuities possible from the point of view of conditions of increasing entropy.

Figs. 3–5 show that along the discontinuity surfaces, which have the ordinary properties of ordinary gasdynamics (Fig. 3), discontinuity surfaces can occur with properties not encountered in the absence of an electromagnetic field. Fig. 4 indicates, for example, that discontinuities are possible in which the density rise decreases with increasing pressure jump. It is particularly important to note the possibility of existence of rarefaction jumps, permissible from the point of view of the increase in entropy (Fig. 5).

In addition to the jumps noted, relations are also possible between the parameters in front of the discontinuity surface, under which the discontinuities become multiple-valued. To verify this let us plot on the p-V plane, in addition to the adiabats, also the curves $j = \rho_1 v_1 = \text{const}$. These curves are given by the equation

$$\left(p_2 - p_1 - \frac{H_1}{8\pi}\right)V_2^2 + \frac{k^2V_1^2}{8\pi} = j^2V_2^2(V_1 - V_2) \qquad [1.13]$$

It is easy to check that the line $V = 0$ is an asymptote for the curves [1.13]. Furthermore, curves [1.10] and [1.13] have in general three points of intersection. This gives rise to a situation wherein the parameters behind the discontinuity surface are not determined uniquely from the parameters specified ahead of it (p_1, ρ_1, H_1, k, j). An example of such an arrangement of the curves is shown in Fig. 5. In this case two discontinuities B and C are possible, satisfying all the conditions, for specified stream and field parameters.

In conclusion let us note that if the values of ρ_1, p_1, H_1 and k are specified in front of the discontinuity surface, the adiabat [1.10] becomes specified in the p-V plane. If we now specify one of the quantities on the discontinuity surface, for example, the pressure, we find the point of intersection between the line $p_2 = \text{const}$ and the adiabat [1.10]. The curve $j = \text{const}$ passing through this point determines the mass flow j corresponding to the discontinuity surface with a given pressure drop, and consequently the velocity and the intensity of

the electric field in the incident stream. If, on the other hand, the quantities specified ahead of the discontinuity surface are p_1, ρ_1, H_1 and E_1, then it is possible to plot on the p-V plane a family of adiabats [1.10] corresponding to different values of the parameter k, as well as a family of curves j = const, which depends on the two parameters k and j. If we now specify the pressure jump, we find on the line p_2 = const the point of intersection of the curves [1.10 and 1.13], which correspond to the same value of k. This point determines the value of j and all the parameters of the stream behind the discontinuity surface. Naturally, it is necessary to verify in each case whether the conditions of increasing entropy are satisfied.

2 To determine the structure of a discontinuity surface with a conductivity jump, we proceed in analogy with (3, 6 and 7).

We consider one-dimensional, stationary motions of nonvicous and non-heat-conducting gas with a conductivity that varies along the x axis. The intensities of the electric and magnetic fields are considered directly perpendicular to each other and lying in a plane perpendicular to the x axis. In this case the system of equations of magnetohydrodynamics can be reduced to four integrals and one ordinary differential equation

$$\rho v = c_1 \qquad p + \rho v^2 + \frac{H^2}{8\pi} = c_2 \qquad \rho v[(1/2)v^2 + i] - \frac{c}{4\pi} EH = c_3$$

$$cE = c_4 \qquad \frac{c^2}{4\pi\sigma}\frac{dH}{dx} - vH = c_4 \qquad \text{[2.1]}$$

We shall assume that up to a certain finite point $x = x_0$ the conductivity of the gas in zero. At $x < x_0$ the flow is considered moving with specified parameters, i.e., the constants c_1, c_2, c_3 and c_4 are determined on the stream for $\sigma = 0$. For $x > x_0$, the flow is described by Equation [2.1] with the right halves specified, and the conductivity in this region may either be constant or a certain function of x. In order to determine the flow, we obtain the dependence of v on H from the first four equations

$$v = \frac{\gamma}{\gamma+1}\frac{1}{c_1}\left(c_2 - \frac{1}{8\pi}H^2\right) \pm \left\{\left[\frac{\gamma}{\gamma+1}\frac{1}{c_1}\left(c_2 - \frac{1}{8\pi}H^2\right)\right]^2 - \frac{2(\gamma-1)}{\gamma+1}\left(\frac{c_3}{c_1} + \frac{c_4}{4\pi c_1}H\right)\right\}^{1/2} \qquad \text{[2.2]}$$

Inserting this expression in the latter equation and integrating, we obtain the function $H(x)$ and then use all the final formulas to obtain all the parameters of motion.

Leaving aside the exact solution of the problem, let us study the behavior of the curves $v = v(H)$, specified by relation [2.2] in the v-H plane. The expression under the square root in [2.2] vanishes at four (or two) values of H, which are roots of the equation

$$\left[\frac{\gamma}{(\gamma+1)c_1}\left(c_2 - \frac{H^2}{8\pi}\right)\right]^2 - \frac{2(\gamma-1)}{\gamma+1}\left(\frac{c_3}{c_1} + \frac{c_4 H}{4\pi c_1}\right) = 0$$

At these values of H the straight line, H = const, is tangent to the curve $v = v(H)$. The geometric locus of such points is a parabola

$$v = \frac{\gamma}{(\gamma+1)c_1}\left(c_2 - \frac{H^2}{8\pi}\right) \qquad \text{[2.3]}$$

Since the momentum and the energy flux for the gas should be positive in order to realize this kind of flow, the branches of

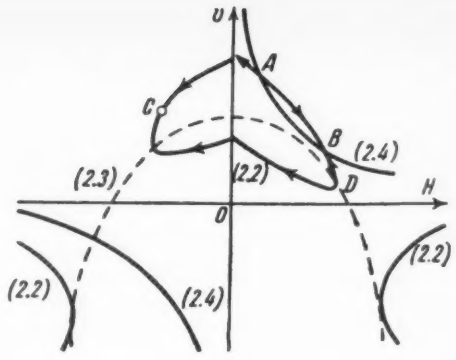

Fig. 7

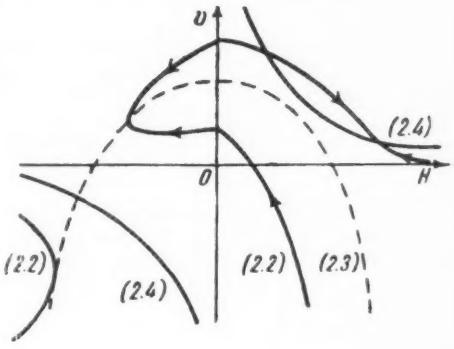

Fig. 8

the curves $v = v(H)$ for which $c_2 - H^2/8\pi < 0$ and $c_3 + c_4 H/4\pi < 0$ must be considered as nonrealizable.

The form of the curves $v = v(H)$ will depend on the behavior of the function

$$f(H) = \left[\frac{\gamma}{(\gamma+1)c_1}\left(c_2 - \frac{H^2}{8\pi}\right)\right]^2 - \frac{2(\gamma-1)}{\gamma+1}\left(\frac{c_3}{c_1} + \frac{c_4 H}{4\pi c_1}\right)$$

Let us consider the case $c_4 < 0$ (for $c_4 > 0$ the situation will be analogous if the sign of H is reversed). The qualitative behavior of the function $f(H)$ for $f(0) > 0$ is shown in Fig. 6, and the realization of positions *1* and *2* will depend on the relation between the constants contained in $f(H)$. The characteristic placement of the curves $v = v(H)$ for cases *1* and *2* is indicated in Figs. 7 and 8. The same figures show a plot of the hyperbola

$$E = -(1/c)vH \qquad \text{[2.4]}$$

The points of this hyperbola correspond to the points of the stream, where the conductivity is $\sigma = \infty$ or else to those points, after which there is no change in the flow parameters with x. The latter of the equations [2.1] establishes a definite direction on the curve $v = v(H)$, in which the representative point should move. In the case of a finite conductivity of the stream (3) in all points $-\infty < x < \infty$, the initial and final points should be located on the curve [2.4]. In this case any discontinuity, defined by the laws of conservation [1.1], can be put in correspondence with a certain continuous flow (AB in Fig. 7). In our case the initial point can be located at any point C of the upper half plane. It is easy to see here that continuous motions, which can be continued to infinity, are possible for certain initial conditions; these correspond to the points located above [2.4], and the points in the segment DB lying below curve [2.4], if such points exist. On the other hand, if the initial parameters are such that the initial point falls in the region DCA on the curve $v = v(H)$, then it is impossible to have continuous motion which can

be continued to infinity. We note that for these initial data the discontinuity surfaces with conductivity jumps, defined by relation [1.1], will become feasible and the condition of entropy increase can be satisfied for them.

We note that if the initial parameters are such that the curves [2.3 and 2.4] do not intersect, then there always exists a region of initial data, corresponding to *DB*, from which stationary rarefaction flows are possible. These flows do not have any analogies in ordinary gasdynamics and correspond to the rarefaction jumps noted above.

Thus, an examination of the structure of the discontinuity surface in the formulation used here, leads to the conclusion that not all the discontinuity surfaces, corresponding to the conservation laws [1.1], can be considered as the limits of continuous flows with variable conductivity. The discontinuity surfaces with conductivity jumps, which can be considered as the limit of continuous flows, are either jumps of increasing density with increasing magnetic field, or else jumps of decreasing density with decreasing magnetic field.

Allowance for the viscosity and heat conduction of the gas shows that stationary flows are possible only under definite initial values of the parameters. This circumstance allows an electromagnetic wave, which changes the initial parameters of the field to be propagated in front of a discontinuity surface with a conductivity jump, contained in a stream of ideal gas.

3 Discontinuity surfaces with conductivity jumps, with energy liberated on the front of the discontinuity, can be considered in analogy with the foregoing. Relations [1.1] continue to hold in this case, with the exception of the condition of conservation of energy, to which one adds an additional term q, connected with the amount of energy liberated on the front of the wave.

The detonation adiabat can be represented in the form

$$i_2 - i_1 - (V_1 + V_2)\left(\frac{p_2 - p_1}{2} - \frac{H_2^2 - H_1^2}{16\pi}\right) - \frac{H_2 V_2}{4\pi}(H_1 - H_2) + q = 0 \quad [3.1]$$

This relation shows that the qualitative behavior of the detonation adiabat in the p-V plane is the same as of adiabat [1.10], except that in the region $V_2 > (\gamma - 1)V_1/(\gamma + 1)$ the adiabat [3.1] lies above the adiabat [1.10] ($q < 0$), and in the region $0 < V_2 < (\gamma - 1)V_1/(\gamma + 1)$ it lies below the adiabat [1.10].

It is easy to show that when $V_2 > 2(\gamma - 1)V_1/3(\gamma + 1)$ the detonation adiabat is steeper than the adiabat [1.10], and that for $0 < V_2 < 2(\gamma - 1)V_1/3(\gamma + 1)$ it slopes more gently than adiabat [1.10].

These considerations enable us to plot in the p-V plane the detonation adiabats, the forms of which will be analogous to the curves shown in Figs. 3–5. It is also possible to plot in the p-V plane the curve j = const, corresponding to the sonic velocity of the gas behind the detonation wave

$$\left[(p_2 - p_1) - \frac{H_1^2}{8\pi}\right] V_2^2 + \frac{k^2 V_1^2}{8\pi} = \left(\gamma p_2 V_2^{-1} + \frac{k^2}{4\pi}\frac{V_1^2}{V_2^2}\right) V_2^2 (V_1 - V_2) \quad [3.2]$$

If the curve [3.2] intersects the adiabat [3.1] below the Poisson adiabat, then, after Jouguet, a detonation at these values of the initial parameters will be impossible. There will also be realized an "overcompressed" detonation with the gas moving behind the wave at a velocity less than the velocity of sound. In ordinary gasdynamics the realization of detonation modes under which the velocity of gas behind the wave is greater than the velocity of sound is impossible without energy being taken away at the detonation front. If the detonation occurs in an electromagnetic field and the conductivity of the medium experiences a jump behind the detonation wave, such modes become possible at certain values of the initial parameters. The parameters of such detonation waves were given by us in (8), but the cases possible here are naturally not confined to these examples.

Thus, an examination of the stationary discontinuity surfaces on which, in addition to the flow parameters, there is also a discontinuity in the conductivity of the medium, displays certain new properties of discontinuity surfaces, which have no analogies in ordinary gasdynamics.

References

1 Landau, L. D. and Lifshitz, E. M., "Mekhanika sploshnykh sred" (Mechanics of Continuous Media), Gostekhizdat, Moscow, 1954.

2 Landau, L. D. and Lifshitz, E. M., "Elektrodinamika sploshnykh sred" (Electrodynamics of Continuous Media), Gostekhizdat, Moscow, 1957.

3 Marshall, W., "Structure of Magnetohydrodynamic Shock Waves," Russian translation in *Problems of Modern Phys.*, no. 7, 1957.

4 Syrovatskii, S. I., "Stability of Shock Waves in Magnetohydrodynamics," *J. Exptl. Theoret. Phys.* (USSR), vol. 35, 1958, p. 1466; translation in *Soviet Phys. JETP*, vol. 8, 1959, p. 1024.

5 Lyubimov, G. A., "Shock Wave with Conductivity Jump in an Electromagnetic Field," *Doklady Akad. Nauk SSSR* (*Trans. USSR Acad. Sci.*,) vol. 126, no. 2, 1959.

6 Burgers, J. M., "Penetration of a Shock Wave in a Magnetic Field," Russian translation in "Magnetohydrodynamics," Atomizdat, Moscow, 1958.

7 Kulikovskii, A. G. and Lyubimov, G. A. "Possible Types of Surface Discontinuities with Conductivity Jumps", *Izvestiia Akad. Nauk SSSR, Otd. Tekh. Nauk* (*Bull. Akad. Sci. USSR, Div. Tech. Sci.*), no. 4, 1959.

8 Lyubimov, G. A., "Effect of Electromagneitic Field on the Detonation Mode," *Doklady Akad. Nauk SSSR* (*Trans. USSR. Acad. Sci.*, vol. 126, 1959, p. 532; translation in *Soviet Phys.—Doklady*, vol. 4, 1959, p. 526.

Reviewer's Comment

The previous studies of the magnetohydrodynamic jump conditions (see, for example (1)), and the possible paths of transition from one state to another ((2), for example), have dealt with the case in which the end points are both in a region where the product of the gas conductivity and the length over which the flow parameters change is very large. In this case the "infinite conductivity" relation $\mathbf{E} = -\mathbf{v} \times \mathbf{B}$ holds. The present paper differs from those studies in that this relation is taken to hold only in back of the shock, while in front the conductivity is taken to be zero so the corresponding relation is that $\mathbf{E}$ there is arbitrary. This difference leads the author to some interesting phenomena which are different from those found in the usual "infinite conductivity" case. Only the special case where the magnetic field is parallel to the shock front and the fluid velocity is perpendicular to it, is considered.

It should be noted that not all these phenomena may occur in physical cases because, for example, some of them may be unstable. Such is the case with the "infinite conductivity" shocks, where switch-on and switch-off shocks (reference 3 below), as well as shocks which cause the tangential component of magnetic field to change sign (references 4 and 5 below) have been shown to be unstable to small disturbances.

The reviewer would like to express his appreciation to Dr. Harry Petschek for his kind assistance.

—Nelson H. Kemp
Avco-Everett Research Laboratory

1 Ericson, W. B. and Baser, J., "Hydromagnetic Shocks," *Astrophys. J.*, vol. 129, no. 3 May 1959, pp. 758–785.

2 Ludford, G. S. S., "The Structure of a Hydromagnetic Shock in Steady Plane Motion," *J. Fluid Mech.*, vol. 5, *pt.* 1, Jan. 1959, pp. 67–80.

3 Syrovatskii, S. I., "The Stability of Shock Waves in Magnetohydrodynamics," *Soviet Phys. JETP*, vol. 35 (8), no. 6, June 1959, pp. 1024–1027.

4 Akhiezev, A. I., Liubarskii, G. Ia. and Polovin, R. V., "The Stability of Shock Waves in Magnetohydrodynamics, "*Soviet Phys. JETP*, vol. 35 (8), no. 3, March 1959, pp. 507–511.

5 Kontorovich, V. M., "On the Interaction Between Small Disturbances and Discontinuities in Magnetohydrodynamics and On the Stability of Shock Waves," *Soviet Phys. JETP*, vol. 35 (8), no. 5, May 1959, pp. 851–858.

(*Continued from page 372*)

Transfer from a 1000-mile Earth orbit, to an orbit placing the transferring body in the vicinity of the moon:

$$\lambda = \frac{r_{des}}{r} = \frac{244{,}000 \text{ miles}}{5000 \text{ miles}} = 48.8$$

$$\gamma = \frac{r}{r_0} = \frac{5000 \text{ miles}}{4000 \text{ miles}} = 1.25$$

$$V_{escref} = 11.2 \text{ km/sec} = 7 \text{ miles/sec}$$

Earth is the primary gravitational source. From Fig. 1, corresponding to the values of λ and γ

$$k = 0.99 \qquad \epsilon = 0.9$$

Therefore

$$V_{req} = k\,\epsilon\,V_{escref} = (0.99)(0.9)(7 \text{ miles/sec}) = 6.23 \text{ miles/sec}$$

Assuming the initial orbit to be circular, the initial velocity is

$$V_{circle} = \sqrt{\frac{u}{r}} = \sqrt{\frac{9.76 \times 10^4}{5 \times 10^3}} = 4.42 \text{ miles/sec}$$

The necessary increase in velocity is thus

$$\Delta V = V_{req} - V_{circle} = 1.81 \text{ miles/sec}$$

Successive transfers from a 200-mile Earth orbit to a 22,400-mile "stationary" (24-hr period) orbit:

$$\lambda = \frac{r_{des}}{r} = \frac{26{,}400 \text{ miles}}{4200 \text{ miles}} = 6.29$$

$$\gamma = \frac{r}{r_0} = \frac{4200 \text{ miles}}{4000 \text{ miles}} = 1.05$$

From Fig. 1, $k = 0.933$ and $\epsilon = 0.98$. Therefore

$$V_{req} = k\,\epsilon\,V_{escref} = (0.933)(0.98)(7 \text{ miles/sec}) = 6.4 \text{ miles/sec}$$

From Equation [7]

$$V = \frac{V_{req}}{\lambda} = \frac{6.4 \text{ miles/sec}}{6.29} = 1.02 \text{ miles/sec}$$

To remain in the 22,400-mile orbit, it is necessary to modify V so as to effect a circular orbit at r_{des}. The necessary change in V is also given by Fig. 1, as follows (subscript 2 is used to designate conditions at r_{des})

$$\lambda_2 = \frac{r_{des}}{r} = 1.0 \qquad \gamma_2 = \frac{r}{r_0} = \frac{26{,}400 \text{ miles}}{4000 \text{ miles}} = 6.6$$

Therefore

$$k_2 = 0.707 \qquad \epsilon_2 = 0.39$$

$$V_{req2} = k_2\,\epsilon_2\,V_{escref} = (0.707)(0.39)(7 \text{ miles/sec}) = 1.925 \text{ miles/sec}$$

The necessary velocity change at r_{des} is then

$$\Delta V = V_{req2} - V = 0.905 \text{ mile/sec}$$

Interplanetary transfer (considering only effect of sun) from Earth to Mars:

$$\lambda = \frac{1.5 \text{ A.U.}}{1.0 \text{ A.U.}} = 1.5$$

$$\gamma = \frac{93 \times 10^6 \text{ miles}}{4.35 \times 10^5 \text{ miles}} = 214$$

$$V_{escref} = 386 \text{ miles/sec}$$

The sun is the primary gravitational source. Therefore

$$k = 0.77 \qquad \epsilon = 0.07$$

$$V_{req} = k\,\epsilon\,V_{escref} = (0.77)(0.07)(386 \text{ miles/sec}) = 20.8 \text{ miles/sec}$$

Assuming the transferring body to be initially traveling at Earth's orbital speed of 18.5 miles per sec, the necessary change in velocity is

$$\Delta V = 20.8 - 18.5 = 2.3 \text{ miles/sec}$$

To effect a "soft" landing on Mars (assuming Mars is properly oriented at takeoff to insure interception by the transferring body) or to transfer to the Martian orbit, the velocity V at r_{des} (see Eq. [7]) must be modified to the Martian orbital velocity of 15.1 mile per sec. The necessary change in velocity at r_{des} may be computed, using Fig. 1, as was done previously.

Interplanetary transfer (considering only effect of sun) from Earth to Venus:

$$\lambda = \frac{0.75 \text{ A.U.}}{1.0 \text{ A.U.}} = 0.75$$

$$\gamma = 214$$

as shown previously. Therefore

$$k = 0.655 \quad \epsilon = 0.07$$

$$V_{req} = k\,\epsilon\,V_{escref} = (0.655)(0.07)(386 \text{ miles/sec}) = 17.7 \text{ miles/sec}$$

Note that $V_{req} < 18.5$ miles per sec, as required for transfer to an interior ellipse. V as given by Equation [7] must be modified, as before, at r_{des} to insure a "soft" landing on Venus.

The last two examples are based on assumptions similar to those made in computing the Hohmann interplanetary transfer ellipses (i.e., only the effect of the sun is considered, and takeoff and arrival are made tangentially to the initial and terminal orbits); the results are thus identical to the Hohmann results. Since the curves of Fig. 1 are based on orbital transfers which depart and arrive tangentially to the initial and desired radii, all transfer requirements given by Fig. 1 are, in fact, minimum energy (Hohmann) transfer requirements.

Nomenclature

V_{escref}	=	reference escape velocity $\equiv \sqrt{2g_0r_0}$, escape velocity at surface of primary gravitational source (V_{escref} = 11.2 km/sec = 7 miles/sec for Earth, V_{escref} = 618 km/sec = 386 miles/sec for sun)
a	=	semimajor axis of elliptical orbit
r_a	=	apogee radius of elliptical orbit
r_p	=	perigee radius of elliptical orbit
u	=	$g_0r_0^2$, gravitational constant associated with primary gravitational source, $u = 9.76 \times 10^4$ miles^3/sec^2 for Earth
g_0	=	gravitational acceleration at surface of primary gravitational source
λ	$\equiv$	desired radius to initial radius ratio, r_{des}/r
k	$\equiv$	required velocity to escape velocity ratio, V_{req}/V_{esc}
γ	$\equiv$	initial radius to gravitational source radius ratio, r/r_0
ϵ	$\equiv$	escape velocity to reference escape velocity ratio, V_{esc}/V_{escref}
r	=	initial radial distance from center of primary gravitational source
r_{des}	=	desired radial distance from center of primary gravitational source after transfer is effected (perigee or apogee radius of transfer ellipse, depending, respectively, on whether $r_{des} < r$ or $r_{des} > r$)
r_0	=	radius of primary gravitational source (r_0 = 4000 miles for Earth, $r_0 = 4.35 \times 10^5$ miles for sun)
V_{req}	=	required *total* velocity, at initial point of transfer, to effect desired new orbit
V_{esc}	=	$\sqrt{2u/r}$, escape velocity associated with initial radius r

Nonlinear Pressure Oscillations in a Combustion Field[1]

GERALD ROSEN[2]

Guggenheim Jet Propulsion Center,
Princeton, N. J.

The unsteady combustion of liquid propellant droplets entrained in a burned gas flow is studied in terms of an idealized mathematical model. We use the model to derive an associated equation for nonlinear pressure oscillations. Two necessary and sufficient conditions for unstable oscillations follow from a discussion of this equation.

MAJOR practical importance has been attached to the problem of high frequency combustion instability, in particular, the unstable pressure oscillations which may affect the performance of a rocket motor. A thorough mathematical treatment of the linearized aspects of this problem has been given by Crocco and Cheng (1–3).[3] Basing their theory on the *sensitive time lag* postulate, these authors have derived certain necessary conditions for the unstable operation of a rocket motor. However, the work of Crocco and Cheng does not elucidate the nonlinear dynamics of instability. There is a question of whether or not an acoustical perturbation will grow to become a pressure oscillation of large amplitude and destructive capabilities. An answer to this question is not within the scope of linearized theory.

Existing mathematical methods do not permit a complete theoretical analysis of nonlinear combustion instability. Nevertheless, it is possible to understand the qualitative dynamics of finite amplitude pressure oscillations if the combustion field is represented by a relatively simple model. The present paper reports a number of theoretical conclusions which are derived from such a model. Of primary interest is the fact that a mechanism for instability follows from an ordinary equation for the burning rate, without evoking the postulate of a *time lag*. The stability of a pressure wave is essentially determined by the frequency of the oscillation and the pressure sensitivity of the burning rate function, in qualitative agreement with the original ideas advanced by Crocco (4).

Mathematical Model

Let us consider a special model of a one-dimensional combustion field in which physical and chemical processes transform liquid propellant droplets into burned gas. If the average Reynolds number of the droplets is sufficiently small, the droplets will remain entrained in the burned gas flow. This we take as a basic feature of the model. Let us put

ρ, gr/cm^3 = density of the mixture
u, cm/sec = mixture velocity in the x-direction
P, gr/cm-sec^2 = pressure

The equations of mass and momentum conservation take the form

$$\frac{\partial \rho}{\partial t} + \frac{\partial}{\partial x}(\rho u) = 0 \qquad [1]$$

$$\rho \frac{\partial u}{\partial t} + \rho u \frac{\partial u}{\partial x} + \frac{\partial P}{\partial x} = 0 \qquad [2]$$

A term due to longitudinal viscous effects has been neglected in writing Equation [2].

The entropy of the completely burned gas is assumed to be constant. Letting ω denote the weight fraction of the burned gas, it follows that the density of the burned gas ($\omega\rho$) is given by the isentropic relation

$$\omega\rho = aP^{1/\gamma} \qquad [3]$$

in which a and γ are appropriate constants.

The rate of production of burned gas is described by the equation

$$\frac{\partial \omega}{\partial t} + u \frac{\partial \omega}{\partial x} = f(\omega, P;\ \text{fluid element}) \qquad [4]$$

The function f embodies the rate controlling physical and/or chemical processes which govern the combustion of the droplets. In general, f is not simple and depends parametrically on the fluid element (through the local fuel/oxidizer ratio, the local spectrum of the droplets, etc.). However, the burning rate function must be required to vanish for all fluid elements at the initial and final states of combustion

$$f(\omega_0, P;\ \text{fluid element}) = f(1, P;\ \text{fluid element}) = 0 \qquad [5]$$

where the initial weight fraction of the burned gas is denoted by ω_0.

Equations [1 to 4] suffice to determine the dynamical behavior of the four dependent variables ρ, u, P and ω. Suitable boundary and initial conditions are required for a unique solution to Equations [1 to 4]. Here we shall be interested in the class of solutions characterized by the boundary conditions

$$\lim_{x \to -\infty} \omega = \omega_0 \qquad [6a]$$

$$\lim_{x \to +\infty} \omega = 1 \qquad [6b]$$

In view of Equations [5 and 6] the region of combustion is confined to those finite values of x which make f greater than zero. Within this region the liquid droplets are consumed, and the weight fraction of the burned gas increases from ω_0 to 1.

Equation for Pressure Oscillations

By eliminating the density and the velocity (5,6), the system [1 to 4] can be reduced to a pair of coupled equations. First we evoke Equation [1] in order to define a *mass coordinate* ψ which satisfies

$$d\psi = \rho dx - \rho u dt \qquad [7]$$

Observe that ψ is a Lagrange coordinate, in the sense that a fixed value of ψ refers to a particular fluid element. Expressing the dependent variables in Equations [1, 2 and 4] in terms of ψ and t, we have

$$\frac{\partial}{\partial t}\left(\frac{1}{\rho}\right) - \frac{\partial u}{\partial \psi} = 0 \qquad [8]$$

$$\frac{\partial u}{\partial t} + \frac{\partial P}{\partial \psi} = 0 \qquad [9]$$

$$\frac{\partial \omega}{\partial t} = f(\omega, P;\ \psi) \qquad [10]$$

In the latter, as well as in all subsequent equations, $\partial/\partial t$ refers to a time differentiation with ψ held fixed; ψ has been used to represent the parametric dependence of the burning rate function in Equation [4].

The combination of Equations [8, 9 and 3] produces

$$\frac{\partial^2}{\partial t^2}\left(\frac{\omega}{aP^{1/\gamma}}\right) + \frac{\partial^2 P}{\partial \psi^2} = 0 \qquad [11]$$

Although the coupled Equations [10, 11] do not involve ρ and

Received Oct. 5, 1959.
[1] This work was sponsored by Project SQUID which is supported by the Office of Naval Research, Department of the Navy, under Contract Nonr 1858(25) NR-098-038. Reproduction in full or in part is permitted for any use of the United States Government.
[2] Research Associate, Department of Aeronautical Engineering.
[3] Numbers in parentheses indicate References at end of paper.

u, these two equations express the full content of the system [1 to 4].

Let us now work out the time differentiations in Equation [11]. Making use of Equation [10], we eventually obtain

$$\omega \frac{\partial^2 P}{\partial t^2} - \gamma a P^{1+1/\gamma} \frac{\partial^2 P}{\partial \psi^2} + \left(2f - \gamma P \frac{\partial f}{\partial P}\right) \frac{\partial P}{\partial t} = \frac{(\gamma + 1)\omega}{\gamma P} \left(\frac{\partial P}{\partial t}\right)^2 + \gamma f \frac{\partial f}{\partial \omega} P \quad [12]$$

a result which displays the essential mechanism for nonlinear pressure oscillations in the combustion field.

Dynamical Interpretation

The first and second terms on the left side of Equation [12] determine the characteristics. These terms propagate a pressure pulse with the local mass coordinate velocity

$$d\psi/dt = \pm \sqrt{\gamma a P^{1+1/\gamma}/\omega} = \pm \sqrt{\gamma P \rho}$$

Recalling Equation [7], we can convert this to the classical propagation velocity

$$dx/dt = u \pm \sqrt{\gamma P/\rho}$$

Thus, the inclusion of combustion does not modify the local phase velocity of waves.

The third term on the left side of Equation [12] is a "friction term" which comes from the interaction of a pressure oscillation with the combustion processes. If the "friction coefficient" $[2f - \gamma P(\partial f/\partial P)]$ is positive, the amplitude of a pressure wave suffers exponential damping as the wave passes through the combustion region. On the other hand, if the friction coefficient is negative, the amplitude of a pressure wave increases in an exponential fashion as the wave traverses the combustion region. Hence, a condition for the unstable growth of a wave is

$$\frac{\partial \ln f}{\partial \ln P} > \frac{2}{\gamma} \quad [13]$$

The right side of Equation [12] gives intrinsic "source terms" for the generation of pressure waves. The first term on the right side is positive-definite in character and stems from the convective nonlinearity in Equations [1 and 2]. This term creates and amplifies waves of a higher frequency, thereby steepening a pressure pulse of finite amplitude. Low frequency pressure waves associated with the combustion process are generated by the second term on the right side of Equation [12]. For the case of steady deflagration this term gives rise to a weak rarefaction wave.

Finally, let us consider the order of magnitude of the friction term on the left side of Equation [12] in comparison to the order of magnitude of the source terms on the right side. The friction term is of the order $f|\partial P/\partial t|$, whereas the source terms are of the order $P^{-1}|\partial P/\partial t|^2$ and f^2P, respectively. Hence, the friction term will be negligible in comparison to one or the other source terms if $(fP)^{-1}|\partial P/\partial t|$ is not of the order unity. The condition

$$\frac{1}{fP}\left|\frac{\partial P}{\partial t}\right| \sim 1 \quad [14]$$

defines a range of frequencies and amplitudes for which instability is possible. Notice that in the case of small amplitude acoustical perturbations, [14] requires the period of an unstable oscillation to be much less than the characteristic time required for the droplet combustion.

The relations stated in [13 and 14] seem to be necessary and sufficient conditions for nonlinear combustion instability.

References

1 Crocco, L. and Cheng, S. I., "Theory of Combustion Instability in Liquid Propellant Rocket Motors," AGARD Monograph no. 8, Butterworths Scientific Publications, London, 1956.

2 Crocco, L. and Cheng, S. I., "High-Frequency Combustion Instability in Rocket Motors with Concentrated Combustion," JOURNAL OF THE AMERICAN ROCKET SOCIETY, vol. 23, no. 5, Sept.-Oct. 1953, pp. 302-313.

3 Crocco, L., Grey, J. and Harrje, D. T., "On the Importance of the Sensitive Time Lag in Longitudinal High-Frequency Combustion Instability," JET PROPULSION, vol. 28, no. 12, Dec. 1958, pp. 841-843.

4 Crocco, L., "Aspects of Combustion Instability in Liquid Propellant Rocket Systems, Part I," JOURNAL OF THE AMERICAN ROCKET SOCIETY, vol. 21, no. 6, Nov.-Dec. 1951, pp. 163-178; Part II, *ibid.*, vol. 22, Jan.-Feb. 1952, pp. 7-16.

5 Rosen, G., "Integration Theory for One-Dimensional Viscous Flow," *Phys. Fluids*, vol. 2, Sept.-Oct. 1959.

6 Rosen, G., "Entropy Production and Pressure Waves," *Phys. Fluids*, vol. 3, March-April 1960.

Forced Convection Heat Transfer to Gaseous Hydrogen at High Heat Flux and High Pressure in a Smooth, Round, Electrically Heated Tube[1]

J. R. McCARTHY[2] and H. WOLF[3]
Rocketdyne Division, North American Aviation, Inc., Canoga Park, Calif.

INFORMATION concerning the heat transfer characteristics of hydrogen under conditions of high heat flux is of prime interest in the design considerations of high performance rocket engines and of reactors for nuclear powered rocket engines. The results presented here summarize experiments conducted over a sufficiently wide range of pressure and heat flux to be of immediate interest, although the gas temperature at the inlet to the test section was greater than −100 F. Heat fluxes as high as 14.8 B/sec in.^{2} and pressures to 1350 psia were achieved. The data presented herein are the initial results of a program directed toward the determination of the heat transfer characteristics of gases under conditions of very high surface to fluid bulk temperature ratios T_w/T_b. It is anticipated that values of the ratio T_w/T_b as high as 10 can be achieved with the present apparatus.

The experiments were conducted in two electrically heated stainless steel test sections 13-in. long, having an ID of 0.194 and 0.305 in. (L/D = 67 and 42.6, respectively). Isothermal starting lengths 10-in. long were provided to insure a fully developed velocity profile and a uniform temperature profile at the entrance. The gas flow rate was measured with calibrated sharp edged orifices, and the gas bulk temperatures at the inlet and exit from the test section were measured with four calibrated Range I, iron-constantan thermocouples in each of two specially designed mixing chambers. Power was supplied to the test section by four d-c motor-generator units and was computed from the measured current through the test section and the voltage drop along it. The inner wall

Received Nov. 11, 1959.

[1] This work was performed at the Combustion and Heat Transfer Laboratory of the Research Center at the Propulsion Field Laboratory, Santa Susana, Calif., and was sponsored by Rocketdyne.

[2] Research Engineer.

[3] Technical Specialist. Member ARS.

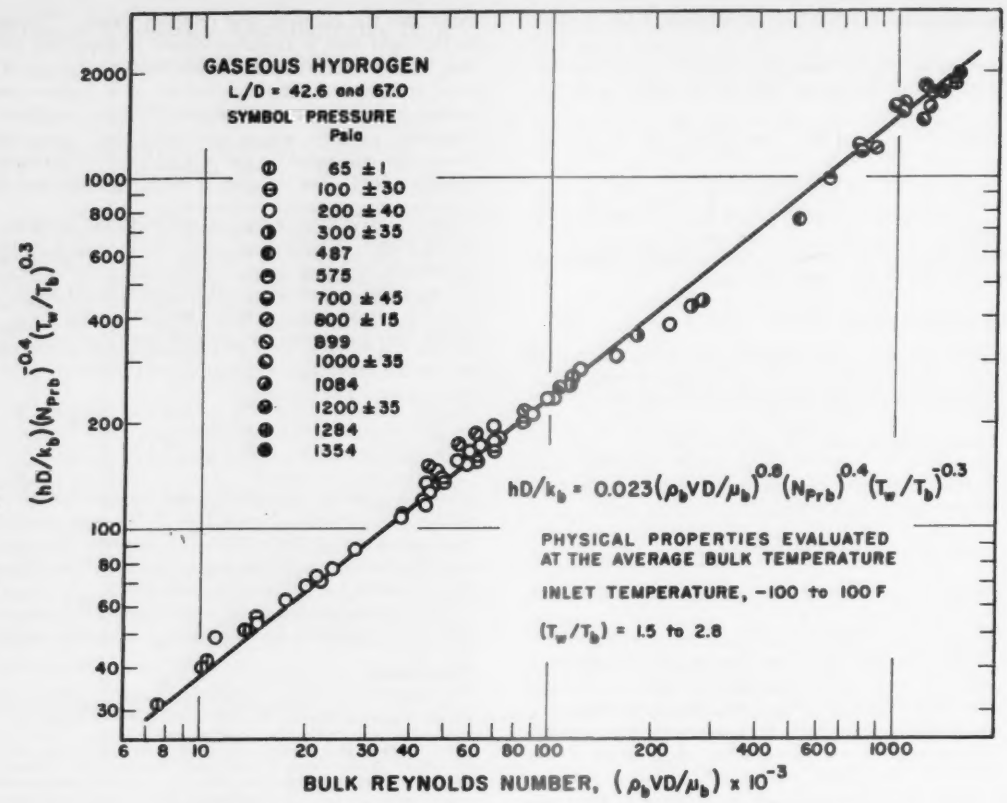

Fig. 1 Correlation of forced convection heat transfer results for hydrogen at different pressures

temperature was calculated from the measured outer wall temperature and the energy generated in the tube wall according to the method given in (1).[4]

The gas exhausting from the test apparatus was burned at a vent approximately 30 ft from ground level. During the course of the experiments, flares were kept burning in the test cell. Accordingly, several leaks and a ruptured test section (caused by a malfunction in flow control) resulted only in fires; no explosions occurred.

The heat transfer results presented are average values for the region of flow having fully developed velocity and temperature profiles. Reference (2) demonstrated that the local heat transfer coefficient approaches to within 5 per cent of its fully developed value in less than eight diameters for the Reynolds number range to 500,000. Accordingly, the heat transfer coefficients employed in the Nusselt number were computed from Newton's law of cooling for the center 10-in. length of the test section. The energy flux through the heat transfer surface was assumed equal to the electrical energy dissipated in the center 10-in. length less the energy conducted through the insulation. Heat balances for the experiments were always less than ±10 per cent.

In correlating the heat transfer results the thermal conductivity at 1-atm pressure was taken from the National Bureau of Standards tables (6), and the effect of pressure was accounted for according to the experimental results of Keyes in (7). The values for viscosity and the pressure effect upon viscosity were those given by Hilsenrath and Touloukian (8). The specific heat, Prandtl number and the compressibility data are those reported in (6).

[4] Numbers in parentheses indicate References at end of paper.

Fig. 1 presents the forced convection heat transfer results for hydrogen in a smooth round tube as a function of the bulk Reynolds number, at different pressures with the physical properties evaluated at the average bulk temperature of the gas. A correlation based upon bulk temperature has been selected, since its use in design calculations is more convenient than correlations based upon other reference temperatures. The results encompassed the following range of variables:

Bulk Reynolds number	7.8 (10^3)–1.50 (10^6)
Bulk inlet temperature	360–560 R
Average wall to average bulk temperature ratio	1.5–2.8
Average wall temperatures	860–1640 R
Average bulk temperature	559–729 R
Inlet pressure	64–1354 psia

The figure demonstrates that pressure, per se, has no influence on the convective heat transfer characteristics of the gas.

References (3 and 4) show that the results of heating experiments having a uniform heat flux boundary condition cannot be correlated with the McAdams equation without including the surface to bulk fluid temperature ratio T_w/T_b. The influence of the ratio T_w/T_b was obtained by crossplotting the values of $N_{Nu}/N_{Pr}^{0.4}$ at constant wall temperature and Reynolds number as a function of T_w/T_b. The resulting slopes varied from 0.29 to 0.31. An average of 0.30 was selected for the correlation; the equation for the line shown in Fig. 1 is

$$\frac{hD}{k_b} = 0.023 \left(\frac{\rho_b VD}{\mu_b}\right)^{0.8} (N_{Prb})^{0.4} \left(\frac{T_w}{T_b}\right)^{-0.3} \quad [1]$$

where

h = heat transfer coefficient, B/hr ft²R

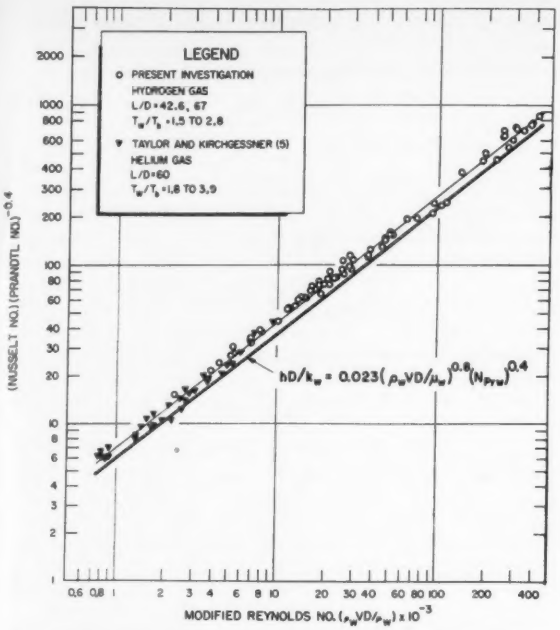

Fig. 2 **Comparison of forced convection heat transfer results for hydrogen with those for helium from (5). Properties evaluated at the wall temperature**

D = test section ID, ft
k_b = thermal conductivity evaluated at T_b, B/hr ft R
ρ_b = fluid density at the average bulk temperature, lb/ft^3
V = average bulk velocity of the fluid, fps
μ_b = viscosity of the fluid evaluated at T_b, lb/ft sec.
N_{Prb} = Prandtl number evaluated at T_b
T_w, T_b = average inner wall and bulk temperature, R

The correlation at Reynolds numbers less than 10^5 can be improved by reducing the exponent on the Reynolds number to 0.76 and increasing the value of the constant in Equation [1] to 0.038.

It is of interest to compare the present results with the heat transfer results for helium gas reported by Taylor and Kirchgessner (5). Fig. 2 illustrates the hydrogen data (presented in Fig. 1) correlated with the modified Reynolds number, properties evaluated at the wall temperature, as recommended in (5). The solid line represents the equation

$$\frac{hD}{k_w} = 0.023 \left(\frac{\rho_w VD}{\mu_w}\right)^{0.8} (N_{Prw})^{0.4} \qquad [2]$$

where the subscript w signifies evaluation at the wall temperature. A very satisfactory correlation of the hydrogen and the helium data in Fig. 2 results if the constant in Equation [2] is increased to 0.027.

The authors would like to express their appreciation to the management of Rocketdyne for permission to publish these results, and to the personnel at the Combustion and Heat Transfer Laboratory for their assistance in conducting the experiments.

References

1 Kaufman, S. J. and Isley, F. D., "Preliminary Investigation of Heat Transfer to Water Flowing in an Electrically Heated Inconel Tube," NACA RM E50G31, Sept. 27, 1950.
2 Wolf, H., "Heating and Cooling Air and Carbon Dioxide in the Thermal Entrance Region of a Circular Duct with Large Gas to Wall Temperature Differences," ASME paper no. 59-SA-15, June 18, 1959.
3 Humble, L. V. and Lowdermilk, W. H., "Measurements of Average Heat Transfer and Friction Coefficients for Subsonic Flow of Air in Smooth Tubes at High Surface and Fluid Temperatures," NACA Rep. 1020, 1951.
4 Deissler, R. G., "Turbulent Heat Transfer and Friction in the Entrance Region of Smooth Passages," Trans. ASME, vol. 77, Nov. 1955, p. 1221.
5 Taylor, M. F. and Kirchgessner, T. A., "Measurements of Heat Transfer and Friction Coefficients for Helium Flowing in a Tube at Surface Temperatures up to 5900 R," ARS preprint no. 850–59, June 1959.
6 Hilsenrath, J. et al., "Tables of Thermal Properties of Gases," Nat. Bur. Standards Circular 564, U. S. Department of Commerce, Washington, D. C., Nov. 1, 1955, p. 254.
7 Reid, R. C. and Sherwood, T. K., "The Properties of Gases and Liquids," McGraw-Hill Book Co., Inc., N. Y., 1958, p. 236.
8 Hilsenrath, J. and Touloukian, Y. S., "The Viscosity, Thermal Conductivity and Prandtl Number for Air, O_2, N_2, NO, H_2, CO, CO_2, H_2O, He, and A," Trans. ASME, vol. 76, Aug. 1954, p. 967.

Lateral Speed Indicator

ROBERT L. SOHN[1]

Space Technology Laboratories, Inc., Los Angeles, Calif.

THIS note describes a lateral speed sensor which can measure the transverse, or drift speed, of an object with respect to the surface of a satellite or planet as the object approaches the body from a remote distance, e.g., the lateral speed of a missile approaching the moon from several thousand miles distance.

For soft landings on the surface, the speed of the vehicle with respect to the body must be reduced by retrorockets. In order to cancel the *total* velocity, both the vertical and lateral components of speed must be known. Determination of vertical speed is accomplished relatively easily by a radar altimeter. But measurement of the lateral speed component is much more difficult, since measurements must be made from altitudes of over several miles, where optical devices are not too practical.

Received Nov. 5, 1959.
[1] Head, System Design Section. Member ARS.

Some lateral speed measurement schemes operate on the principle of scanning the horizon with three or more sensors. To illustrate: As the vehicle approaches the surface, the angles subtended by the horizon sensors vary in proportion to both vertical and lateral speed. By noting the rates of change in each of the subtended angles, lateral speed can be computed. But the great difficulty with this system lies in the fact that the angular rates are extremely small, so that good accuracy cannot be obtained. This note describes a lateral speed indicator that does not depend upon *rate* information, but only upon position information.

Analytical Background

Consider, for example, the case in which a vehicle is approaching the surface of the moon. Nominally, the vehicle would be designed to impact vertically, with no lateral speed component. In actuality, the vehicle probably will be off course by a certain distance. As a result, the vehicle will not approach along a radius and impact vertically, but will approach along a slightly curved path and impact with some residual lateral speed. This is illustrated in Fig. 1.

It can be shown that the lateral speed is uniquely related to the angle through which the trajectory curves during ap-

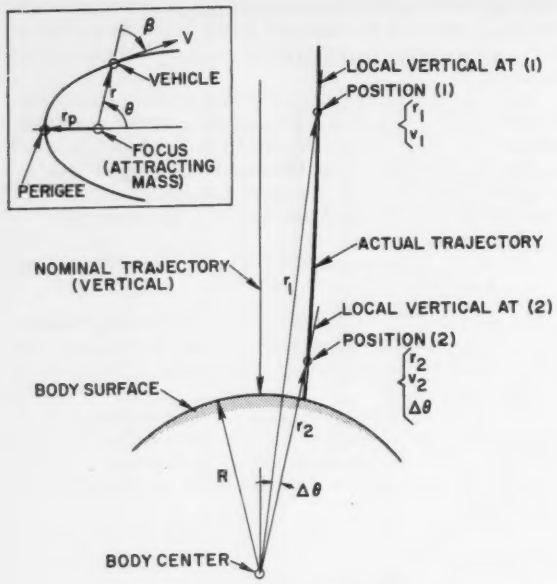

Fig. 1 Trajectory path and nomenclature

proach. In other words, lateral speed can be predicted by combining certain known quantities, such as initial speed and altitude, with a measurement of the angle through which the trajectory curves during approach. For example, a horizon scanner can be used to establish a local vertical when the vehicle begins its approach to the body (position 1). A second measurement of the local vertical is made as the vehicle draws near to the surface (position 2). The difference between these angles (the local vertical at position 1 is noted by a gyro) is, then, a unique indication of lateral speed both as to direction and magnitude. Since vehicle motion with respect to the gyro reference system (three-axis gyros) is nulled, sufficient information is known to orient a retrorocket so as to null the lateral speed as well as vertical speed.

Analytical Development

The motion of a body in a central force field has been analyzed in several texts.[2] Fig. 1 (from the cited reference) illustrates the nomenclature. It should be noted that the case of a hyperbolic orbit has been selected because a vehicle approaching the moon, for example, normally will be traveling faster than escape speed with respect to the moon. The derivation can be developed easily for the case of parabolic or elliptic paths.

First of all assume that a horizon scanner will measure local vertical at positions 1 and 2; thus $\Delta\theta$ will be known, since the angle of rotation of the local vertical is precisely $\Delta\theta$. (A gyro will be used to store the local vertical angle at position 1.) Also the altitudes at positions 1 and 2 will be measured by a *C-W* range and range rate radar altimeter (which is directed along the local vertical); thus r_1 and r_2 will be known. Further, measurement of range rate along the local vertical at position 1 will give V_1 to a very close approximation. Actually the vehicle velocity vector at position 1 will be rotated very slightly from the local vertical (by less than 2 deg, as will be shown later). The true velocity will then vary from the measured velocity by the cosine of the rotation angle. But since this angle is usually small, the measured velocity will differ only slightly from the true velocity.

The pertinent equations are as follows

$$\lambda = V^2 r/GM \qquad [1]$$

$$\frac{r}{\lambda - 2} = \frac{r_p}{e - 1} \qquad [2]$$

$$\beta = \sin^{-1}\sqrt{\frac{(e+1)r_p/r}{2 - (1-e)/(r_p/r)}} \qquad [3]$$

$$\theta = \cos^{-1}\frac{1}{e}\left[1 - (1+e)\left(\frac{r_p}{r}\right)\right] \qquad [4]$$

At position 1, V and r are measured, so that λ_1 can be computed

$$\lambda_1 = V_1^2 r_1/GM$$

As noted, $\Delta\theta$ is measured by the lateral speed sensory instrumentation. From Equation [4]

$$\Delta\theta = \cos^{-1}\frac{1}{e}\left[1 - (1+e)\left(\frac{r_p}{r_1}\right)\right] - \cos^{-1}\frac{1}{e}\left[1 - (1+e)\left(\frac{r_p}{r_2}\right)\right] \qquad [5]$$

Equation [2] can be rearranged to solve for r_p

$$r_p = r_1(e-1)/(\lambda_1 - 2) \qquad [6]$$

Combining Equations [5 and 6] gives

$$\Delta\theta = \cos^{-1}\frac{1}{e}\left[1 - \frac{e^2-1}{\lambda_1 - 2}\right] - \cos^{-1}\frac{1}{e}\left[1 - \frac{e^2-1}{\lambda_1 - 2}\left(\frac{r_1}{r_2}\right)\right] \qquad [7]$$

All quantities in Equation [7] are measured, except the eccentricity e. Hence a solution can be obtained for e. Actually, the computer incorporated into the lateral speed indicator will solve the equation by an iterative process.

Finally, it is necessary to solve for the flight path angle and velocity at the surface of the body. The radius of the body R will be known beforehand, of course. The solution for the velocity is as follows. From Equation [2]

$$\lambda_b = (\lambda_1 - 2)(R/r_1) + 2 \qquad [8]$$

and from Equation [1]

$$V_b = \sqrt{\frac{\lambda_b}{\lambda_1}\frac{r_1}{R}\,V_1^2} \qquad [9]$$

Combining Equations [8 and 9] gives

$$V_b = \sqrt{\frac{2 + (\lambda_1 - 2)R/r_1}{\lambda_1}\left(\frac{r_1}{R}\right)V_1^2} \qquad [10]$$

and by combining Equations [3 and 6]

$$\beta_b = \sin^{-1}\sqrt{\frac{[(e^2-1)/(\lambda_1 - 2)]r_1/R}{2 + (\lambda_1 - 2)/(r_1/R)}} \qquad [11]$$

A direct solution for the lateral speed at the surface of the body can now be given as

$$V_{l_b} = V_b \sin\beta_b = \frac{r_1}{R}\sqrt{\frac{GM(e^2-1)}{r_1(\lambda_1 - 2)}} \qquad [12]$$

Numerical Example

A vehicle approaches the moon for a controlled landing. It is assumed to be off course by 100 nautical miles, with a resultant lateral speed component of 435 fps, which is computed by the sensor as previously described.

[2] A summary of the pertinent relations is given in "A Proposed Kepler Diagram," by R. L. Sohn, ARS JOURNAL, vol. 29, no. 1, Jan. 1959, pp. 51–54.

Description

A vehicle is approaching the moon along a nominally radial path. However at a distance of 25,000 nautical miles from the center of the moon, the vehicle is proceeding parallel to its nominal path, but 100 nautical miles to one side. Speed at this point is 3930 fps. It is desired to predict impact speed as described.

At position 1. Assume that position 1 is 1000 nautical miles above the surface of the moon. The lateral speed indicator measures the following: Velocity, 6480 fps (radar range rate); altitude, 1000 nautical miles (radar range); local vertical, by means of horizon scanner.

At position 2. Assume that position 2 is 100 nautical miles above the surface of the moon. The lateral speed indicator measures the following: Velocity, 8380 fps; altitude, 100 nautical miles; $\Delta\theta$, 1.38 deg (by comparing horizon scanner reading with position 1 horizon scanner reading).

Computation

From Equation [7], eccentricity e is 1.00123.
From Equation [10], V_b is 8570 fps.
From Equation [11], β_b is 2.92 deg.
From Equation [12], V_{lb} is 435 fps. (Direction of motion is given by comparing the horizon scanner reading with the three-axis gyro reference.)

Error Analysis

The sensitivity of the lateral speed indicator to errors in the measured quantities ($\Delta\theta$, r_1, r_2) can be determined as follows. Equation [7] can be rewritten as shown by inserting Equation [12]

$$\Delta\theta = \cos^{-1}\frac{1}{e}\left[1 - \frac{R^2}{r_1\,GM}\,V_{lb}{}^2\right] - \cos^{-1}\frac{1}{e}\left[1 - \frac{R^2}{r_2\,GM}\,V_{lb}{}^2\right] \quad [13]$$

By assuming that

$$e \backsimeq 1.0 \qquad \cos\theta \backsimeq 1 - \frac{\theta^2}{2!} \quad [14]$$

the following relations are obtained

$$\theta_1 = \sqrt{\frac{2R^2}{GM}}\,\frac{1}{\sqrt{r_1}}\,V_{lb}$$

$$\theta_2 = \sqrt{\frac{2R^2}{GM}}\,\frac{1}{\sqrt{r_2}}\,V_{lb}$$

Hence

$$V_{lb} = \sqrt{\frac{GM}{2R^2}}\,\frac{\Delta\theta}{(1/\sqrt{r_1} - 1/\sqrt{r_2})} \quad [15]$$

The sensitivity equations are then obtained with suitable differentiation

$$\frac{\partial V_{lb}}{\partial\Delta\theta} = \sqrt{\frac{GM}{2R^2}}\left(\frac{1}{1/\sqrt{r_1} - 1/\sqrt{r_2}}\right) \quad [16]$$

$$\frac{\partial V_{lb}}{\partial r_1} = \sqrt{\frac{GM}{2R^2}}\,\frac{\Delta\theta}{(1/\sqrt{r_1} - 1/\sqrt{r_2})^2}\,\frac{1}{2r_1{}^{3/2}} \quad [17]$$

$$\frac{\partial V_{lb}}{\partial r_2} = \sqrt{\frac{GM}{2R^2}}\,\frac{\Delta\theta}{(1/\sqrt{r_1} - 1/\sqrt{r_2})^2}\,\frac{1}{2r_2{}^{3/2}} \quad [18]$$

By using the numerical example presented previously the following sensitivities are indicated

$$h_1 = r_1 - R$$
$$h_2 = r_2 - R$$
$$\%\delta V_{lb} = 0.847\%\delta(\Delta\theta)$$
$$\%\delta V_{lb} = 0.598\%\delta(h_1)$$
$$\%\delta V_{lb} = -0.152\%\delta(h_2)$$

where the terms on the left are percentage changes in V_{lb} with percentage changes in measured inputs. The percentage error in $\Delta\theta$ is likely to be larger than those of the altimeter. For example, the time of flight between points 1 and 2 is approximately 0.2 hr. If a gyro drift of 1 deg per hr is assumed, a 0.2-deg error in $\Delta\theta$ will be introduced. The corresponding error in V_{lb} is 53 fps.

It should be noted that the assumptions of Equation [14] are valid for the example chosen, but cannot be used in the general case.

New Method for Studying Polymerization of Solid Propellants and Propellant Binders

R. W. WARFIELD[1]

U. S. Naval Ordnance Laboratory, Silver Spring, Md.

TODAY'S great usage of solid propellants has emphasized the need for new experimental techniques to study the polymerization of these composite systems. In general, the conventional methods are not applicable because of the polyfunctional nature of the propellant binder, and because of the presence of large amounts of inorganic oxidizer particles and other additives. The author has recently shown (1, 2)[2] that electrical volume resistivity measurements, made continuously and isothermally, can be used to quantitatively define the bulk polymerization characteristics of thermosetting polymers. This technique has now been applied to the study of the polymerization of solid propellants and propellant binders. It is the purpose of this note to indicate how resistivity measurements may be used to study the polymerization of solid propellants and to describe briefly the types of data which may be obtained.

The continuous current monitoring device (CCMD), which is a simple application of Ohm's Law, is used to determine the resistivity of the propellant during and after polymerization (3). This device consists of a Keithley Model 210 electrometer, a Keithley Model 2008 decade shunt and a sample cell. With this instrumentation it is possible to monitor the large change in resistivity (10^6 to 10^{16} ohm-cm) which propellants may undergo during polymerization. The sample cell, in which polymerization is conducted, consists of two small concentric cylinders between which about 13 gm of the liquid propellant or binder are poured. A small laboratory oven was used to maintain the isothermal conditions within ±0.5 C.

Received Nov. 23, 1959.
[1] Physical Chemist, Chemistry Research Department.
[2] Numbers in parentheses indicate References at end of paper.

The temperature dependence of the resistivity of the polymerized propellant was determined by monitoring the resistivity as the sample was heated at the rate of about 15 C per hr. The sample cell and experimental arrangement employed to continuously record the electrical volume resistivity have been previously reported (3).

From a series of these polymerizations conducted on both the binder and the composite propellant, it is possible to determine the rates of polymerization at various temperatures and the overall activation energies for the polymerization process of both the binder and the composite propellant. From the values of the activation energies it can be determined if the presence of oxidizer and/or additives serves to catalyze and/or accelerate the polymerization. It is expected that a catalyzed reaction would exhibit a lower activation energy than an uncatalyzed reaction. A rapid and simple method for determining catalysis in these systems is particularly significant, in view of the work of Mishuck and Carleton (4) who have reported that the presence of ammonium perchlorate will accelerate the polymerization of a polyester-styrene propellant. Results obtained in this laboratory (5) by the electrical resistivity method indicate that the presence of ammonium perchlorate will catalyze the polymerization of a polyurethane propellant.

By studying the rates of polymerization at different temperatures, it is possible to select the optimum manner in which to conduct polymerization and thus obtain the optimum physical properties. Also, providing that the polymerizations are conducted over a broad temperature range, Arrhenius plots may be used to determine if different reaction mechanisms occur. It has been previously suggested (6) that the method employing electrical resistivity during an isothermal polymerization may give results superior to those obtained by conventional dilatometric techniques.

The temperature dependence of the resistivity of the polymerized propellant can be used as an index of the extent of polymerization. It has been shown (1, 2) that during polymerization the temperature dependence of the resistivity increases with the extent of polymerization. Incomplete polymerization is evidenced by a resistivity vs. temperature plot exhibiting a reduced slope and a displacement toward lower temperatures when compared with a plot of the completely polymerized material.

It is suggested that electrical volume resistivity measurements may be used for long-term surveillance testing of composite propellants. On the basis of past work on thermosetting polymers, it would be expected that volume resistivity measurements would be sensitive to degradation, decomposition, crystallation, and possibly could be used to study deterioration at the binder-oxidizer interface (7) and other effects encountered in long-term aging.

References

1 Warfield, R. W. and Petree, M. C., "The Use of Electrical Resistivity in the Study of the Polymerization of Thermosetting Polymers," *J. Polymer Sci.*, vol. 37, 1959, p. 305.

2 Warfield, R. W. and Petree, M. C., "A Study of the Polymerization of Epoxide Polymers by Electrical Resistivity Techniques," paper presented at the 136th Meeting of the American Chemical Society, Atlantic City, Sept. 15, 1959.

3 Warfield, R. W., "Studying the Electrical Properties of Casting Resins," *Soc. Plastics Eng. J.*, vol. 14, no. 11, 1958, p. 39.

4 Mishuck, E. and Carleton, L. T., "Chemical Principles of Solid Propellants," paper presented at the 136th Meeting of the American Chemical Society, Atlantic City, Sept. 17, 1959.

5 Warfield, R. W., Naval Ordnance Laboratory Rep. no. 6653, 1959. *Classified*, not available for general circulation.

6 Aukward, J. A., Warfield, R. W. and Petree, M. C., "Change in Electrical Resistivity of Some High Polymers During Isothermal Polymerization," *J. Polymer Sci.*, vol. 27, 1958, p. 199.

7 Boyars, C., "Surveillance of Solid Propellant Rockets," ARS JOURNAL, Feb. 1959, vol. 29, no. 2, pp. 148–150.

Technical Comments

Comment on "Effect of Thrust Termination Process Upon Range Dispersion of a Ballistic Missile"

STEPHEN L. JOHNSTON[1]

Army Rocket and Guided Missile Agency, Redstone Arsenal, Ala.

THE ELLIPTICAL range equation has appeared in many forms. The recent article by Kelly (1)[2] presents the following range Equation [14] in (1)

$$\Delta\phi = 3\cos^{-1}\left(\frac{-2cZ_h + b}{\sqrt{b^2 + 4ac}}\right) - \cos^{-1}\left(\frac{-2cZ_R + b}{\sqrt{b^2 + 4ac}}\right)$$

Although Kelly indicated that this equation was taken from the 1953 edition of (2), he did not show the derivation by which he obtained this form. Equation [14] does not appear in the 1957 edition of (2).

The range equation given by Baker and Hart (3) indicates that Kelly's Equation [14] may be incorrect. Baker and Hart's equation in Kelly's notation is

$$\phi = \cos^{-1}\left(\frac{b - 2cZ_h}{\sqrt{b^2 + 4ac}}\right) + \cos^{-1}\left(\frac{b - 2cZ_R}{\sqrt{b^2 + 4ac}}\right)$$

The quantity c must be redefined[3] as $[(r_0 + h_0)U_0 \cos\theta_0]^2$. Other quantities are as defined by Kelly.

No attempt was made to verify Equations [16 and 17] of (1), but their values for the sample problem were compared with results obtained by using the equations of (4). These equations were obtained by differentiating Baker and Hart's range Equation [2]. This comparison is shown in Table 1. The small value of $\partial R/\partial\theta_0$ (57.3 nautical mile/radian) quoted

Received by Oct. 15, 1959.

[1] Chief, Guidance and Control Branch, Systems Analysis Laboratory, Ordnance Missile Division.

[2] Numbers in parentheses indicate References at end of paper.

[3] Alternatively, quantity c could remain as defined by Kelly provided θ_0 were redefined as the angle with the vertical rather than the horizontal. Inspection of Table 1 indicates that Kelly may have inadvertently done this in his calculations. For example, compare his value of 480 naut mile for R_t for $\theta_0 = 30$ deg with the value of 482 naut mile for $\theta_0 = 60$ deg in Table 1.

by Kelly indicates that $\theta_0 \approx \theta_{opt}$. In fact, for the h_0 and U_0 values shown, $\theta_{opt} = 40.954$ deg. It was not possible to obtain Kelly's values of R, $\partial R/\partial U_0$, and $\partial R/\partial \theta_0$ for any one value of θ. The results shown in Table 1 for (4) were obtained on an IBM 704 computer for various values of θ and were rounded off for use herein. Values of g and r_0 are the same as those used by Kelly.

Comparison of Kelly's values [method of (1)] indicates that there may be errors in his Equations [16 and 17] in addition to his errors in Equation [14] and his confusion over θ_0.

While a generalized approach as was used by Kelly is very desirable, two possible simplifications for many practical applications should be mentioned. The angle ξ used by Kelly is actually the angle of attack. Both load factor considerations and control system linearity problems demand that ξ be small, especially in the vicinity of thrust termination. For the preliminary analysis purposes of Kelly's paper, it would be permissible to use $\xi \approx 0$ and thus to simplify Equation [11] to $Q = \partial R/\partial U_0$.

A further justification for this simplification of Equation [11] arises from maximum range considerations. It is well known that maximum free flight range is obtained for that value of θ_0 for which $\partial R/\partial \theta_0 = 0$. In the initial design consideration of a missile, performance aspects at maximum range are of principal interest. For this case $\partial R/\partial \theta_0 = 0$, and again simplification of Equation [11] and the elimination of Equation [17] are permitted.

For most cases (i.e., $\partial R/\partial \theta_0 = 0$ and/or $\xi = 0$), Equation [16] can also be eliminated. From Fig. 4 of (4), it can be seen that for optimum trajectories $\partial R/\partial U_0$ is very insensitive to changes in values of h_0 for a gross evaluation. Similarly, $\partial R/\partial U_0$ is approximately a linear function of free-flight range.

Table 1 Comparison of results obtained by methods of references (4) and (1)

θ_0, deg	R_t, naut miles	$\partial R/\partial U_0$, naut miles/fps	$\partial R/\partial \theta_0$, naut miles/rad
	{Method of (4)}		
30	554.3	0.1138	400.0
40	592.8	0.1218	35.57
50	567.0	0.1150	−326.2
60	481.9	0.0961	−637.2
	{Method of (1)}		
30	480	0.117	57.3

Thus Equation [11] could be further simplified to the form $Q = K_1 + K_2 R_t$ where

$$K_1 = 0.0335 \text{ naut mile/fps} \qquad K_2 = 1.33 \times 10^{-4} \text{ sec/ft}$$

These values of K_1 and K_2 are valid for missiles having ranges of approximately 200 to 2500 nautical miles.

References

1 Kelly, A. J., "Effect of Thrust Termination Process Upon Range Dispersion of a Ballistic Missile," ARS JOURNAL, vol. 29, no. 6, June 1959, pp. 432–442.

2 Goldstein, H., "Classical Mechanics," Addison-Wesley Publishing Co., Reading, Mass., 1957.

3 Baker, C. D., and Hart, J. J., "Maximum Range of a Projectile in a Vacuum," *Amer. J. Phys.*, vol. 23, no. 5, May 1955, pp. 253–255.

4 Gilman, E. L., and Johnston, S. L., "First and Second Order Partial Derivatives of Free-Flight Range and Time Equations for Impact Accuracy of Ballistic Missiles," Redstone Arsenal/OML Rep. 6R7F, April 10, 1958.

Aeromechanical Effects in Ablation

MARK V. MORKOVIN[1]

The Martin Co., Baltimore, Md.

IN HIS article on "Recent Advances in Ablation" (1)[2] Adams states that "Mechanical erosion, though not discussed here, will reduce the effective heat of ablation. Since surface erosion effects cannot be separated from ablation as such, the shear and pressure forces anticipated for application should be duplicated in laboratory ablation tests." At the discussion on ablation at the Conference on Physical Chemistry and Space Flight, held Sept. 1–3, 1959 at the University of Pennsylvania in Philadelphia, Barry and Gruntfest of the General Electric Co. emphasized that good mechanical strength of the char is an important property of good ablators. The following is the essence of the comments at the same conference by the author on the question of laboratory simulation of the mechanical erosion aspects of ablation.

Let us consider another possible interplay between fluid mechanics and the rate of ablation. The importance of mechanical strength of the char suggests that the dynamic aspects of the local air loads during the testing and during flight should be considered.

From information presented at the International Symposium on Fluid Mechanics in the Ionosphere (2), it appears highly unlikely that there are any irregularities in that part of Earth's atmosphere where ablation may be important which has a scale of less than 5 m. Thus for all practical purposes the ablating vehicle encounters a uniform and steady (or quasi-steady) free stream and the aerodynamic disturbances present must arise in the boundary layer of the vehicle itself (or due to the vibrations of the body).

The situation is quite different in the aerodynamic testing facilities where one should distinguish between steady and unsteady temperature, sound, and turbulence nonuniformities of the free stream (3). For instance, steady nonuniformity in velocity has been observed to cause considerable unevenness in ablation rate in the Caltech Hypersonic Tunnel which is otherwise a clean and quiet facility (private communication by Lees[3]). In hot jets with diameters less than 2 diam of the tested body the steady nonuniformities are also likely to be important. However, in hot jets, plasma jets and rocket exhausts, the unsteady temperature, sound, and turbulence nonuniformities may well be most important and often critical. While nothing definite is known about the effect of rather intense moving hot-spots on the body, we know that the extremely high sound levels encountered in rocket exhausts can be highly destructive of structural components. This may occur in a number of ways depending upon the frequency of the sound, since in one way or another the critical effects are usually associated with resonance of local structural elements or of aerodynamic cavities. Strong sound fluctuations may create local spots hotter than stagna-

Received Jan. 15, 1960.

[1] Principal Scientist, Research Staff, Manned Vehicles Division.

[2] Numbers in parentheses indicate References at end of paper.

[3] Lester Lees, Professor of Aeronautics, Guggenheim Aeronautical Laboratory, California Institute of Technology, Pasadena, Calif.

tion temperature and local instantaneous high pressure regions, especially inside cavities, which must be detrimental to the structure, see e.g., (4) on "frontal" cavities, and unpublished data on "side" cavities. (Even the mild pressure and shear fluctuations associated with a low speed turbulent boundary layer are known to accelerate substantially the mechanical scrubbing of paint from ship hulls.) Finally, besides the above direct effects of the nonuniformities in the testing facilities, there must be an indirect effect, namely the earliest possible transition to turbulent flow over the model itself with consequent higher heat transfer and still higher pressure fluctuations.

Clearly, all these effects depend upon the amplitudes of the disturbances which have not been measured in the hot facilities. Whatever these amplitudes may be, the gross information indicates that they are one or two orders of magnitude larger than those we are used to in ordinary aerodynamic tests and those the ablating vehicle is likely to encounter in actual flight. The reported importance of the mechanical strength of the char seems to indicate that the "aerodynamic abrasion" in the "noisy" testing facilities may have to be considered in evaluating the significance of the tests and that actual flight vehicles may ablate slower.

References

1 Adams, M. C., "Recent Advances in Ablation," ARS JOURNAL, vol. 29, no. 9, Sept. 1959, pp. 625–632.

2 International Symposium on Fluid Mechanics in the Ionosphere, Cornell University, July 9–15, 1959, Proceedings, published in *J. Geophys. Res.*, vol. 64, no. 12, Dec. 1959.

3 Morkovin, M. V. "On Supersonic Wind Tunnels With Low Free-Stream Disturbances," *J. Appl. Mech.*, vol. 26, no. 3, Sept. 1959, pp. 319–324.

4 Sprenger, H. "Ueber Thermische Effekte in Resonanzrohren, Mitteilung," Inst. of Aerodynamik, Tech. Hochschule, Zurich, no. 21, Publ. Leemann, Zurich, 1954.

Book Reviews

Ali Bulent Cambel, Northwestern University, *Associate Editor*

Analysis and Design of Aircraft Structures, Vol. I, Analysis for Stress and Strain, by E. F. Bruhn, assisted by A. F. Schmitt, Tri-State Offset Co., Cincinnati, Ohio, 1958.

Reviewed by GEORGE GERARD
New York University

In approaching a subject as broad as aircraft structures, there are certain courses available to an author: He may present a large volume of material that can cover most of the problem areas likely to be encountered in one's professional career; or, he may proceed in a highly selective manner by choosing broad areas of importance where the student is thoroughly grounded in the scientific principles of the subjects selected. With this fundamental background, one can proceed to handle the specific problems which arise in his professional work, as well as treat the new developments characteristic of this rapidly evolving field.

A large measure of the success of the earlier editions of this book, as measured by its routine use in industry, can probably be attributed to the use of the first approach. The current edition consists of two volumes, the one under review and Volume II, "Strength Analysis and Design" yet to appear. Thus, there is a distinct effort to cover much more material in detail in the present revision.

To this reviewer, the needs of the modern academic world are more consistent with the second approach discussed, since progressive engineering education tends to emphasize the science rather than the art of the profession. The great amount of detailed material covered in "Analysis and Design of Aircraft Structures" will require each instructor to make his individual selection of material. The fierce competition for the student's time in his education as an aeronautical-astronautical engineer necessitates considerable judgment in selection of subject material for aircraft structures courses. Thus a major role that should be performed by the author of a textbook has been left to the instructor.

The material covered in Volume I is concerned with the stress analysis of statically determinate and indeterminate structures, axial loads and shear flow in thin wall shells, and contains an introduction to wing and fuselage analysis. The excellent photographs of modern aircraft structural components throughout the book are commendable.

To the stress analyst in industry, the appearance of this new edition may be of considerable interest particularly because of the enlarged coverage. To those concerned with the educational aspects of aeronautical structures, the enlarged scope of the work may prove these volumes to be unattractive as a text.

Hypersonic Aerodynamics, by Robert Wesley Truitt, The Ronald Press Co., New York, 1959, 474 pp. $10.

Reviewed by WILLIAM H. DORRANCE
Convair Scientific Research Laboratory

As stated in the Preface, "the purpose of this book is to present the fundamental principles of hypersonic aerodynamics and their application to missile design problems." In the opinion of this reviewer the author comes closer to the latter than to the former, as will be elaborated upon in what follows.

This book has some merit. The stated objective is excellent, the organization by chapter headings good and the references at the end of each chapter excellent. Certainly the inclusion of problems with their answers, according to methods presented in the book, is a meritorious accomplishment for teachers and those who learn by example. The subject matter suggested by the table of contents is excellent. It is organized into 10 chapters which, starting with an introduction to hypersonics, ranges through methods applicable in analyzing the two- and three-dimensional flow about bodies, the development of minimum drag bodies using impact (Newtonian) theory and impact theory with centrifugal force corrections, hypersonic small disturbance theory, hypersonic slender body theory, hypersonic flow over blunt bodies, complete configurations, stability and control, and ends with a chapter on real gas effects.

This reviewer found Chapter 3 useful. It is on impact theory (Newtonian), modified to account for centrifugal force effects for bodies of revolution, and empirical methods of estimating cone-cylinder normal force and pitching moment. Similarly, Chapter 4 on the development of minimum drag bodies using impact (Newtonian) and impact plus centrifugal force correction theories, Chapter 6 on Cole's slender body theory, and Chapter 9 on stability and control, are well organized and, probably useful, chapters. In most cases the author's efforts to compare theory with experiment were clearly and pertinently presented.

Despite the virtues cited, this reviewer is of the opinion that this is not a good book. The virtues are primarily those of the author's source material; the shortcomings, for the most part, are those contributed by the author. For example, in pages 34–36 the author sets out to derive the potential flow equation for compressible flow (although he doesn't identify it that way but instead calls it the "Governing Differential Equation for Hypersonic Flow," certainly an unnecessarily restrictive description). He uses what at first glance appears to be vector analysis but which makes no acknowledgment as to the formalities of the use of scalar and vector products. He persists in calling the Euler equation the "Navier-Stokes" equation. Certainly a book dedicated to elaborating the fundamental principles should avoid this error.

The author consistently ignores the contribution of axial force distribution to

EXCELCO

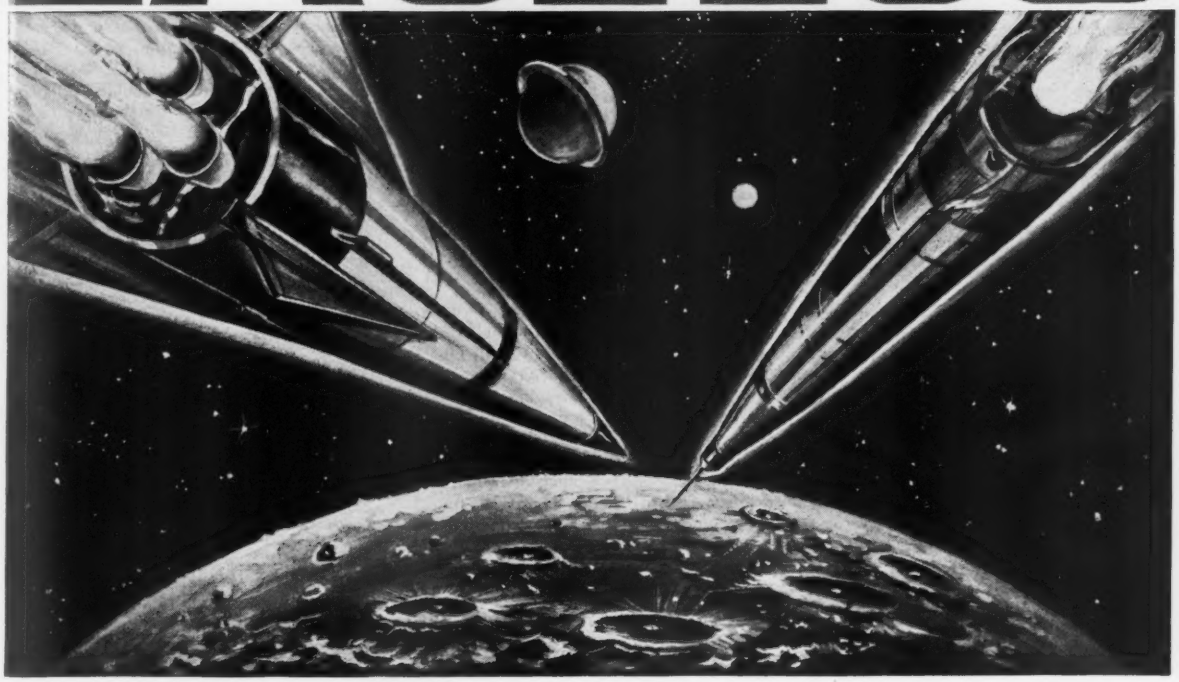

RV-A-10 • SERGEANT
AIR FORCE — RE-ENTRY X-17
POLARIS — RE-ENTRY X-36
JUPITER JR. • JUPITER SR.
POLARIS 0 • POLARIS A
POLARIS AIX • POLARIS A2-MOD 1-2-3
NIKE HERCULES • NIKE ZEUS
MINUTEMAN • PERSHING
N.A.S.A. PROGRAMS • SCOUT
LITTLE JOE

•

and many other classified projects

Builders of more large, thin wall, high strength solid propellant rocket engine cases and nozzles for development purposes than any other company in America.

A small experienced organization geared to handle your development and prototype requirements for static and flight tests in the shortest possible time.

Call or write:

EXCELCO DEVELOPMENTS

MILL STREET • SILVER CREEK, NEW YORK

pitching moment and to the location of the center of pressure, both for axially symmetric and nonsymmetric bodies. For example, on page 84 he gives the center of pressure location for a cone as two thirds the length, whereas, because of the axial force distribution, it is actually $^2/_3[1 + \tan^2\theta_c]$ where θ_c is the cone semivertex angle. For a cone with $\theta_c = 25$ deg (not unreasonable for ICBM-type nose cones) the author's expression is in error by about 20 per cent. For practicing engineers such an omission can be damaging.

The book varies in sophistication from chapter to chapter. Chapter 8 on complete configurations is so elementary as to suggest (however improperly) that the more difficult material presented earlier (such as hypersonic small disturbance theory, or hypersonic flow over blunt bodies) is superfluous for a practical engineer. This chapter detracts from the material presented fairly skillfully in Chapters 3 and 4.

The important areas of hypersonic boundary layer theory and nonequilibrium hypersonic flow are merely mentioned, and their treatment is inadequate.

The use of three references for Chapter 8, which were papers "presented at the Engineering Section of the Virginia Academy of Sciences," certainly raises a question as to their availability to the general reader.

Analysis of Linear Systems, by David K. Cheng, Addison-Wesley Publishing Co., Inc., Reading, Mass., 1959, xiii + 431 pp.

Reviewed by J. L. Stewart
University of Southern California

For many years, one classic work has dominated the market for senior-graduate books for electrical engineers and others, in the general area of linear systems analysis by means of the Laplace transform method.

The book reviewed here is typical of recent books, although it is above average in the care of its presentation and in its thoroughness.

The content of the text is typical in that the principal purpose is the exposition of the Laplace transform method. The author is aware of the shortcomings of presenting the Laplace method as a mere definition in the form of a suddenly presented formula. So he has wisely prefaced his book (Chapters 1 and 2) with material on classical differential equations.

The author also believes that adequate exposition of the Laplace method demands knowledge of the equations of specific systems. He thus gives a fairly general presentation of electric circuit analysis in Chapter 3, and of mechanical and electromechanical circuits in Chapter 4; these subjects come well before the introduction of transform methods.

The familiar procedure is followed in Chapter 5; the Fourier series and the Fourier integral are introduced as a preliminary step to a derivation of the Laplace transform. The author does pause however, to discuss the invaluable concept of the frequency spectrum.

Chapters 6, 7 and 8 contain the principal material on the Laplace method. The presentation is fairly thorough (considering the fact that contour integration is presumed to be beyond the level of the book), although to some it may be disappointingly lacking in novelty.

Later chapters concern themselves with the usual supplementary material, such as feedback and block diagrams (Chapter 9), the Z transformation (Chapter 10) and systems with distributed constants (Chapter 11). An appendix on numerical factoring methods is also provided.

The book is a careful and highly conservative presentation of a widely taught group of subjects; it is in fact superior to most books of its type. However, in its conservatism it has the same oversights and is subject to the same limitations as its predecessors. For example, the pole-zero interpretation is given almost no attention. The author still shows inhibitions to the effect that the rudiments of contour integration are somehow too mysterious to explain. Numerous additional items of this type can be cited.

This reviewer believes the book to be adapted to the needs of a number of institutions; it is a good example of its type. However, the reason for its existence apart from that of furnishing competition can be questioned; it adds little to the literature.

Space Flight, by Carsbie C. Adams, McGraw Hill-Book Co., Inc., New York, 1959, xvi + 373 pp. $6.50.

Reviewed by F. C. Durant III
Avco—Research and Development

An increasing flood of works on space flight have been appearing on the book market in the past few years. No longer can the "aficianado" add to his library everything published on astronautics. Selection is difficult. Many books are narrow in scope, highly technical state of the art surveys, aimed at a limited audience. Others, intended to be educational on a general level, are compilations of summaries of other writings. Often the authors of the latter type are professional writers who are new to their subject, but are educating themselves as they assemble facts and figures in a mechanically skilled manner.

Seldom does a general work appear which is not only broad in scope and selectively documented, but imaginative and stimulating as well, as history evolves into present-day projects and the paths into space become defined. Dr. Adams with his collaborators, F. I. Ordway III, Heyward E. Canney Jr. and Ronald C. Wakeford, have produced a remarkable book of wide readership value. For different reasons "Space Flight" should satisfy the needs of public and technical libraries, college undergraduates, the motivated high school senior and the professional rocket engineer and scientist. The layman needs education in the interplay of widely differing disciplines of science and technology which are the components of astronautics. The professional often desperately needs a view of the "forest" while he is daily applying his calipers to the individual "tree."

In his Forward, Dr. Wernher von Braun writes that he has "no doubt that 'Space Flight' will become the spaceman's book on space flight," and that he is "certain that it will soon attain the stature on one of the few great classics on this fascinating and many-faceted subject." This is high praise by a leader in the field.

The technique of presentation follows an excellent organizational pattern in which historical review in each case leads the reader to the present. Dr. Adams uses skill and good judgment in his treatment of the recent past with regard to the development of satellite plans, programs, controversies and the personalities concerned. In particular, the positions of the USSR and the United States is finely drawn with respect to capabilities, drives and accomplishments. Much of this recent history has not appeared before as completely or as well.

Particularly refreshing are the footnote references and extensive bibliographies listed at the end of all but one of the 15 chapters. A perusal of these selected references is like opening a door to a whole new library of material. Many of these are the classic, technical papers written for meetings of the American Rocket Society, British Interplanetary Society and the International Astronautical Federation. Librarians of universities and industrial research organizations can usually obtain these papers without much effort. British, French, German and Italian works are also referenced. The writings of persons who have played key roles in the identification of astronautical problems and approaches to their solutions are listed, including not only the well-known names of von Braun, Van Allen, Singer, Whipple, Ehricke, Stehling, Stuhlinger, Bonney and Merrill, but foreign writers, such as Clarke, Cleaver, Moore, Saenger, Gartmann, Partel, Burgess, Lawden, Gatland, Carter, Ananoff, and dozens more.

The writing style is light in touch—a difficult and seldom achieved objective. There is humor and whimsy, as appropriate, in treatment of history and philosophy. Fundamental parameters of rocketry and orbital and celestial mechanics are developed with refreshingly little mathematics.

No critical review could fail to find faults in every book. The treatment of atmospheric re-entry could and should be stronger. The section on electric propulsion seems too short, but the reviewer recognizes his own personal bias in this regard. Offsetting these shortcomings is the remarkably fine discussion of human factors and space medicine of which the author is professionally well aware. A few typographical errors, such as misspellings of: "fuze," and "Allegany" Ballistics Laboratory, and at least one incorrect middle initial in names. But this is carping, and a new edition will undoubtedly make these corrections.

In short, "Space Flight" is a valuable and exciting book—informative, thought provoking and readable. It is definitely recommended for the layman and the professional.

Technical Literature Digest——

M. H. Smith, *Associate Editor*
The James Forrestal Research Center, Princeton University

Propulsion and Power (Combustion Systems)

An Investigation of Ejectors Without Induced Flow—Phase I, by D. L. Barton and D. Taylor, *Arnold Engng. Dev. Center, AEDC TN* 59-145, Dec. 1959, 42 pp.

Dimensioning Tables for Ramjet Engines. Part 2. One-dimensional internal Flow With Chemical Heating at Flight Mach Numbers 1 to 6 and Altitudes from 0 to 42 Km, by Irene Sänger-Bredt and Hermann Stümke, *Forschungsinst. für Physik der Strahlantriebe*, Stuttgart, *Mitteilungen* no. 18, Aug. 1959, 829 pp. (In German.)

Propulsion and Power (Non-Combustion)

Experimental Investigations of Plasma Accelerators for Space Vehicle Guidance and Propulsion, by B. Gorowitz, K. Moses and P. Gloersen, *General Electric Co., Missile & Space Vehicle Dept., TIS* R598D466, Nov. 1959, 25 pp.

Magnetohydrodynamic Channel Flow of a Perfect Gas for the Generation of Electrical Power, by G. W. Sutton, *General Electric Co., Missile & Space Vehicle Dept., TIS* R598D472, Dec. 1959, 29 pp.

Ion Wave Instabilities, by Ira Bernstein, Edward Frieman, Russel Kulsrud and Marshall N. Rosenbluth, *Princeton Univ., Proj. Matterhorn, Matt-23*, Nov. 1959, 7 pp.

Stability of Large Amplitude Waves in the One-dimensional Plasma, by David Montgomery, *Princeton Univ., Proj. Matterhorn, Matt-24*, Nov. 1959, 9 pp.

Electromagnetic Radiation from an Ionized Hydrogen Plasma, by S. M. Berman, *Space Tech. Labs., Inc., Physical Res. Lab., PRL* 9-29, Sept. 1959, 25 pp.

Space Charge Limited Current Flow from a Plane, Plasma "Cathode," by B. D. Fried and L. O. Heflinger, *Space Tech. Labs., Inc., Physical Res. Lab., Tech. Rep.* 59-0000-00870, Oct. 1959, 12 pp.

Akademiia Nauk, SSSR, Institute Atomnoi Energii, **Physics of Plasmas and Problems of Controlled Thermonuclear Reactions,** Moscow, Akademiia Nauk, 1958, 4 vol. (in Russian). *Vol. 1* (300 pp.):

Theory of the Magnetic Thermonuclear Reactor, by I. E. Tamm, pp. 3–19 (Chap. 1) (1951).

Theory of the Magnetic Thermonuclear Reactor, by A. D. Sakharov, pp. 20–30 (Chap. 2) (1951).

Theory of the Magnetic Thermonuclear Reactor, by I. E. Tamm, pp. 31–41 (Chap. 3) (1951).

Questions Associated with the Drift of Particles in a Toroidal Magnetic Thermonuclear Reaction Chamber, by G. I. Budker, pp. 66–67 (1951).

Stationary Conditions of a Magnetic Thermonuclear Reactor, by D. N. Zubarev and N. V. Klimov, pp. 249–288 (1952).

Vol. 3 (363 pp.):

Thermonuclear Reactions in a System with Magnetic Mirrors, by G. I. Budker, pp. 4–31 (1954).

Propellants and Combustion

Electrical Initiation of Insensitive Explosives, by D. B. Moore and G. M. Muller, *Stanford Res. Inst., Poulter Labs., Tech. Rep.* 016-59, Nov. 1959, 36 pp.

Some Safety and Handling Characteristics of a Mixture of 70% Propyne and 30% Allene, by Lloyd E. Line Jr., *Experiment Inc., TM-1104*, July 1959, 17 pp.

Experimental Investigation of Flame Stabilization in a Deflected Jet, by Gunnar Erik Broman, *Calif. Inst. Tech., Jet Prop. Lab., Rep.* 30-5, Sept. 1959, 60 pp.

Mathematical Approach to Solid Propellant Grain Design, by H. K. Lumpkin, *Army Rocket & Guided Missile Agency, Ord. Missile Labs. Div., ARGMA TN* 1G5N, Dec. 21, 1959, 30 pp.

Special Report; Detonation Characteristics of PBAA Propellant, by R. C. McCauley, *Thiokol Chem. Corp., Redstone, Rep.* 43-59, 15 pp.

Absorption and Dispersion of Microwaves in Flames, by Jürgen Schneider and F. W. Hofman, *Phys. Rev.*, vol. 116, Oct. 15, 1959, pp. 244–249.

The Effect of an Electromagnetic Field on the Detonation Regime, by G. A. Lyubimov, *Soviet Physics-Doklady*, vol. 4 (Russian vol. 126, nos. 1–6), no. 3, Dec. 1959, pp. 526–528.

Exact Solutions for the Propagation of Explosion Waves in a Gravitating Gas with Zero Temperature Gradient, by E. V. Ryazanov, *Soviet Physics-Doklady*, vol. 4 (Russian vol. 126, nos. 1–6), no. 3, Dec. 1959, pp. 537–540.

On Particularities Near the Detonation Center and on the Appearance of Two Shock Waves, by N. N. Kochina, *Soviet Physics-Doklady*, vol. 4 (Russian vol. 126, nos. 1–6), no. 3, Dec. 1959, pp. 544–548.

Reverse In Situ Combustion, by R. P Gilbert, *Zeitschrift für Angewandte Math. und Phys.*, vol. 10, no. 6, 1959, pp. 544–551.

Materials and Structures

Nuclear Radiation Effects on Structural Plastics and Adhesives, Part I: Literature Survey, by Edwin M. Kinderman and Shirley B. Radding, *Wright Air Dev. Center, Tech. Rep.* 56-534, Part I, June 1957, 71 pp.

Nuclear Radiation Effects on Structural Plastics and Adhesives, Part II: Extension of Literature Survey, by R. Y. Mixer and Shirley B. Radding, *Wright Air Dev. Center, Tech. Rep.* 56-534, Part II, June 1959, 33 pp.

Nuclear Radiation Effects on Structural Plastics and Adhesives, Part III: Experimental Research, by R. Y. Mixer and D. B. Parkinson, *Wright Air Dev. Center, Tech. Rep.* 56-534, Part III, Aug. 1957, 44 pp.

EDITOR'S NOTE: Contributions from Professors E. R. G. Eckert, J. P. Hartnett, T. F. Irvine Jr. and P. J. Schneider of the Heat Transfer Laboratory, University of Minnesota, are gratefully acknowledged.

The Effects of Irradiation on Graphite, by G. H. Kinchin, *Atomic Energy of Canada, Ltd., Chalk River Proj., AECL* 846, June 1959, 23 pp.

Fluid Dynamics, Heat Transfer and MHD

On the Stable Shape of a Slender Ablating Graphite Body, by George W. Sutton, *J. Aero/Space Sci.*, vol. 26, Oct. 1959, pp. 681–682.

Shock Waves and Dissipation in a Resonance Tube, by Ascher H. Shapiro, *J. Aero/Space Sci.*, vol. 26, Oct. 1959, pp. 684–685.

On the Influence of Viscosity and Heat Conduction on the Gas Flow Behind a Strong Shock Wave, by L. I. Sedov, M. P. Michailova and G. G. Chernyi (trans. by Ronald F. Probstein from *Vestnik, Moskovskovo Universitela,* no. 3, 1953, pp. 95–100), *Wright Air Dev. Center, TN* 59-349, Oct. 1959, 11 pp.

Experimental Supersaturation of Gases in Hypersonic Wind Tunnels, by P. D. Arthur and H. T. Nagamatsu, *Calif. Inst. Tech., Hypersonic Wind Tunnel Memo.* 10, July 15, 1952, 99 pp.

Some Heat Transfer Problems in Hypersonic Flow, by Antonio Ferri, *Brooklyn Polytech. Inst., PIBAL Rep.* 473, July 1959, 51 pp. (*AFOSR TN* 59-806).

Instrumentation and Communications

Temperature Response of a Hot-Wire Anemometer to Shock and Rarefaction Waves, by S. G. Datar, *Univ. Toronto, Inst. Aerophys., UTIA TN* 28, June 1959, 20 pp.

High-speed Rotating Mirror Streak Camera, by Charles H. Bagley, *Stanford Res. Inst., Poulter Labs., Tech. Rep.* 024-57, Jan. 1957, 14 pp.

A Rough Estimate of the Attenuation of Telemetering Signals Through the Ionized Gas Envelope Around a Typical Re-entry Missile, by S. C. Lin, *AVCO-Everett Res. Lab., Res. Rep.* 74, Feb. 1956, 43 pp.

High-speed Plotting of Telemetering Data, by R. L. Sapirstein, *Electronics,* vol. 33, Jan. 8, 1960, pp. 41–43.

Conversion Circuits for Earth Satellites, by D. N. Carson and S. K. Dhawan, *Electronics,* vol. 33, Jan. 15, 1960, pp. 82–84.

The Effects of Fluctation Noise in Frequency-Modulation Systems, by V. A. Smirnov, *Radio Engng. (trans of Radiotekhnika),* vol. 13, no. 9, Sept. 1959, pp. 7–18.

A Circuit for the Measurement of Weak Signals with Continuous Spectra, by V. S. Voiutskii and A. I. Slutskovskii, *Radio Engng. (trans. of Radiotekhnika),* vol. 13, no. 9, Sept. 1959, pp. 29–34.

Diffused Propagation of Ultra-short Waves in the Troposphere with High-directivity Antenna, by D. M. Vysokovskii, *Telecommunications (trans of Elektrosviaz'),* no. 5, Aug. 1959, pp. 488–497.

Atmospheric and Space Physics

Deduction of Vertical Thermal Structure of a Planetary Atmosphere from a Satellite, by Jean I. F. King, *General Electric Co., Missile and Space Vehicle Dept., TIS* R59SD47, Dec. 1959, 10 pp.

Some Preliminary Reports of Experiments in Satellites 1958 Alpha and 1958 Gamma, *IGY World Data Center, A. Rockets and Satellites, IGY Satellite Report Series* no. 3, May 1, 1958, 92 pp.

Satellite Micrometeorite Measurements by E. Manring and M. Dubin, pp. 25–30.

Satellite Temperature Measurements for 1958 Alpha, by E. P. Buwalda and A. R. Hibbs, pp. 31–72.

The Observation of High Intensity Radiation by Satellites 1958 Alpha and Gamma, by J. A. Van Allen, G. H. Ludwig, E. C. Ray and C. E. McIlwain, pp. 73–100.

Ephemeris of Satellite 1957 Alpha 2 and Collected Reports on Satellite Observations, *IGY World Data Center, A. Rockets and Satellites, IGY Satellite Report Series* no. 8, June 15, 1959, 122 pp.

The Earth's Gravitational Potential as Derived from Satellites 1957 Beta One and 1958 Beta Two, by L. G. Jacchia, pp. 75–78.

The Earth's Gravitational Potential Derived from the Motion of Satellite 1958 Beta Two, by Yoshihide Kozai, pp. 79–84.

Atmospheric Densities from Explorer IV, by G. F. Schilling and C. A. Whitney, pp. 93–102.

The Structure of the High Atmosphere, I: Linear Models, by C. A. Whitney, pp. 93–102.

The Structure of the High Atmosphere, II: A Conduction Model, by C. A. Whitney, pp. 115–121.

Symposium on Scientific Effects of Artificially Introduced Radiations at High Altitudes, *IGY World Data Center, A. Rockets and Satellites, IGY Satellite Report Series* no. 9, Sept. 15, 1959, pp. 1141–1228.

The Argus Experiment, by N. C. Christofilos, pp. 1144–1152.

Satellite Observations of Electrons Artificially Injected into the Geomagnetic Field, by James A. Van Allen, Carl E. McIlwain and George H. Ludwig, pp. 1152–1171.

Project Jason Measurement of Trapped Electrons from a Nuclear Device by Sounding Rockets, by Lew Allen Jr., James L. Beaver, William A. Whitaker, Jasper A. Welch and Roddy B. Walton, pp. 1171–1190.

The Theory of Geomagnetically Trapped Electrons from an Artificial Source, by Jasper A. Welch Jr. and William A. Whitaker, pp. 1190–1208.

Optical, Electromagnetic, and Satellite Observations of High-altitude Nuclear Detonations, Part I, by Philip Newman, pp. 1208–1221.

Optical, Electromagnetic and Satellite Observations of High-altitude Nuclear Detonations, Part II, by Allen M. Peterson, pp. 1221–1228.

On the Problem of the Energy of Gravitation Fields, by H. G. Schöpf, *Annalen der Physik,* vol. 5, nos. 1–2, Oct. 31, 1959, pp. 1–3. (In German.)

Question of the Existence of a Lunar Magnetic Field, by Marcia Neugebauer, *Phys. Rev. Letters,* vol. 4, Jan. 1960, pp. 6–7.

Low Frequency Electromagnetic Radiation Associated with Magnetic Disturbances, by G. R. A. Ellis, *Planetary & Space Sci.*, vol. 1, Sept. 1959, pp. 253–258.

Distribution of Density in a Planetary

Exosphere, by E. J. Öpik and S. F. Singer, *Phys. Fluids*, vol. 2, Nov.-Dec. 1959, pp. 653–655.

Atmospheric Densities from Satellites and Rocket Observation, by K. W. Champion and R. A. Minzner, *Planetary & Space Sci.*, vol. 1, Sept. 1959, pp. 259–264.

Characteristics of the Radiation Emerging from the Top of a Rayleigh Atmosphere, I, by K. L. Coulson, *Planetary & Space Sci.*, vol. 1, Sept. 1959, pp. 265–271.

Characteristics of the Radiation Emerging from the Top of a Rayleigh Atmosphere, II, by K. L. Coulson, *Planetary & Space Sci.*, vol. 1, Sept. 1959, pp. 272–284.

Lines of Force of the Geomagnetic Field in Space, by E. H. Vestine and W. L. Sibley, *Planetary & Space Sci.*, vol. 1, Sept. 1959, pp. 285–290.

Artificial Electron Clouds, II: General Considerations, by F. F. Marmo, J. Pressman and L. M. Aschenbrand, *Planetary & Space Sci.*, vol. 1, Sept. 1959, pp. 291–305.

Artificial Electron Clouds, III: Release of Atomic Potassium at 121 km, by F. F. Marmo, L. M. Aschenbrand and J. Pressman, *Planetary & Space Sci.*, vol. 1, Sept. 1959, pp. 306–318.

The Association of Solar Radio Bursts with Auroral Streams, by A. Maxwell, A. R. Thompson and G. Garmire, *Planetary & Space Sci.*, vol. 1, Sept. 1959, pp. 325–332.

The Photolysis of Nitrous Oxide in the Far Ultraviolet, by W. E. Groth and H. Schierholz, *Planetary & Space Sci.*, vol. 1, Sept. 1959, pp. 333–342.

Ionizing Radiation Detected by Pioneer II, by A. Rosen, P. J. Coleman Jr. and C. P. Sonett, *Planetary & Space Sci.*, vol. 1, Sept. 1959, pp. 343–349.

Diffusion of Ions in a Static F_2 Region, by J. E. C. Gliddon, *Quart. J., Mech. & Appl. Math.*, vol. 12, Aug. 1959, pp. 340–346.

Use of Green's Function in the Solution of Ionospheric Diffusion Problems, by J. E. C. Gliddon, *Quart. J. Mech. & Appl. Math.*, vol. 12, Aug. 1959, pp. 347–353.

Some Properties of Primary Electromagnetic Disturbances Caused by Lightning Discharges, by V. E. Kashprovskii, *Telecommunications (trans. of Electrosviasz')*, no. 7, Oct. 1959, pp. 717–731.

Ultraviolet Reflectivities of Mars and Jupiter, by A. Boggess III and L. Dunkelman, *Astrophys. J.*, vol. 129, nos. 1 & 2, Jan. and Feb. 1959, pp. 236–241.

Some Aspects of the Electrical Properties of the Upper Atmosphere, by F. A. Goldberg, *J. Aero/Space Sci.*, vol. 26, Dec. 1959, pp. 63–68.

Gravitation and Electromagnetism, by A. H. Klotz, *Nuovo Cimento*, vol. 14, no. 1, Oct. 1959, pp. 135–141.

Measurement of Phase and Amplitude Fluctuations of Radio Waves Which Have Traversed the Ionosphere, by V. V. Vitkevich and Iu. L. Kokurin, *Radio Engng. & Electronics (trans. of Radiotekhnika i Elektronika)*, vol. 3, no. 11, 1958, pp. 70–78.

Combined Photographic and Radio Echo Observations of Meteors, by J. Davis, J. S. Greenhow and J. E. Hall, *Proc., Roy. Soc., London*, vol. A 253, Nov. 17, 1959, pp. 121–129.

The Effect of Attachment of Radio Echo Observations of Meteors, by J. Davis, J. S. Greenhow and J. E. Hall, *Proc., Roy. Soc., London*, vol. A 253, Nov. 17, 1959, pp. 130–139.

Index to Advertisers